

17. Norman S., Vertommen D., Heath R., Neumann D., Mouton V., Woods A., Schlattner U., Wallmann T., Carling D., Hue L., Rider M.H. (2006) Insulin antagonizes ischemia-induced Thr172 phosphorylation of AMP-activated protein kinase alpha-subunits in heart via hierarchical phosphorylation of Ser485/491. *J Biol Chem* 281: 5335–40.
18. Kasi D., Adachi T., Deng L., Nagano-Fujii M., Sada K., Ikeda M., Kato N., Ide Y.H., Shoji I., Hotta H. (2009) HCV replication suppresses cellular glucose uptake through down-regulation of cell surface expression of glucose transporters. *J Hepatol* 50: 883–94.
19. Blight K.J., McKeating J.A., Rice C.M. (2002) Highly permissive cell lines for subgenomic and genomic hepatitis C virus RNA replication. *J Virol* 76: 13001–14.
20. Bungyoku Y., Shoji I., Makine T., Adachi T., Hayashida K., Nagano-Fujii M., Ide Y.H., Deng L., Hotta H. (2009) Efficient production of infectious hepatitis C virus with adaptive mutations in cultured hepatoma cells. *J Gen Virol* 90: 1681–91.
21. Inubushi S., Nagano-Fujii M., Kitayama K., Tanaka M., An C., Yokozaki H., Yamamura H., Nuriya H., Kohara M., Sada K., Hotta H. (2008) Hepatitis C virus NS5A protein interacts with and negatively regulates the non-receptor protein tyrosine kinase Syk. *J Gen Virol* 89: 1231–42.
22. Lindenbach B.D., Evans M.J., Syder A.J., Wolk B., Tellinghuisen T.L., Liu C.C., Maruyama T., Hynes R.O., Burton D.R., McKeating J.A., Rice C.M. (2005) Complete replication of hepatitis C virus in cell culture. *Science* 309: 623–6.
23. Shuda U., Hatani T., Nakashima K., Ogi K., Sada K. (2009) Tyrosine phosphorylation of 3BP2 regulates B cell receptor-mediated activation of NFAT. *J Biol Chem* 284: 33719–28.
24. Sada K., Miah S.M., Maeno K., Kyo S., Qu X., Yamamura H. (2002) Regulation of Fc epsilon RI-mediated degranulation by an adaptor protein 3BP2 in rat basophilic leukemia RBL-2H3 cells. *Blood* 100: 2138–44.
25. Qu X., Sada K., Kyo S., Maeno K., Miah S.M., Yamamura H. (2004) Negative regulation of Fc epsilon RI-mediated mast cell activation by a ubiquitin-protein ligase Cbl-b. *Blood* 103: 1779–86.
26. Mankouri J., Tedbury P.R., Gretton S., Hughes M.E., Griffin S.D., Dallas M.L., Green K.A., Hardie D.G., Peers C., Harris M. (2010) Enhanced hepatitis C virus genome replication and lipid accumulation mediated by inhibition of AMP-activated protein kinase. *Proc Natl Acad Sci U S A* 107: 11549–54.
27. Thomas C.B., Meade J.C., Holmes E.W. (1981) Aminoinimidazole carboxamide ribonucleoside toxicity: a model for study of pyrimidine starvation. *J Cell Physiol* 107: 335–44.
28. Sabina R.L., Holmes E.W., Becker M.A. (1984) The enzymatic synthesis of 5-amino-4-imidazolecarboxamide riboside triphosphate (ZTP). *Science* 233: 1193–5.
29. Owen M.R., Doran E., Halestrap A.P. (2000) Evidence that metformin exerts its anti-diabetic effects through inhibition of complex I of the mitochondrial respiratory chain. *Biochem J* 348(Pt 3): 607–14.
30. El-Mir M.Y., Nogueira V., Fontaine E., Averet N., Rigoulet M., Leverve X. (2000) Dimethylbiguanide inhibits cell respiration via an indirect effect targeted on the respiratory chain complex I. *J Biol Chem* 275: 223–8.
31. Foretz M., Hebrard S., Leclerc J., Zarrinpasheh E., Soty M., Mithieux G., Sakamoto K., Andreelli F., Viollet B. (2010) Metformin inhibits hepatic gluconeogenesis in mice independently of the LKB1/AMPK pathway via a decrease in hepatic energy state. *Clin Invest* 120: 2355–69.
32. Kawaguchi T., Yoshida T., Harada M., Hisamoto T., Nagao Y., Ide T., Taniguchi E., Kumemura H., Hanada S., Maeyama M., Baba S., Koga H., Kumashiro R., Ueno T., Ogata H., Yoshimura A., Sada M. (2004) Hepatitis C virus down-regulates insulin receptor substrates 1 and 2 through up-regulation of suppressor of cytokine signaling 3. *Am J Pathol* 165: 1499–508.
33. Kawaguchi T., Ide T., Taniguchi E., Hirano E., Itou M., Sumie S., Nagao Y., Yanagimoto C., Hanada S., Koga H., Sada M. (2007) Clearance of HCV improves insulin resistance, beta-cell function, and hepatic expression of insulin receptor substrate 1 and 2. *Am J Gastroenterol* 102: 570–6.
34. Yamada T., Kamon J., Minokoshi Y., Ito Y., Waki H., Uchida S., Yamashita S., Noda M., Kita S., Ueki K., Eto K., Akanuma Y., Froguel P., Foufelle F., Ferre P., Carling D., Kimura S., Nagai R., Kahn B.B., Kadokawa T. (2002) Adiponectin stimulates glucose utilization and fatty-acid oxidation by activating AMP-activated protein kinase. *Nat Med* 8: 1288–95.
35. Saha A.K., Avilucea P.R., Ye J.M., Assifi M.M., Kraegen E.W., Ruderman N.B. (2004) Pioglitazone treatment activates AMP-activated protein kinase in rat liver and adipose tissue *in vivo*. *Biochem Biophys Res Commun* 314: 580–5.
36. Zhou G., Myers R., Li Y., Chen Y., Shen X., Fenyo-Melody J., Wu M., Venre J., Doeberer T., Fujii N., Musi N., Hirshman M.F., Goodyear L.J., Moller D.E. (2001) Role of AMP-activated protein kinase in mechanism of metformin action. *J Clin Invest* 108: 1167–74.
37. Miyanari Y., Atsuzawa K., Usuda N., Watanuki K., Hishiki T., Zayas M., Bartenschlager R., Wakita T., Hijikata M., Shimotohno K. (2007) The lipid droplet is an important organelle for hepatitis C virus production. *Nature Cell Biology* 9: 1089–97.
38. Leu G.Z., Lin T.Y., Hsu J.T. (2004) Anti-HCV activities of selective polyunsaturated fatty acids. *Biochem Biophys Res Commun* 318: 275–80.
39. Kapadia S.B., Chisari F.V. (2005) Hepatitis C virus RNA replication is regulated by host geranylgeranylation and fatty acids. *Proc Natl Acad Sci U S A* 102: 2561–6.
40. Ye J., Wang C., Sumpter R. Jr., Brown M.S., Goldstein J.L., Gale M. Jr. (2003) Disruption of hepatitis C virus RNA replication through inhibition of host protein geranylgeranylation. *Proc Natl Acad Sci U S A* 100: 15865–70.
41. Pietschmann T., Lohmann V., Rutter G., Kurpanek K., Bartenschlager R. (2001) Characterization of cell lines carrying self-replicating hepatitis C virus RNAs. *J Virol* 75: 1252–64.
42. Zhu Q., Guo J.T., Seeger C. (2003) Replication of hepatitis C virus subgenomes in nonhepatic epithelial and mouse hepatoma cells. *J Virol* 77: 9204–10.
43. Donadon V., Balbi M., Mas M.D., Casarin P., Zanette G. (2010) Metformin and reduced risk of hepatocellular carcinoma in diabetic patients with chronic liver disease. *Liver Int* 30: 750–8.
44. Romero-Gomez M., Diago M., Andrade R.J., Calleja J.L., Salmeron J., Fernandez-Rodriguez C.M., Sola R., Garcia-Samaniego J., Herreras J.M., De la Mata M., Moreno-Otero R., Nunez O., Oliveira A., Duran S., Planas R. (2009) Treatment of insulin resistance with metformin in naïve genotype 1 chronic hepatitis C patients receiving peginterferon alfa-2a plus ribavirin. *Hepatology* 50: 1702–8.

SUPPORTING INFORMATION

Additional supporting information may be found in the online version of this article:

Fig. S1. Exogenous lipid has no effect on AICAR-mediated suppression of HCV. Huh-7.5 cells were infected with HCV at a MOI of 3.0 for 4 hr. The cells were

treated with 1 mM AICAR for 20 hr with or without supplementation with 100 μ M mevalonolactone (Sigma) and 100 μ M oleic acid (Sigma) (Lipid). Cell lysates were separated by SDS-PAGE and analyzed by immunoblotting as shown in Figure 1b. Molecular size markers are indicated at the left in kilodaltons. The results are representative of three independent experiments.

Fig. S2. Cell confluence activates AMPK and suppresses HCV replication. 10^5 (sub-confluent) or 4×10^5 Huh-7.5 cells (confluent) were seeded in 24-well plates overnight. 4×10^5 Huh-7.5 cells resulted in a 100% confluent monolayer of cells in the culture plates. The cells

were infected with HCV at a MOI of 3.0 for 4 hr and incubated for 20 hr. Cell lysates were separated by SDS-PAGE and analyzed by immunoblotting as shown in Figure 1b. Molecular size markers are indicated at the left in kilodaltons. The results are representative of three independent experiments.

Please note: Wiley-Blackwell are not responsible for the content or functionality of any supporting materials supplied by the authors. Any queries (other than missing material) should be directed to the corresponding author for the article.



Mechanism of action of ribavirin in a novel hepatitis C virus replication cell system

Kyoko Mori^a, Masanori Ikeda^a, Yasuo Ariumi^a, Hiromichi Dansako^a, Takaji Wakita^b, Nobuyuki Kato^{a,*}

^a Department of Tumor Virology, Okayama University Graduate School of Medicine, Dentistry, and Pharmaceutical Sciences, 2-5-1 Shikata-cho, Okayama 700-8558, Japan

^b Department of Virology II, National Institute of Infectious Diseases, 1-23-1 Toyama, Shinjuku-ku, Tokyo 162-8640, Japan

ARTICLE INFO

Article history:

Received 16 November 2010

Received in revised form 4 February 2011

Accepted 4 February 2011

Available online 12 February 2011

Keywords:

HCV

HCV RNA replication system

RBV

IMPDH inhibitor

ABSTRACT

Ribavirin (RBV) is a potential partner of interferon (IFN)-based therapy for patients with chronic hepatitis C. However, to date, its anti-hepatitis C virus (HCV) mechanism remains ambiguous due to the marginal activity of RBV on HCV RNA replication in HuH-7-derived cells, which are currently used as the only cell culture system for robust HCV replication. We investigated the anti-HCV activity of RBV using novel cell assay systems. The recently discovered human hepatoma cell line, Li23, which enables robust HCV replication, and the recently developed Li23-derived drug assay systems (ORL8 and ORL11), in which the genome-length HCV RNA (O strain of genotype 1b) encoding renilla luciferase efficiently replicates, were used for this study. At clinically achievable concentrations, RBV unexpectedly inhibited HCV RNA replication in ORL8 and ORL11 systems, but not in ORG (an HuH-7-derived assay system). The anti-HCV activity of RBV was almost cancelled by an inhibitor of equilibrative nucleoside transporters. The evaluation of the anti-HCV mechanisms of RBV proposed to date using ORL8 ruled out the possibility that RBV induces error catastrophe, the IFN-signaling pathway or oxidative stress. However, we found that the anti-HCV activity of RBV was efficiently cancelled with guanosine, and demonstrated that HCV RNA replication was notably suppressed in inosine monophosphate dehydrogenase (IMPDH)-knockdown cells, suggesting that the antiviral activity of RBV is mediated through the inhibition of IMPDH. In conclusion, we demonstrated for the first time that inhibition of IMPDH is a major antiviral target by which RBV at clinically achievable concentrations inhibits HCV RNA replication.

© 2011 Elsevier B.V. All rights reserved.

1. Introduction

Hepatitis C virus (HCV) infection causes chronic hepatitis, which often leads to liver cirrhosis and hepatocellular carcinoma (Thomas, 2000). Since approximately 170 million people are infected with HCV worldwide, HCV infection is a serious global health problem (Thomas, 2000). HCV is an enveloped positive single-stranded RNA virus of the *Flaviviridae* family. The HCV genome encodes a large

polyprotein precursor of approximately 3000 amino acids, which is cleaved into in the following order: Core, envelope 1 (E1), E2, p7, non-structural protein 2 (NS2), NS3, NS4A, NS4B, NS5A, and NS5B (Kato et al., 1990).

The current standard therapy for patients with chronic hepatitis C is a combination of pegylated-interferon (PEG-IFN) and ribavirin (RBV). This treatment currently achieves a sustained virological response (SVR) greater than 50% (Chevaliez et al., 2007). However, the mechanism of RBV activity in patients with chronic hepatitis C is still ambiguous. To date, five distinct mechanisms have been proposed: (a) RBV acts as an RNA mutagen that causes mutations of the HCV RNA genome and induces a so-called "error catastrophe" (Feld and Hoofnagle, 2005); (b) RBV enhances the IFN-signaling pathway (Feld et al., 2010; Thomas et al., 2011); (c) RBV induces GTP depression by inhibiting inosine monophosphate dehydrogenase (IMPDH) (Zhou et al., 2003); (d) RBV directly inhibits NS5B-encoded RNA-dependent RNA polymerase (Feld and Hoofnagle, 2005); (e) RBV enhances host T-cell mediated immunity by switching the T-cell phenotype from type 2 to type 1 (Lau et al., 2002). Unfortunately, no groups have clarified the anti-HCV mechanism of RBV at clinically achievable concentrations (5–14 μM) (Feld et al., 2010; Pawlotsky et al., 2004; Tanabe et al.,

Abbreviations: HCV, hepatitis C virus; E1, envelope 1; NS2, nonstructural protein 2; PEG, polyethylene glycol; IFN, interferon; RBV, ribavirin; SVR, sustained virological response; IMPDH, inosine monophosphate dehydrogenase; RL, renilla luciferase; EC₅₀, 50% effective concentration; VE, vitamin E; NBMPR, S-(4-nitrobenzyl)-6-thiouridine; MPA, mycophenolic acid; CSA, cyclosporine A; STAT1, signal transducer and activator of transcription 1; ENT, equilibrative nucleoside transporter; RT-PCR, reverse-transcription polymerase chain reaction; ISG, IFN-stimulated gene; IRF7, IFN regulatory factor 7; IP-10, IFN-gamma-inducible protein-10; GAPDH, glyceraldehyde-3-phosphate dehydrogenase; 5'-UTR, 5'-untranslated region; Neo^R, neomycin-resistance gene; CNT, concentrative nucleoside transporter; EC₅₀, 90% effective concentration; CFE, colony-forming efficiency; MMPD, merimepodib.

* Corresponding author. Tel.: +81 86 235 7385; fax: +81 86 235 7392.

E-mail address: nkato@md.okayama-u.ac.jp (N. Kato).

2004). Although most of the above mechanisms were proposed based on studies using HuH-7 (human hepatoma cell line)-derived cells, which are currently used as the only cell culture system for robust HCV replication, the effective concentrations (50–1000 μM) of RBV were much higher than the clinically achievable concentrations (Feld and Hoofnagle, 2005; Feld et al., 2010; Lau et al., 2002; Pawlotsky et al., 2004; Thomas et al., 2011; Zhou et al., 2003). Indeed, our HuH-7-derived cell assay system (ORG) (Ikeda et al., 2005; Naka et al., 2005), in which genome-length HCV RNA (O strain of genotype 1b) encoding renilla luciferase (RL) efficiently replicates, also showed that the 50% effective concentration (EC₅₀) of RBV was approximately 100 μM (Naka et al., 2005).

Recently, we found a new human hepatoma cell line, Li23, that enables robust HCV RNA replication (Kato et al., 2009). We showed by microarray analysis that Li23 cells possessed expression profiles rather different from those in HuH-7 cells (Kato et al., 2009), and that the expression profile of Li23 cells was distinct from those of frequently used other hepatoma cell lines (Mori et al., 2010). We further developed Li23-derived cell culture assay systems (ORL8 and ORL11) in which genome-length HCV RNA (O strain of genotype 1b) encoding RL efficiently replicates (Kato et al., 2009). Here, we unexpectedly observed through the use of these cell culture assay systems the first evidence of anti-HCV activity of RBV at clinically achievable concentrations, and obtained the convincing data that the anti-HCV mechanism of RBV is mediated through the inhibition of IMPDH.

2. Materials and methods

2.1. Cell cultures

HuH-7-derived cells harboring an HCV replicon or genome-length HCV RNA were maintained with medium containing G418 (0.3 mg/ml) as described previously (Ikeda et al., 2005). Li23-derived polyclonal sORL8 and sORL11 cells harboring an HCV replicon were established by the transfection of ORN/C-5B/QR, KE, SR RNA (Kato et al., 2009) into the cured ORL8 and ORL11 cells, respectively. Li23-derived cells harboring an HCV replicon or genome-length HCV RNA were maintained as described previously (Kato et al., 2009). Cured cells, from which the HCV RNA had been eliminated by IFN treatment, were also maintained as described previously (Kato et al., 2009).

2.2. RL assay

RL assay was performed as described previously (Ikeda et al., 2005; Kato et al., 2009). The experiments were performed at least in triplicate.

2.3. Reagents

RBV was kindly provided by Yamasa (Chiba, Japan). Human IFN-α, vitamin E (VE), phloridzin dihydrate, S-(4-nitrobenzyl)-6-thiouridine (NBMPR), and mycophenolic acid (MPA) were purchased from Sigma-Aldrich (St. Louis, MO). Cyclosporine A (CsA) was purchased from Calbiochem (San Diego, CA). Guanosine and adenosine were purchased from Wako Pure Chemical Industries, Ltd. (Osaka, Japan).

2.4. Cell viability

Cell viability was examined by the method described previously (Kato et al., 2009). The experiments were performed in triplicate.

2.5. Western blot analysis

The preparation of cell lysates, sodium dodecyl sulfate-polyacrylamide gel electrophoresis and immunoblotting analysis with a PVDF membrane were performed as previously described (Kato et al., 2003). The antibodies used in this study were those against Core (CP11; Institute of Immunology, Tokyo, Japan), NS5B (a generous gift from Dr. M. Kohara, Tokyo Metropolitan Institute of Medical Science), signal transduction and activator of transcription 1 (STAT1) and phospho-STAT1 (Tyr701) (BD Transduction Laboratories, Lexington, KY) and equilibrative nucleoside transporter 1 (ENT1) (Abgent, San Diego, CA). β-actin antibody (Sigma-Aldrich) was used as the control for the amount of protein loaded per lane. Immunocomplexes were detected by using a Renaissance enhanced chemiluminescence assay (Perkin Elmer Life Sciences, Boston, MA).

2.6. Reverse transcription-polymerase chain reaction (RT-PCR)

Total RNA from the cultured cells was extracted with an RNeasy Mini Kit (Qiagen, Valencia, CA). RT-PCR was performed by a method described previously (Dansako et al., 2003) using the following primer pairs: IFN-stimulated gene (ISG) 15 (346 bp), 5'-GCCTTCAGCAGCGCTGGC-3' and 5'-CCAGCGCAGCATGAAACACGG-3'; IFN regulatory factor 7 (IRF7) (221 bp), 5'-AGCTGGCTACACGGAGAACACAG-3' and 5'-CCACAGCTTGGAGAACAGAC-3'; IFN-gamma-inducible protein-10 (IP-10) (111 bp), 5'-GGCCATCAAGAAATTACTGAAGCCA-3' and 5'-TCTGTGTGTCATCTTGGAA-3'; ENT1 (382 bp), 5'-GAGTTCACTCTCCAACCTCTCAG-3' and 5'-GCATCGTCTCGAAGACACAGCAG-3'; ENT2 (306 bp), 5'-CTTGTTGTCCTTCACAGTCAC-3' and 5'-GGTGTGATGAACTAGGCATCTCTG-3'; ENT3 (350 bp), 5'-GTCTCTTCATCACCAGCCTCATC-3' and 5'-GTGCTGAGGTAGCCGTGCTCAG-3'; glyceraldehyde-3-phosphate dehydrogenase (GAPDH) (334 bp), 5'-GACTCATGACCACAGTCATGC-3' and 5'-GAGGACACACCCTGGTCTCAG-3'.

2.7. Infection of cells with secreted HCV

The inoculum was prepared from HCV-JFH1 (Wakita et al., 2005)-infected HuH-7-derived RSc cells (Ariumi et al., 2007; Kato et al., 2009) at 5 days postinfection and then stored at -80 °C after filtering through a 0.20-μm filter (Kurabo, Osaka, Japan) until use. ORL8c or RSc cells (each 5 × 10⁴) were cultured for 24 h before infection. The cells were infected with 50 μl (equivalent to a multiplicity of infection of 0.05–0.1) of inoculum and maintained for several days until RBV treatment.

2.8. Quasispecies analysis of HCV RNA

ORL8 cells were treated with or without RBV (50 μM) for 72 h. Total RNA from the cultured cells was extracted with an RNeasy Mini Kit (Qiagen). To amplify genome-length HCV RNA, RT-PCR was performed separately in two fragments using KOD-plus DNA polymerase (Toyobo) as described previously (Ikeda et al., 2005; Kato et al., 2003). The two PCR products (the 6.0 kb region covering 5'-untranslated region (5'-UTR) to NS3 and the 6.1 kb region covering NS2 to NS5B) were subcloned into the *Xba*I site of pBR322MC, and sequence analysis of the region encoding RL to the neomycin-resistance gene (Neo^R) (1953 nts), NS5A (1341 nts), or NS5B (1773 nts) was performed as described previously (Ikeda et al., 2005). Synonymous and nonsynonymous substitutions at variance with the parental ORN/C-5B/QR, KE, SR sequences (Kato et al., 2009) were determined. To examine the error frequency of KOD-plus DNA polymerase in the PCR amplification, PCR using the plasmid containing ORN/C-5B/QR, KE, SR sequences was performed separately in the

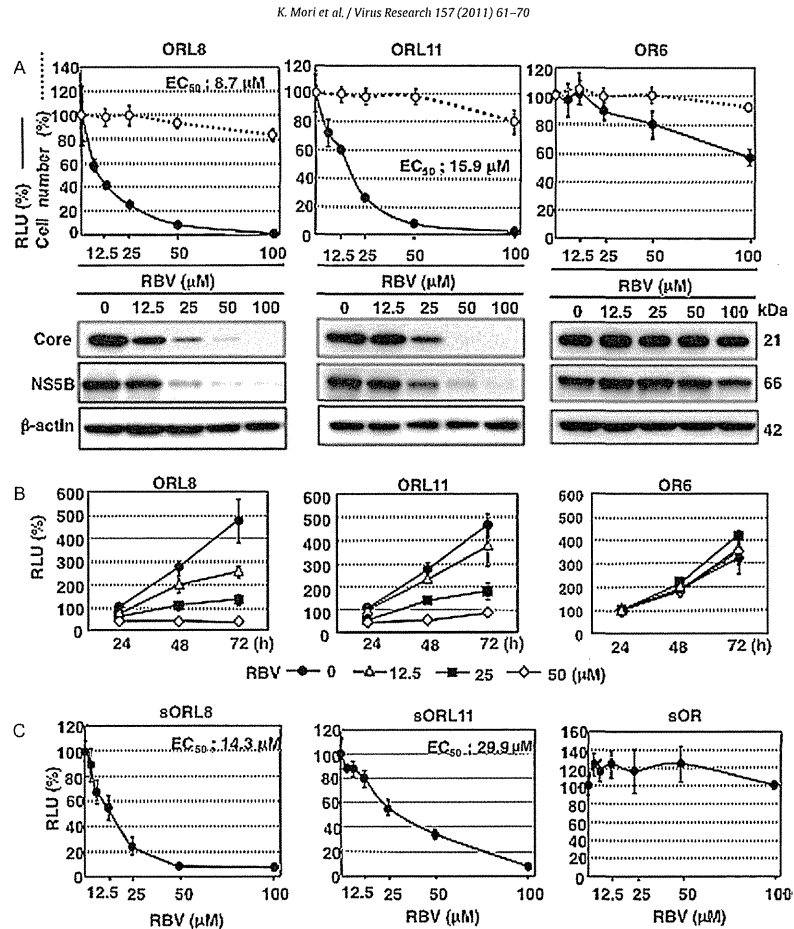


Fig. 1. Anti-HCV activity of RBV detected in the ORL8 and ORL11 system. (A) RBV sensitivities on genome-length HCV RNA replication in ORL8, ORL11, and OR6. The ORL8, ORL11 and OR6 cells were treated with RBV for 72 h, and then an RL assay (bold line in the upper panel) was performed. The relative luciferase activity (RLU) (%) calculated at each point, when the level of luciferase activity in non-treated cells was assigned to be 100% is presented here. The cell number (dotted line in the upper panel) at each concentration was determined as described in Section 2. Western blot analysis of RBV-treated ORL8, ORL11, and OR6 cells for HCV proteins, Core and NS5B, was also performed (lower panel). (B) Time-dependent anti-HCV activity of RBV. The ORL8, ORL11, and OR6 cells were treated with RBV, and an RL assay was performed at 24, 48, and 72 h after the treatment. The RLU (%) calculated at each time point, when the luciferase activity of non-treated cells at 24 h was assigned to be 100% is shown. (C) Anti-HCV activity of RBV was observed in Li23-derived replicon assay systems (sORL8 and sORL11), but not in HuH-7-derived replicon assay system (sOR). RBV treatment and RL assay were performed as described for panel A.

two parts (6.0 kb covering 5'-UTR to NS3 and 6.1 kb covering NS3 to NS5B) and the two PCR products were subcloned for the sequence analysis as described above.

2.9. RNA interference and quantitative RT-PCR

SiRNA duplexes targeting the coding regions of human IMPDH1 (Dharmacon; catalog no. M-009687-01) and IMPDH2 (Dharmacon; catalog no. M-004330-02) were chemically synthesized. SiRNA duplex non-targeting (Dharmacon; catalog no. D-001206-13) was

also used as a control. ORL8 cells were transfected with the indicated siRNA duplexes using Oligofectamine (Invitrogen) (Dansako et al., 2007). Extraction of total RNA and quantitative RT-PCR analysis for HCV RNA were performed by real-time LightCycler PCR as described previously (Ikeda et al., 2005).

2.10. Statistical analysis

Statistical comparison of the luciferase activities between the treatment groups and controls was performed using the Student's

t-test. *P* values of less than 0.05 were considered statistically significant.

3. Results

3.1. Anti-HCV activity of RBV was clearly observed in the Li23-derived assay systems, but not in the HuH-7-derived assay system

Recently we demonstrated that Li23-derived assay systems (ORL8 and ORL11), in which genome-length HCV RNA (O strain of genotype 1b) encoding RL robustly replicates, were frequently more sensitive to anti-HCV reagents such as IFNs and statins than the corresponding HuH-7-derived assay system (OR6) (Kato et al., 2009). Since we had observed a marginal anti-HCV activity of RBV in OR6 system, we assumed that the anti-HCV activity of RBV might also be illuminated by ORL8 or ORL11 system. Indeed, marked differences were observed between OR6 and both of the other assay systems: RBV at clinically achievable concentrations effectively inhibited HCV RNA replication in both ORL8 and ORL11, but not in OR6 (Fig. 1A). The EC₅₀ values of RBV in ORL8, ORL11, and OR6 were 8.7, 15.9, and >100 μM, respectively, without suppression of cell growth (upper panels in Fig. 1A). These pronounced differences in the anti-HCV activity of RBV were confirmed by Western blot analysis (lower panels in Fig. 1A). In addition, time course assays revealed that the anti-HCV activity of RBV was dose- and time-dependent in ORL8 and ORL11, but not in OR6 (Fig. 1B). We next examined the activity of RBV using monoclonal cell-based assay systems (sORL8, sORL11, and sOR) (Ikeda et al., 2005) harboring HCV replicon RNA. The results revealed that the EC₅₀ values of RBV in sORL8 and sORL11 were 14.3 and 29.9 μM, respectively, whereas RBV showed no anti-HCV activity in sOR (Fig. 1C), suggesting that the anti-HCV activity of RBV was not either a clone-specific or genome-length HCV RNA-specific phenomenon. Moreover, we demonstrated by Western blot (upper panel of Fig. 2) and quantitative RT-PCR (lower panel of Fig. 2) analyses that RBV suppressed HCV RNA replication in HCV-JFH1-infected ORL8c cells, but not in HCV-JFH1-infected RSc cells, which HCV could infect and efficiently replicate within (Arimi et al., 2007; Kato et al., 2009). These results also indicate that only the Li23-derived assay system can illuminate the anti-HCV activity of RBV.

3.2. An ENT inhibitor cancelled anti-HCV activity of RBV

As one possible explanation for the pronounced differences in RBV activity between the Li23- and HuH-7-derived assay systems, we considered that the efficiencies in the cellular uptake of RBV might have differed between the two types of cells. To date, two families of nucleoside transporter proteins have been identified: the ENT family (ENT1, ENT2, and ENT3) and the concentrative nucleotide transporter (CNT) family (CNT1, CNT2, and CNT3) (Pastor-Anglada et al., 2005). Two recent reports showed that ENT1 and CNT3 might be responsible for RBV uptake in HuH-7 cells (Ibarra and Pfeiffer, 2009), and that ENT1, but not ENT2 or CNTs, is a major RBV uptake transporter in human hepatocytes (Fukuchi et al., 2010). To test these points, we first examined the effects of an ENT inhibitor, NBMPR, and a CNT inhibitor, phloridzin dihydrate, on the anti-HCV activity of RBV (50 μM; 90% effective concentration [EC₉₀]) in ORL8 system. The results revealed that 5 μM NBMPR partially attenuated the anti-HCV activity of RBV in ORL8 (Fig. 3A). The marginal activity of RBV was also not changed in OR6 system treated with these transporter inhibitors (data not shown). A significant dose-dependency of the cancellation by NBMPR was also observed in ORL8 (Fig. 3B). Since we observed a lack of expression of CNT family members in ORL8 cells (data not shown), these

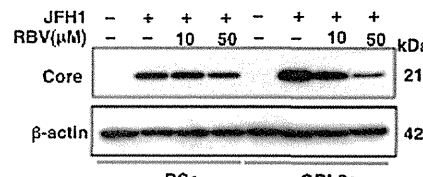


Fig. 2. RBV inhibited HCV production in JFH1-infected ORL8c cells, but not in JFH1-infected RSc cells. JFH1-infected ORL8c and RSc cells were treated with RBV for 72 h, and subjected to Western blot analysis using anti-Core or β-actin antibody (upper panel), and to quantitative RT-PCR analysis (lower panel). Asterisks indicate significant differences compared to the control treatment. ***P*<0.01; NS: not significant.

results suggest that cellular uptake of RBV is mediated by ENT member(s). Accordingly, we next examined the levels of ENT mRNAs in ORL8 and OR6 cells. However, the expression levels of ENT1, ENT2, and ENT3 mRNAs were comparable between ORL8 and OR6 cells (Fig. 3C). In addition, sequence analysis of ENT1, ENT2, and ENT3 mRNAs (data not shown) and Western blot analysis of ENT1 protein (Fig. 3D) revealed no differences between the two cell lines. These results suggest that the expression levels of ENT members are not associated with the differences in RBV activity.

3.3. RBV did not act as a mutagen in HCV RNA replication

Since the suppressive effect of RBV on HCV RNA replication was clearly observed in ORL8 system, we expected that ORL8 cells would be suitable for analysis of the anti-HCV mechanism of RBV. In regard to the anti-HCV mechanism of RBV, several groups have proposed that RBV (50–400 μM) acts as an RNA mutagen and induces error catastrophe in HCV RNA replication (Contreras et al., 2002; Zhou et al., 2003). Therefore, we first examined whether or not error catastrophe theory is involved in the anti-HCV activity of RBV observed in ORL8 system. To test the mutagenic effect of RBV, ORL8 cells were treated with or without RBV (50 μM; EC₉₀ level in ORL8 system) for 72 h, and then genome-length HCV RNA from the ORL8 cells was amplified by RT-PCR. We performed HCV quasispecies analysis by sequencing of RL to the Neo^R, NS5A, and NS5B regions using at least 10 independent clones for each region. To estimate the mutation rate, the total number of mutations and the ratio of nonsynonymous to synonymous mutations in each region were determined by comparison with the parental HCV sequences (Kato et al., 2009). The results revealed that the overall mutation rate and the ratio of nonsynonymous to synonymous mutations in each

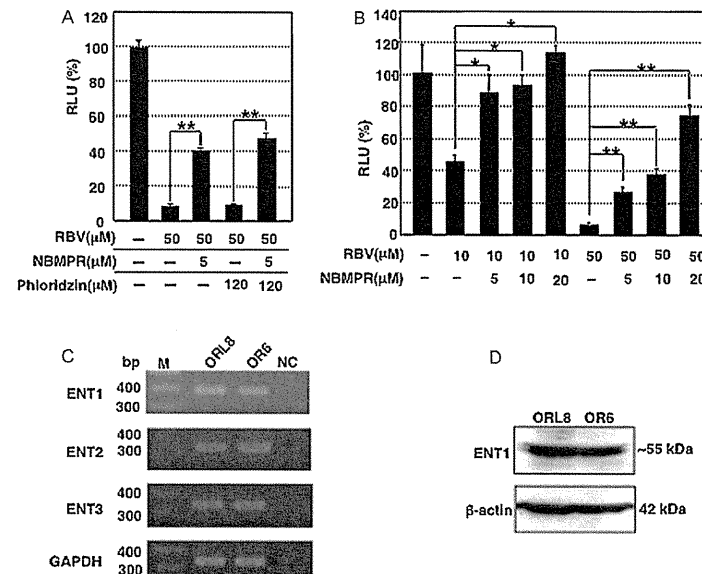


Fig. 3. An ENT inhibitor abolished anti-HCV activity of RBV. (A) An ENT inhibitor, NBMPR, canceled the anti-HCV activity of RBV in ORL8. ORL8 cells were pretreated with NBMPR and/or phloridzin dihydrate for 30 min, and then treated with RBV for 72 h, after which an RL assay was performed. Asterisks indicate significant differences compared to the control treatment. **P<0.01. (B) Dose-dependent cancellation by NBMPR of the activity of RBV. ORL8 cells were pretreated with NBMPR for 30 min, and then treated with RBV for 72 h, after which an RL assay was performed. Asterisks indicate significant differences compared to the control treatment. *P<0.05. **P<0.01. (C) RT-PCR analysis of ENTs. Total RNAs prepared from ORL8 and OR6 cells were subjected to RT-PCR using the primer sets for ENT1, ENT2, ENT3, and GAPDH as described in Section 2. RT-PCR products were detected by staining with ethidium bromide after 3% agarose gel electrophoresis. (D) Western blot analysis of ORL8 and OR6 cells for ENT1. The primary antibody used was ENT1. β-actin was used as a control for the amount of protein loaded per lane.

region were not increased irrespective of the presence or absence of RBV treatment (Table 1). To confirm that mutation frequencies given in Table 1 are overwhelmingly above the error level associated with the PCR, we sequenced independent five clones (6.0 kb covering 5'-UTR to NS3 and 6.1 kb covering NS3 to NS5B) obtained by PCR using KOD-plus DNA polymerase and a plasmid containing the parental HCV sequences (Kato et al., 2009) as a template. No mutations were detected in these sequenced clones, indicating that KOD-plus DNA polymerase possesses extremely high fidelity, and suggesting that the mutations obtained in the present study are not produced by the errors associated with the PCR. Therefore, these results indicate that RBV does not act as a mutagen in HCV RNA replication in ORL8 cells, and suggest that the anti-HCV activity of RBV (EC₅₀: 8.7 μM) observed in ORL8 system is not due to the induction of error catastrophe in the HCV RNA genome.

3.4. RBV did not activate the IFN-signaling pathway

Regarding HCV, Liu et al. (Liu et al., 2007) have reported that RBV (40–500 μM) enhances the IFN-signaling pathway in *in vitro* cell culture systems. Furthermore, a recent report showed that RBV improved early responses to PEG-IFN through enhanced IFN signaling in the treatment of patients with chronic hepatitis (Feld et al., 2010). In that study, it was shown that the RBV concentration in patients at day 3 was correlated with IP-10 induction at 12 h, but only in patients with an adequate first phase viral decline (Feld et al., 2010). Therefore, we expected that RBV would enhance the IFN-signaling pathway in our new cell culture system. Accordingly, we first examined the effect of RBV in combination with IFN-α on HCV RNA replication using ORL8 system. OR6 system was also used for purpose of comparison. The results showed that RBV had an additive effect in decreasing HCV RNA replica-

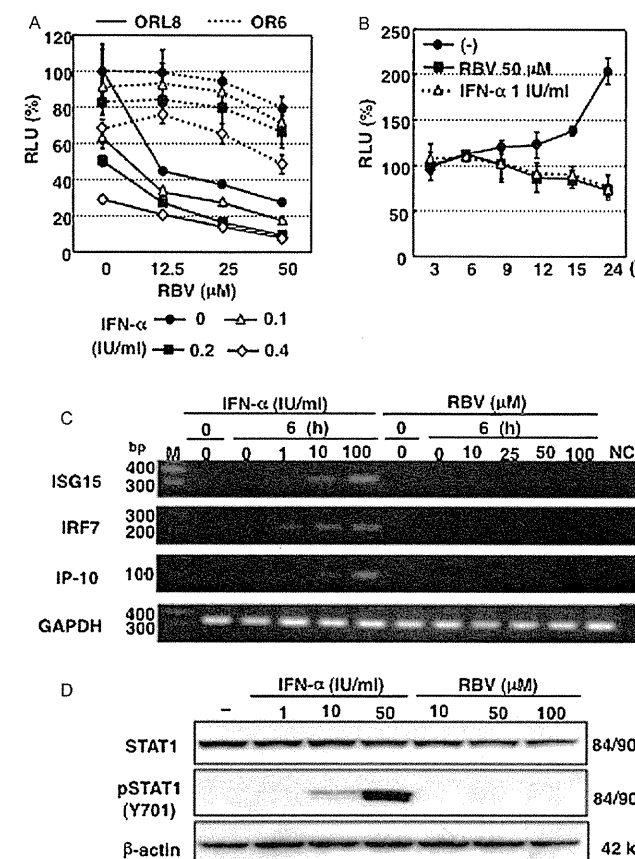


Fig. 4. RBV did not activate the IFN-signaling pathway in ORL8 cells. (A) Additive effect of RBV in combination with IFN-α. ORL8 and OR6 cells were treated with a combination of IFN-α and RBV for 72 h, after which the RL assay was performed. (B) Time course assay of the anti-HCV activity of RBV or IFN-α. ORL8 cells were treated with RBV or IFN-α, and an RL assay was performed at 3, 6, 9, 12, 15, and 24 h after treatment. Presented here is the RLU (%) calculated at each point, when the RL activity of non-treated cells at 3 h was assigned to be 100%. (C) ISGs were not induced by RBV treatment. ORL8 cells were treated with IFN-α or RBV for 6 h, and then the total RNAs extracted from the cells were subjected to RT-PCR using the primer sets for ISG15, IRF7, IP-10, and GAPDH as described in Section 2. RT-PCR products were detected by staining with ethidium bromide after 3% agarose gel electrophoresis. (D) Phosphorylation of STAT1 was not induced by RBV treatment. ORL8 cells were treated with IFN-α or RBV for 30 min, and subjected to Western blot analysis using anti-STAT1, anti-phospho-STAT1(Y701), and anti-β-actin antibodies.

tion in both assay systems, but its activity was greater in ORL8 than in OR6 (Fig. 4A). A comparative time course assay using RBV or IFN-α demonstrated that RBV- and IFN-α-treated ORL8 cells had the same anti-HCV kinetics, leading to decreased RL activity at 9 h after treatment (Fig. 4B). These results suggest that RBV induces some anti-HCV signaling pathway, such as an IFN-signaling pathway, rather than inducing IFN or directly inhibiting RNA replication.

We next examined the ability of RBV to activate ISGs. RT-PCR analysis revealed that RBV treatment (6 h) did not cause an induction of representative ISGs, ISG15, IRF7, and IP-10, in ORL8 cells, although phosphorylation of STAT1 was observed even after the treatment with 1 IU/ml of IFN-α (Fig. 4D). Together, these results indicate that RBV does not activate the IFN-signaling pathway.

Table 1
Mutation frequencies in RL-Neo^R, NS5A, and NS5B regions.

Region	Condition	Total no. of clones	Total no. of mutations	Nonsynonymous/synonymous substitutions (ratio)
RL-Neo ^R (1953 nts)	Control	12	59	39/20 (1.95)
	RBV (50 μM)	12	49	31/18 (1.72)
NS5A (1341 nts)	Control	10	35	24/11 (2.18)
	RBV (50 μM)	10	36	24/12 (2.00)
NS5B (1773 nts)	Control	10	10	3/7 (0.43)
	RBV (50 μM)	10	9	2/7 (0.29)

and IRF7) or 10 IU/ml (IP-10) of IFN-α could induce these ISGs (Fig. 4C). Similar results were also obtained in OR6 cells and Huh7.5 cells (data not shown). In addition, enhancement of these ISGs was also not observed in the ORL8 cells co-treated with IFN-α and RBV (data not shown). Furthermore, we examined the phosphorylation status of STAT1 after RBV treatment. The results revealed that RBV treatment (up to 100 μM for 30 min) did not induce the phosphorylation of STAT1 in ORL8 cells, although phosphorylation of STAT1 was observed even after the treatment with 1 IU/ml of IFN-α (Fig. 4D). Together, these results indicate that RBV does not activate the IFN-signaling pathway.

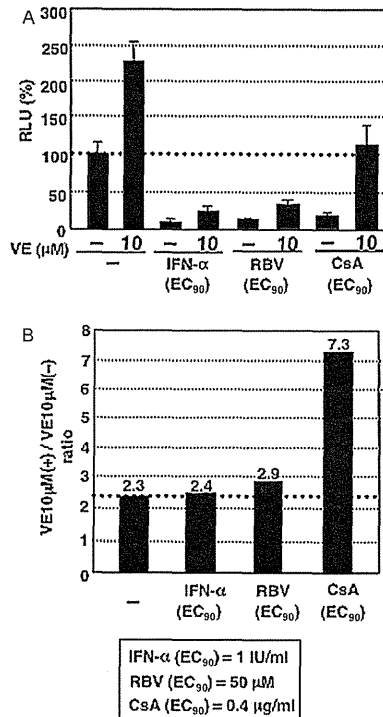


Fig. 5. The anti-HCV activity of RBV was not canceled by addition of VE. (A) Effects of VE on IFN- α , RBV, and CsA at the EC₉₀. ORL8 cells were treated with control medium (—), IFN- α , RBV, or CsA in the either the absence or presence of VE for 72 h, and then an RL assay was performed. (B) The ratio of RL activity in the presence of VE to the RL activity in the absence of VE. The above ratio was calculated from the data of panel A. The horizontal line indicates the promotive effect of VE alone on HCV RNA replication by RBV.

3.5. RBV did not induce the oxidative stress or subsequent anti-HCV status

Recently we reported that the antioxidant VE negated the antiviral activities of a broad range of anti-HCV reagents, including CsA, and demonstrated the involvement of the MEK-ERK1/2-signaling pathway in the anti-HCV status induced by oxidative stress (Yano et al., 2007, 2009). Therefore, we next expected that RBV induces oxidative stress. Accordingly, we examined the effect of VE on RBV, IFN- α , or CsA at the EC₉₀ level in ORL8 system. Although the anti-HCV activity of CsA was canceled to a significant level by VE, the inhibitory effects of RBV and IFN- α were hardly influenced by co-treatment with VE (Fig. 5A). We normalized these results by dividing the RL value obtained in the presence of VE by that in the absence of VE as described previously (Yano et al., 2007) (Fig. 5B). The value of RBV was almost the same as that of IFN- α or control, although the value of CsA was somewhat higher (7.3) which was consistent with previous findings (Yano et al., 2007). These results suggest that induction of oxidative stress is not associated with the activity of RBV detected in ORL8 system.

3.6. Guanosine dose-dependently attenuated the anti-HCV activity of RBV

Previously, using a qualitative colony-forming efficiency (CFE) assay of an HCV RNA replicon, Zhou et al. (2003) showed that RBV (50 μM) reduced the CFE by 2-fold in HuH-7 cells, although 10 μM RBV did not result in a significant change in CFE. In that study, when exogenous guanosine, but not adenosine, which would replenish GTP pools via the salvage pathway, was co-administered with RBV, the RBV-induced CFE reduction was partially cancelled (Zhou et al., 2003). From this result, the authors suggested that IMPDH inhibition and subsequent lowering of GTP pools contribute to the observed reduction in CFE. However, they failed to observe the any suppressive effects of the IMPDH inhibitors MPA and Merimepodib (MMPD)/VX-497 on HCV RNA replication (Zhou et al., 2003). Conversely, Henry et al. showed that MPA exerted anti-HCV activity on HCV RNA replication in HuH-7-derived cells (Henry et al., 2006). Therefore, in order to resolve these controversial results, we initially examined the anti-HCV activity of MPA in ORL8 and OR6 systems. The results revealed that MPA strongly inhibited HCV RNA replication in both systems without suppression of cell growth. The EC₅₀ values of MPA in the ORL8 and OR6 were 0.29 and 0.57 μM, respectively (Fig. 6A). Dose-dependent cancellation by guanosine, but not by adenosine, of the activity of MPA, was observed in both systems (Fig. 6B and data not shown for OR6 system). These results suggest that the depression of GTP induced by inhibition of IMPDH decreases the level of HCV RNA replication. From these results, we expected that anti-HCV activity of RBV observed in ORL8 might also have been associated with the inhibition of IMPDH. Indeed, significant dose-dependent cancellation by guanosine, but not by adenosine, of the anti-HCV activity of RBV (10 μM) was observed in ORL8 (Fig. 6C). ORL11 also showed a similar cancellation by guanosine (data not shown). The suppressive effect of guanosine on the activity of RBV in ORL8 was confirmed by Western blot analysis (Fig. 6D). These results suggest that the anti-HCV activity of RBV at clinically achievable concentrations in ORL8 is mediated through the inhibition of IMPDH by RBV.

3.7. IMPDH is required for HCV RNA replication

To confirm the involvement of IMPDH on HCV RNA replication, the endogenous expression of IMPDH was suppressed by siRNA specific to IMPDH. Since IMPDH has two isoforms, IMPDH1 and IMPDH2, which share 84% amino-acid homology (Wang et al., 2008), we prepared IMPDH1- and/or IMPDH2-knockdown ORL8 cells. The effective knockdown of IMPDH1 and/or IMPDH2 in ORL8 cells was confirmed by quantitative RT-PCR (Fig. 7A). We observed that the levels of HCV RNA replication in these knockdown cells were notably reduced compared with the control cells without suppression of cell growth (Fig. 7B). These results suggest that IMPDH is crucial for the maintenance of HCV RNA replication. Taken together, these results indicate that the inhibitory activity of RBV on HCV RNA replication in Li23-derived cells is mediated through the inhibition of IMPDH by RBV.

4. Discussion

In this study, using novel Li23-derived cell culture assay systems, we demonstrated for the first time that RBV at clinically achievable concentrations efficiently inhibited HCV RNA replication, and clarified that its anti-HCV activity was mediated by the inhibition of IMPDH.

To date, several mechanisms as described above have been proposed based on the results of studies using an HuH-7-derived cell culture system (Feld and Hoofnagle, 2005; Feld et al., 2010; Lau

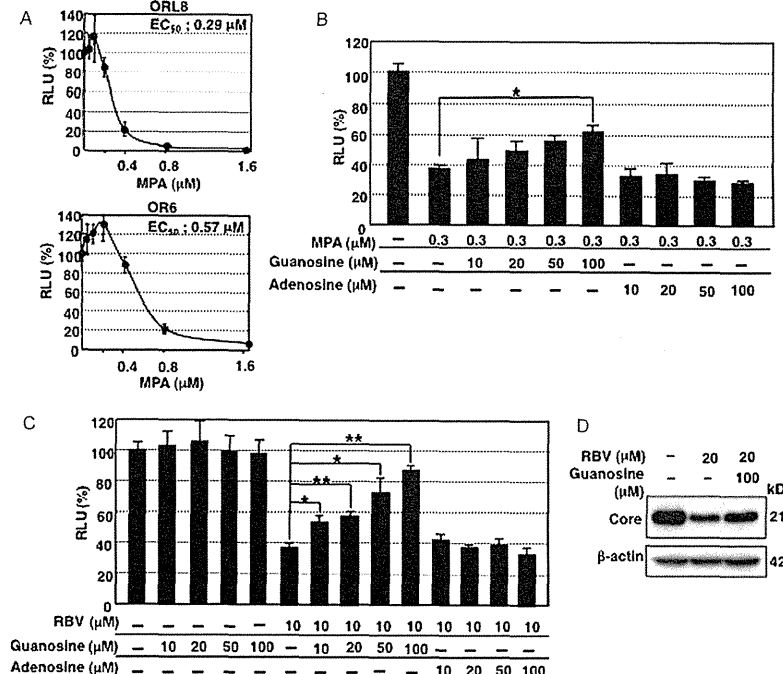


Fig. 6. Guanosine canceled the anti-HCV activity of RBV in ORL8 system. (A) Anti-HCV activity of MPA in ORL8 and OR6. The ORL8 and OR6 cells were treated with MPA for 72 h, and then RL assay was performed. (B) Effect of guanosine or adenosine on MPA in ORL8 system. ORL8 cells were treated with MPA alone or in combination with guanosine or adenosine for 72 h, and then the RL assay was performed. Asterisk indicates a significant difference compared to the control treatment. *P < 0.05. (C) Effect of guanosine or adenosine on RBV in ORL8 system. ORL8 cells were treated with RBV alone or in combination with guanosine or adenosine for 72 h, and then the RL assay was performed. Asterisks indicate significant differences compared to the control treatment. *P < 0.05; **P < 0.01. (D) Effect of guanosine on RBV in ORL8 system. ORL8 cells were treated with RBV alone or in combination with guanosine for 72 h, and subjected to Western blot analysis using anti-Core and β-actin antibodies.

et al., 2002; Thomas et al., 2011; Zhou et al., 2003). Although the effective concentrations (50–1000 μM) of RBV in those studies were much higher than the clinically achievable concentrations (5–14 μM) (Feld et al., 2010; Pawlotsky et al., 2004; Tanabe et al., 2004), the effective concentration of RBV in this study was close to the clinically achievable concentrations. Furthermore, it is noteworthy that the replication of a different HCV strain (JFH1 of genotype 2a) in the Li23-derived cell culture system, but not in the HuH-7-derived cell culture system, was also suppressed with RBV at the concentration of 10 μM (Fig. 1C). These results demonstrate that the Li23 cell-derived assay system is a more sensitive biosensor of RBV than the HuH-7 cell-derived assay system.

The finding that RBV remarkably inhibited HCV RNA replication in our new assay systems led us to analyze the anti-HCV mechanism of RBV. In this study, we evaluated several possible anti-HCV mechanisms of RBV, as described above. Regarding the induction of error catastrophe by RBV, we obtained no evidence that RBV (even at 50 μM) acted as a mutagen in HCV RNA replication. Therefore, we could not explain the mechanism underlying the suppression of HCV RNA replication by RBV according to the theory of error catastrophe. In addition, no increasing mutation rate of HCV RNA in patients receiving RBV monotherapy or a combination of RBV plus IFN- α was observed in a previous clinical study (Chevaliez et al., 2007). In consideration of all these findings, we suggest that the clinically achievable concentrations of RBV do not act as a mutagen in HCV RNA replication. Indeed, our previous study using the replicon cell culture system demonstrated that RBV treatment (6 months at 5 and 25 μM) did not accelerate the mutation rate or increase the genetic diversity of the HCV replicon (Kato et al., 2005). In regard to the effect of RBV on the IFN system, we obtained no evidence that RBV (even at 50 μM) induced ISGs (ISG15, IRF7, and IP-10) or phosphorylation of STAT1 even in the cells co-treated with IFN- α and RBV (data not shown). On the other hand, very recently Thomas et al. (Thomas et al., 2011) reported that RBV treatment (500 μM) resulted in the induction of a distinct set of ISGs including ISG15, IRF7, and IRF9, using HuH-7-derived cell line HuH7.5.1. In that study, they demonstrated that the induction of these ISGs was mediated by a novel mechanism different from those associated with IFN signaling and double stranded RNA sensing pathway, and concluded that the effect of RBV on ISG regulation is IFN-independent. However, in our cell culture system, which is highly sensitive to RBV, the induction of ISG15 and IRF7 by RBV was not observed (Fig. 4C). This kind of controversial results may be dependent on the difference of cell lines used in both studies, since recent microarray analysis revealed that the expression profiles of Li23 and HuH-7 cells, both of which possess an environment

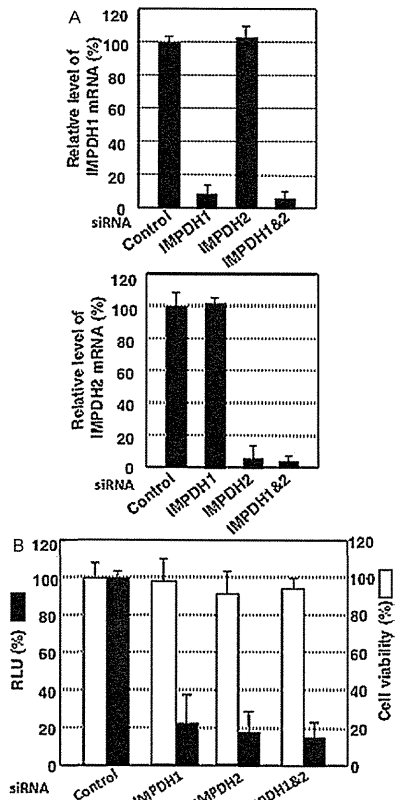


Fig. 7. IMPDH is required for HCV RNA replication. (A) Inhibition of IMPDH1 and IMPDH2 expression by siRNA in ORL8 cells. ORL8 cells were transfected with 8 nM siRNA targeting for IMPDH1 and/or IMPDH2. After 72 h, the expression levels of IMPDH1 and IMPDH2 mRNAs were determined by the quantitative RT-PCR. Experiments were done in triplicate. (B) Suppression of HCV RNA replication in IMPDH1- and/or IMPDH2-knockdown ORL8 cells. The RLU (%) calculated, when the luciferase activity of the cells treated with control siRNA was assigned to be 100%, is shown. The cell viability was determined as described in Section 2.

for robust HCV replication, differed considerably (Kato et al., 2009; Mori et al., 2010). However, Thomas et al. (2011) observed that the addition of guanosine to the medium could block RBV-induced ISGs induction. Therefore, further additional studies would be needed to resolve the differences of results obtained from both studies.

The highlight in this study is that a Li23-derived cell culture system clearly demonstrated an association between the suppression of HCV RNA replication by RBV and IMPDH inhibition by RBV. Although RBV is known to be an IMPDH inhibitor (Lau et al., 2002), it had been considered that such inhibitory activity would not contribute to the anti-HCV activity of RBV, because of the marginal antiviral effect of RBV in HuH-7-derived HCV RNA replicating cells (Naka et al., 2005; Tanabe et al., 2004; Zhou et al., 2003). Although Zhou et al. (2003) previously showed that exoge-

nous guanosine cancelled the RBV-induced CFE reduction using an HuH-7-based HCV replicon system, they did not observe any dose-dependent reversal of the adverse effect of RBV by the addition of guanosine. However, in our Li23-based HCV replication assay system, we observed a near complete cancellation of the activity of RBV in the dose-dependent manner of guanosine (Fig. 6C). This finding indicated that anti-HCV activity of RBV might be mediated through the inhibition of IMPDH by RBV. Indeed, we could demonstrate that HCV RNA replication was notably suppressed in IMPDH-knockdown ORL8 cells (Fig. 7B). Taken together, these results revealed that the Li23-derived assay system was superior to HuH-7-derived assay system in order to clarify the anti-HCV mechanism of RBV.

The remarkable effect of RBV observed in this study was considered to be due to the difference in the cell lines used, because Li23-derived cells possessed rather different gene expression profiles from those in HuH-7-derived cells (Kato et al., 2009; Mori et al., 2010). As one of the possibilities, we examined the expression status of nucleoside transporters (ENT family) involved in cellular uptake of RBV or ATP-binding cassette transporters, including multidrug resistance 1, which is involved in cellular excretion. However, the mRNA levels of these transporters were almost the same in both types of cells (Fig. 3C). Although unfortunately we failed to clarify the mechanism underlying the remarkable differences in the activity of RBV in both types of cells, we observed that the anti-HCV activity of RBV was completely canceled by NBMPR, an ENT inhibitor, suggesting that RBV is taken by ENT member(s) at least in ORL8 cells. This finding supports the recent report describing the involvement of ENT1 on cellular uptake of RBV (Fukuchi et al., 2010; Ibarra and Pfeiffer, 2009). Therefore, a comparative analysis regarding the functions of ENT member(s) derived from both types of cells will be needed. As the other possibility, the differences of activities or expression levels of IMPDH in OR6 and ORL8 cells may contribute to the remarkable effect of RBV observed in ORL8 cells.

On the other hand, it has been known that rapid reduction of the intracellular level of GTP occurs when RBV inhibits IMPDH (Feld and Hoofnagle, 2005). Therefore, it is assumed that the decrease of GTP would lead to a suppression of HCV replication. To date, several studies (Lohmann et al., 1999; Lai et al., 2000; Simister et al., 2009) have shown that high concentration of GTP (approximately 500 μM corresponding to the intracellular concentration) is required for the efficient de novo initiation of RNA synthesis by HCV NS5B RdRp. In addition, Simister et al. (2009) showed that change from 500 μM to 100 μM of GTP concentration decreased a log of the NS5B RdRp activity. From these studies, we expect that the inhibition of IMPDH by RBV may cause rapid decrease of intracellular GTP concentration, resulting in the suppression of de novo RNA synthesis by NS5B. Before our assumption, MMPD/VX-497 has developed as an inhibitor of IMPDH, and it has been shown to exert anti-HCV activity (EC₅₀: 0.39 μM) in an HCV replicon system (Marcellin et al., 2007). However, MMPD/VX-497 monotherapy of patients with chronic hepatitis C had no effect on HCV RNA levels (Marcellin et al., 2007) just as in another study, RBV monotherapy had no effect on HCV RNA levels in patients with chronic hepatitis C (Di Bisceglie et al., 1995). Although we showed that the EC₅₀ value of RBV in this study was equivalent to the clinically achievable concentrations (Feld et al., 2010; Pawlowsky et al., 2004; Tanabe et al., 2004), we considered that the effective concentration for a reduction of HCV RNA levels in monotherapy would be less than the EC₅₀ value. However, an IMPDH inhibitor at EC₅₀ would be effective in combination with IFN-α as an adjuvant. Indeed, combination therapy with IFN-α and MMPD/VX-497 was effective in previously untreated patients with chronic hepatitis C (McHutchison et al., 2005). However, a recent study (Rustgi et al., 2009) showed that the addition of MMPD/VX-497 to PEG-IFN-α and RBV combination

therapy in patients who had been nonresponsive to PEG-IFN-α and RBV combination therapy did not increase the proportion of patients who achieved an SVR. Since we showed that RBV also acted as an IMPDH inhibitor in the present study, it would seem to be a reasonable result that MMPD/VX-497 had no significant effect on patients who were nonresponsive to combination therapy with PEG-IFN-α and RBV.

In conclusion, we clarified the anti-HCV mechanism of RBV in a new HCV cell culture system. The fact that anti-HCV activity of RBV was mediated by the inhibition of IMPDH would provide a clue to the mechanism of the increase of SVR by the current standard combination therapy with PEG-IFN-α and RBV. In addition, our findings should also be useful for the screening and development of new anti-HCV drugs, which inhibit IMPDH, with reduced side effects, including anemia.

Acknowledgments

We would like to thank Naoko Kawahara, Takashi Nakamura, and Keiko Takeshita for their technical assistances. This work was supported by a grant-in-aid for research on hepatitis from the Ministry of Health, Labor, and Welfare of Japan. K. M. was supported by a Research Fellowship from the Japan Society for Promotion of Science for Young Scientists.

References

Ariumi, Y., Kuroki, M., Abe, K., Dansako, H., Ikeda, M., Wakita, T., Kato, N., 2007. DDX3 DEAD-box RNA helicase is required for hepatitis C virus RNA replication. *J. Virol.* 81, 13922–13926.

Chevaliez, S., Brillet, R., Lázaro, E., Hézode, C., Pawlowsky, J.M., 2007. Analysis of ribavirin mutagenicity in human hepatitis C virus infection. *J. Virol.* 81, 7732–7741.

Chevaliez, S., Pawlowsky, J.M., 2007. Interferon-based therapy of hepatitis C. *Adv. Drug Deliv. Rev.* 59, 1222–1241.

Contreras, A.M., Hiasa, Y., He, W., Terella, A., Schmidt, E.V., Chung, R.T., 2002. Viral RNA mutations are region specific and increased by ribavirin in a full-length hepatitis C virus replication system. *J. Virol.* 76, 8505–8517.

Dansako, H., Ikeda, M., Kato, N., 2007. Limited suppression of the interferon-β production by hepatitis C virus serine protease in cultured human hepatocytes. *FEBS J.* 274, 4161–4176.

Dansako, H., Nagamura, A., Nakamura, T., Ikeda, F., Nozaki, A., Kato, N., 2003. Differential activation of interferon-inducible genes by hepatitis C virus core protein mediated by the interferon stimulated response element. *Virus Res.* 97–103.

Di Bisceglie, A.M., Conjeevan, H.S., Fried, M.W., Sallie, R., Park, Y., Yurdaydin, C., Swain, M., Kleiner, D.E., Mahaney, K., Hoofnagle, J.H., 1995. Ribavirin as therapy for chronic hepatitis C. A randomized, double-blind, placebo-controlled trial. *Ann. Intern. Med.* 123, 897–903.

Feld, J.J., Lutchman, G.A., Heller, T., Hara, K., Pfeiffer, J.K., Leff, R.D., Meek, C., Rivera, M., Ko, M., Koh, C., Rotman, Y., Ghany, M.G., Haynes-Williams, V., Neumann, A.U., Liang, T.J., Hoofnagle, J.H., 2010. Ribavirin improves early responses to peginterferon through improved interferon signaling. *Gastroenterology* 139, 154–162.

Feld, J.J., Hoofnagle, J.H., 2005. Mechanism of action of interferon and ribavirin in treatment of hepatitis C. *Nature* 436, 967–972.

Fukuchi, Y., Furihata, T., Hashizume, M., Iikura, M., Chiba, K., 2010. Characterization of ribavirin uptake systems in human hepatocytes. *J. Hepatol.* 52, 486–492.

Henry, S.D., Melselaar, H.J., Lonsdale, R.C., Kok, A., Haagmans, B.L., Tilanus, H.W., van der Laan, L.J., 2006. Mycophenolate acid inhibits hepatitis C virus replication and acts in synergy with cyclosporin A and interferon-α. *Gastroenterology* 131, 1452–1462.

Ibarra, K.D., Pfeiffer, J.K., 2009. Reduced ribavirin antiviral efficacy via nucleoside transporter-mediated drug resistance. *J. Virol.* 83, 4538–4547.

Ikeda, M., Abe, K., Dansako, H., Nakamura, T., Naka, K., Kato, N., 2005. Efficient replication of a full-length hepatitis C virus genome, strain 1, in cell culture, and development of a luciferase reporter system. *Biochem. Biophys. Res. Commun.* 329, 1350–1359.

Kato, N., Hijikata, M., Ootsuyama, Y., Nakagawa, M., Ohkoshi, S., Sugimura, T., Shimotohno, K., 1990. Molecular cloning of the human hepatitis C virus genome from Japanese patients with non-A, non-B hepatitis. *Proc. Natl. Acad. Sci. U.S.A.* 87, 9524–9528.

Kato, N., Mori, K., Abe, K., Dansako, H., Kuroki, M., Ariumi, Y., Wakita, T., Ikeda, M., 2009. Efficient replication systems for hepatitis C virus using a new human hepatoma cell line. *Virus Res.* 146, 41–50.

Kato, N., Nakamura, T., Dansako, H., Namba, K., Abe, K., Nozaki, A., Naka, K., Ikeda, M., Shimotohno, K., 2005. Genetic variation and dynamics of hepatitis C virus replicons in long-term cell culture. *J. Gen. Virol.* 86, 645–655.

Kato, N., Sugiyama, K., Namba, K., Dansako, H., Nakamura, T., Takami, M., Naka, K., Nozaki, A., Shimotohno, K., 2003. Establishment of a hepatitis C virus subgenomic replicon derived from human hepatocytes infected in vitro. *Biochem. Biophys. Res. Commun.* 305, 756–766.

Lau, J.Y., Tam, R.C., Liang, T.J., Hong, Z., 2002. Mechanism of action of ribavirin in the combination treatment of chronic HCV infection. *Hepatology* 35, 1002–1009.

Liu, W.L., Su, W.C., Cheng, C.W., Hwang, L.H., Wang, C.C., Chen, H.L., Chen, D.S., Lai, M.Y., 2007. Ribavirin up-regulates the activity of double-stranded RNA-activated protein kinase and enhances the action of interferon-α against hepatitis C virus. *J. Infect. Dis.* 196, 425–434.

Lohmann, V., Overton, H., Bartenschlager, R., 1999. Selective stimulation of hepatitis C virus and pestivirus NS5B RNA polymerase activity by GTP. *J. Biol. Chem.* 274, 10807–10815.

Luo, G., Hamatake, R.K., Mathis, D.M., Racela, J., Rigat, K.L., Lemm, J., Colombo, R.J., 2000. Do novo initiation of RNA synthesis by the RNA-dependent RNA polymerase (NS5B) of hepatitis C virus. *J. Virol.* 74, 851–857.

Marcellin, P., Horsmans, Y., Nevens, F., Grange, J.D., Bronowicki, J.P., Vetter, D., Purdy, S., Garg, V., Bengtsson, L., McNair, L., Alam, J., 2007. Phase 2 study of the combination of merimepodib with peginterferon-α2b, and ribavirin in nonresponders to previous therapy for chronic hepatitis C. *J. Hepatol.* 47, 476–483.

McHutchison, J.G., Schiff, M.L., Cheung, R.C., Gordon, S.C., Wright Jr., T.L., Pottage, J.C., McNair, L., Ette, E., Moseley, S., Alam, J., 2005. A randomized, double-blind, placebo-controlled dose-escalation trial of merimepodib (VX-497) and interferon-α in previously untreated patients with chronic hepatitis C. *Antivir. Ther.* 10, 635–643.

Mori, K., Ikeda, M., Ariumi, Y., Kato, N., 2010. Gene expression profile of Li23, a new human hepatoma cell line that enables robust hepatitis C virus replication. Comparison with HuH-7 and other hepatic cell lines. *Hepatol. Res.* 40, 1248–1253.

Naka, K., Ikeda, M., Abe, K., Dansako, H., Kato, N., 2005. Mizoribine inhibits hepatitis C virus RNA replication, effect of combination with interferon-α. *Biochem. Biophys. Res. Commun.* 330, 871–875.

Pastor-Anglada, M., Camar-Soldado, P., Molina-Arcas, M., Llosta, M.P., Larráoz, I., Martínez-Picado, J., Casado, F.J., 2005. Cell entry and export of nucleoside analogues. *Virus Res.* 107, 151–164.

Pawlowsky, J.M., Dahari, H., Neumann, A.U., Hézode, C., Germanidis, G., Lonjon, I., Castera, L., Dhumeaux, D., 2004. Antiviral action of ribavirin in chronic hepatitis C. *Gastroenterology* 126, 703–714.

Rustgi, V.K., Lee, W.M., Lawitz, E., Gordon, S.C., Afshai, N., Poordad, F., Bonkovsky, H.L., Bengtsson, L., Chandorkar, G., Harding, M., McNair, L., Alyson, M., Alam, J., Kaufman, R., Gharakhanian, S., McHepatitis Trial, 2005. Merimepodib, pegylated interferon, and ribavirin in nonresponders. *Hepatology* 41, 1719–1726.

Simister, P., Schmitt, M., Geitmann, M., Wicht, O., Danielson, U.H., Klein, R., Bresanelli, S., Lohmann, V., 2009. Structural and functional analysis of hepatitis C virus strain JFH1 polymerase. *J. Virol.* 83, 11926–11939.

Tanabe, Y., Sakamoto, N., Enomoto, N., Kurosaki, M., Ueda, E., Maekawa, S., Yamashiro, T., Nakagawa, M., Chen, C.H., Kanazawa, N., Kakinuma, S., Watanabe, M., 2004. Synergistic inhibition of intracellular hepatitis C virus replication by combination of ribavirin and interferon-α. *J. Infect. Dis.* 189, 1129–1139.

Thomas, D.L., 2000. Hepatitis C epidemiology. *Curr. Top. Microbiol. Immunol.* 242, 25–41.

Thomas, E., Feld, J.J., Li, Q., Hu, Z., Fried, M.W., Liang, T.J., 2011. Ribavirin potentiates interferon action by augmenting interferon-stimulated gene induction in HCV cell culture models. *Hepatology* 53, 32–41.

Wakita, T., Pietschmann, T., Kato, T., Date, T., Miyamoto, M., Zhao, Z., Murthy, K., Habermann, A., Kräusslich, H.G., Mizokami, M., Bartenschlager, R., Liang, T.J., 2005. Production of infectious hepatitis C virus in tissue culture from a cloned viral genome. *Nat. Med.* 11, 791–796.

Wang, J., Yang, J.W., Zeeb, A., Webber, S.A., Girnita, D.M., Selby, R., Fu, J., Shah, T., Pravica, V., Hutchinson, I.V., Burkart, C.J., 2008. IMPDH1 gene polymorphisms and association with acute rejection in renal transplant patients. *Clin. Pharmacol. Ther.* 83, 711–717.

Yano, M., Ikeda, M., Abe, K., Dansako, H., Ohkoshi, S., Aoyagi, Y., Kato, N., 2007. Comprehensive analysis of the effects of ordinary nutrients on hepatitis C virus RNA replication in cell culture. *Antimicrob. Agents Chemother.* 51, 2016–2127.

Yano, M., Ikeda, M., Abe, K., Kawai, Y., Kuroki, M., Mori, K., Dansako, H., Ariumi, Y., Ohkoshi, S., Aoyagi, Y., Kato, N., 2009. Oxidative stress induces anti-hepatitis C virus status via the activation of extracellular signal-regulated kinase. *Hepatology* 50, 678–688.

Zhou, S., Liu, R., Baroudy, B.M., Malcolm, B.A., Reyes, G.R., 2003. The effect of ribavirin and IMPDH inhibitors on hepatitis C virus subgenomic replicon RNA. *Virology* 310, 333–342.

BASIC STUDIES

Anti-ulcer agent teprenone inhibits hepatitis C virus replication: potential treatment for hepatitis C

Masanori Ikeda^{1*}, Yoshinari Kawai^{1,2*}, Kyoko Mori¹, Masahiko Yano^{1,3}, Ken-ichi Abe¹, Go Nishimura¹, Hiromichi Dansako¹, Yasuo Arimi¹, Takaji Wakita⁴, Kazuhide Yamamoto² and Nobuyuki Kato¹

¹ Department of Tumor Virology, Okayama University Graduate School of Medicine, Dentistry, and Pharmaceutical Sciences, Okayama, Japan

² Department of Gastroenterology and Hepatology, Okayama University Graduate School of Medicine, Dentistry, and Pharmaceutical Sciences, Okayama, Japan

³ Division of Gastroenterology and Hepatology, Graduate School of Medical and Dental Sciences, Niigata University, Niigata City, Japan

⁴ Department of Virology II, National Institute of Infectious Diseases, Tokyo, Japan

Keywords

geranylgeranylation – HCV – Selbex – statin – teprenone

Correspondence

Masanori Ikeda, MD, PhD, Department of Tumor Virology, Okayama University Graduate School of Medicine, Dentistry, and Pharmaceutical Sciences, 2-5-1 Shikata-cho, Okayama 700-8558, Japan
Tel: +81-86-235-7386
Fax: +81-86-235-7392
e-mail: maikeda@md.okayama-u.ac.jp

Received 11 October 2010

Accepted 7 February 2011

DOI:10.1111/j.1478-3231.2011.02499.x

Hepatitis C virus (HCV) infection frequently causes persistent hepatitis and leads to cirrhosis and hepatocellular carcinoma (HCC). Currently, the combination therapy of pegylated interferon (IFN) with ribavirin is available for patients with chronic hepatitis C (CH C) and yields a sustained virological response rate of about 50% (1). However, about half of CH C patients are still susceptible to the progression of the disease to fatal cirrhosis and HCC. Therefore, the development of more effective reagents for the treatment of HCV infection is urgent.

*Contributed equally.

Abstract

Background: Previously we reported that 3-hydroxy-3-methylglutaryl coenzyme A reductase inhibitors, statins, inhibited hepatitis C virus (HCV) RNA replication. Furthermore, recent reports revealed that the statins are associated with a reduced risk of hepatocellular carcinoma and lower portal pressure in patients with cirrhosis. The statins exhibited anti-HCV activity by inhibiting geranylgeranylation of host proteins essential for HCV RNA replication. Geranylgeranyl pyrophosphate (GGPP) is a substrate for geranylgeranyltransferase. Therefore, we examined the potential of geranyl compounds with chemical structures similar to those of GGPP to inhibit HCV RNA replication. **Methods:** We tested geranyl compounds [geranylgeraniol, geranylgeranoic acid, vitamin K₂ (VK2) and teprenone] for their effects on HCV RNA replication using genome-length HCV RNA-replicating cells (the OR6 assay system) and a JFH-1 infection cell culture system, because their chemical formulas are similar to that of the GGPP, a substrate for geranylgeranyltransferase in geranylgeranylation (13–15). The anti-ulcer agent, teprenone (also called geranylgeranylacetone) is reported to block the function of GGPP by the competitive inhibition of the mevalonate pathway (16). Teprenone is the major component of the clinically used anti-ulcer reagent, Selbex. We also examined the anti-HCV activities of the geranyl compounds in combination with interferon (IFN)- α or statins. **Results:** Among the geranyl compounds tested, only teprenone exhibited anti-HCV activity at a clinically achievable concentration. However, other anti-ulcer agents tested had no inhibitory effect on HCV RNA replication. The combination of teprenone and IFN- α exhibited a strong inhibitory effect on HCV RNA replication. Although teprenone alone did not inhibit geranylgeranylation, surprisingly, statins' inhibitory action against geranylgeranylation was enhanced by cotreatment with teprenone. **Conclusions:** The anti-ulcer agent, teprenone inhibited HCV RNA replication and enhanced statins' inhibitory action against geranylgeranylation. This newly discovered function of teprenone may improve the treatment of HCV-associated liver diseases as an adjuvant to statins.

To overcome this problem, we developed a genome-length HCV RNA (strain O of genotype 1b) replication system (OR6) with luciferase as a reporter, which facilitated the prompt and precise monitoring of HCV RNA replication in hepatoma cells (HuH-7-derived OR6 cells) (2). Using this OR6 system, we recently reported that 3-hydroxy-3-methylglutaryl coenzyme A (HMG-CoA) reductase inhibitors, statins, inhibited HCV RNA replication efficiently (3–5). Among five statins – fluvastatin (FLV), atorvastatin (ATV), simvastatin (SIV), pravastatin (PRV) and lovastatin (LOV) – FLV exhibited the strongest anti-HCV activity, while PRV had no effect on HCV RNA replication (3, 6). More recently, Bader *et al.* (7) demonstrated that FLV inhibited HCV RNA replication

Teprenone inhibits HCV replication

in humans. Furthermore, recent reports revealed that the statins were associated with a reduced risk of HCC (8) and lower portal pressure in patients with cirrhosis (9).

Statins targeted the mevalonate pathway. This pathway is branched after farnesyl pyrophosphate (FPP) into cholesterol and geranylgeranyl pyrophosphate (GGPP) biosynthesis pathways. The inhibition of GGPP but not of cholesterol is essential for HCV RNA replication in the inhibitory activity of statins (3, 10, 11). To date, one of the proteins, FBL2, was reported as the host protein essential for HCV RNA replication. HCV RNA replication requires geranylgeranylation of FBL2 by geranylgeranyltransferase with GGPP (12).

We have attempted to examine the effects of geranyl compounds [geranylgeraniol (GGOH), geranylgeranoic acid, vitamin K₂ (VK2) and teprenone] on HCV RNA replication using the OR6 assay system and the JFH-1 infection cell culture system, because their chemical formulas are similar to that of the GGPP, a substrate for geranylgeranyltransferase in geranylgeranylation (13–15). The anti-ulcer agent, teprenone (also called geranylgeranylacetone) is reported to block the function of GGPP by the competitive inhibition of the mevalonate pathway (16). Teprenone is the major component of the clinically used anti-ulcer reagent, Selbex.

Here, we reported the inhibitory activity of teprenone on HCV RNA replication and the effect of teprenone in combination with statins on their inhibitory action against geranylgeranylation.

Materials and methods

Reagents and antibodies

Teprenone (Selbex), geranylgeranoic acid, ecabet sodium and sofalcon, gefarnate were purchased from Eisai Co. Ltd (Tokyo, Japan), BIOMOL (Plymouth Meeting, PA, USA), Mitsubishi Tanabe Pharma (Osaka, Japan), Taisho Pharmaceutical Co. (Tokyo, Japan) and Dainippon Sumitomo Pharma Co. Ltd (Osaka, Japan) respectively. GGPP, GGOH, VK2, IFN- α , vitamin E, linoleic acid and mevalonate were purchased from Sigma (St Louis, MO, USA). Cyclosporine A, FLV, LOV and PRV were purchased from Calbiochem (Los Angeles, CA, USA). ATV, SIV and pitavastatin (PTV) were purchased from Astellas Pharma Inc. (Tokyo, Japan), Banyu Pharmaceutical Co. Ltd (Tokyo, Japan), and Kowa Co. Ltd (Nagoya, Japan) respectively.

The antibodies used in this study were those specific to the Core (CP11, Institute of Immunology, Tokyo), NSSA (a generous gift from Dr A. Takamizawa, Research Foundation for Microbial Diseases, Osaka University), NSSB (a generous gift from Dr M. Kohara, Tokyo Metropolitan Institute of Medical Science) and β -actin (Sigma). Anti-heat shock protein (HSP) 90 and anti-HSP70 antibodies were purchased from BD Bioscience (San Jose, CA, USA). Anti-Rap1A (sc-1482) and anti-Rap1 (sc-65) antibodies were purchased from Santa Cruz Biotechnology (Santa Cruz, CA, USA).

Cell cultures

OR6 is a cell line cloned from ORN/C-5B/KE RNA-replicating HuH-7 cells as described previously (2) and cultured in Dulbecco's modified Eagle's medium supplemented with 10% fetal bovine serum, penicillin, streptomycin and G418 (300 μ g/ml; Geneticin, Invitrogen, Carlsbad, CA, USA). ORN/C-5B/KE RNA is derived from HCV-O, and OR6c cells are cured OR6 cells from which HCV RNA was eliminated by IFN- α treatment as described previously (2). HCV-O/RLGE is the authentic HCV RNA containing adaptive mutations of Q111R, P111L, E120G and K160E in the NS3 region and replicates efficiently in OR6c cells.

OR6 reporter assay

For the *Renilla* luciferase (RL) assay, 1.0–1.5 \times 10⁴ OR6 cells were plated onto 24-well plates in triplicate and precultured for 24 h. The cells were treated with each compound for 72 h. Then, the cells were harvested and subjected to an RL assay according to the manufacturer's protocol (2).

Western blot analysis

For western blot analysis, 4–4.5 \times 10⁴ OR6 or OR6c cells harbouring HCV-O/RLGE RNA were plated onto six-well plates and cultured for 24 h, and were then treated with each compound for 72 h. Preparation of the cell lysates, sodium dodecyl sulphate-polyacrylamide gel electrophoresis and immunoblotting were then performed as described previously (17).

Cell growth assay

To examine the effect of each reagent on OR6 cell growth, 6.0–6.5 \times 10³ OR6 cells were plated onto six-well plates in triplicate and were precultured for 24 h. The cells were treated with or without each compound for 72 h, and then the viable cells were counted after trypan blue dye treatment as described previously (18).

WST-1 cell proliferation assay

The OR6 cells (2 \times 10³ cells) were plated onto a 96-well plate in triplicate at 24 h before treatment with each reagent. The cells at 24, 48 and 72 h after treatment were subjected to a WST-1 cell proliferation assay (Takara Bio, Otsu, Japan) according to the manufacturer's protocol.

Reverse transcription-polymerase chain reaction

Reverse transcription-polymerase chain reaction (RT-PCR) for HMG-CoA reductase and for glyceraldehyde-3-phosphate dehydrogenase (GAPDH) was performed by a method described previously (19). Briefly, using cellular total RNAs (2 μ g), cDNA was synthesized using Superscript II with the oligo dT primer. One-tenth of the synthesized cDNA was subjected to PCR with the

following primer pairs: HMG-CoA reductase, 5'-ATGCC ATCCCTGTTGGAGTG-3' and 5'-TGTTCATCCCCATG GCATCCC-3'; and GAPDH, 5'-GACTCATGACCACAG TCCATGC-3' and 5'-GAGGAGACCACCTGGTGCCTCA G-3'.

Hepatitis C virus infection experiment

For the infection experiment with the JFH-1 virus, HuH-7-derived RSc cells (1×10^5 cells) were plated onto six-well plates and cultured for 24 h (20). Then, the cells were infected with 100 μ l (equivalent to a multiple of infection of 0.1–0.2) of inoculum and cultured for 24 h. The cells were treated with each reagent for 72 h. The culture supernatants and cells were collected for quantification of the Core by an enzyme-linked immunosorbent assay (ELISA) (Mitsubishi Kagaku Bio-Clinical Laboratories, Tokyo, Japan) and for western blot analysis respectively.

Statistical analysis

The luciferase activities were statistically compared between the various treatment groups using Student's *t*-test. *P* values of < 0.05 were considered statistically significant. The mean \pm standard deviation is determined from at least three independent experiments.

Results

Anti-hepatitis C virus activity of teprenone is a unique feature not only among geranyl compounds but also among anti-ulcer agents

The mevalonate pathway is divided into two branches: cholesterol synthesis and GGPP synthesis pathways (Fig. 1). The statins exhibited anti-HCV activity via

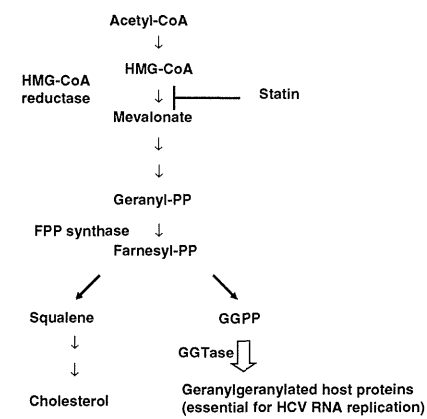


Fig. 1. Schema of the mevalonate pathway.

inhibition of geranylgeranylation of host proteins essential for HCV RNA replication. Therefore, we examined the effects of geranyl compounds [GGOH, geranylgeranoic acid, VK2 and teprenone (Selbex)] on HCV RNA replication using the OR6 assay system, because their chemical structures are similar to that of the GGPP (Fig. 2A) (16). Teprenone inhibited HCV RNA replication in a dose-dependent manner without affecting OR6 cell growth up to a concentration of 20 μ g/ml (Fig. 2B). The 50% effective concentration (EC_{50}) of teprenone is 5.3 μ g/ml. On the other hand, GGOH, geranylgeranoic acid and VK2 did not inhibit HCV RNA replication at the concentration without cytotoxicity (Fig. 2C–E). We also demonstrated that teprenone did not affect cell proliferation within this concentration (supporting information, Fig. S1A). These results suggest that anti-HCV activity of teprenone was not a common feature among geranyl compounds.

Teprenone is used for patients with gastritis and gastric ulcers. Therefore, we examined anti-ulcer agents for their inhibitory effects against HCV RNA replication. The chemical structures of three anti-ulcer agents – ecabet sodium, sofalcon and gefarnate – are shown in supporting information, Figure S1B. None of these agents exhibited inhibitory effects on HCV RNA replication (supporting information, Fig. S1C–E). These results indicate that the anti-HCV activity of teprenone may not be a common feature among anti-ulcer agents.

Teprenone inhibited authentic hepatitis C virus RNA replication

The genome-length HCV RNA replicating in the OR6 cells contained three non-natural elements – RL, neomycin phosphotransferase and encephalomyocarditis virus internal ribosomal entry site. To further confirm that the anti-HCV activity of teprenone was not because of the inhibition of these three exogenous genes or their products, we used authentic 9.6 kb HCV RNA-replicating cells. We introduced *in vitro* synthesized HCV-O/RLGE RNA into cured OR6c cells (Fig. 3A). As shown in Figure 3B, teprenone inhibited Core expression in HCV-O/RLGE-replicating OR6c cells in a dose-dependent manner. These results indicate that the anti-HCV activity of teprenone was because of the inhibition of HCV RNA itself, but not exogenous genes or their products.

Teprenone enhanced anti-hepatitis C virus activity of interferon- α

We examined whether or not teprenone would enhance the anti-HCV activity of IFN- α . We did this by studying the inhibitory effects of combinations of IFN- α (0, 2.5, 5 and 10 IU/ml) and teprenone (0, 10 and 20 μ g/ml) using the OR6 assay system. Teprenone enhanced the anti-HCV activity of IFN- α in a dose-dependent manner (Fig. 4). Teprenone with IFN- α also inhibited Core expression (Fig. 4). We also demonstrated that teprenone did not

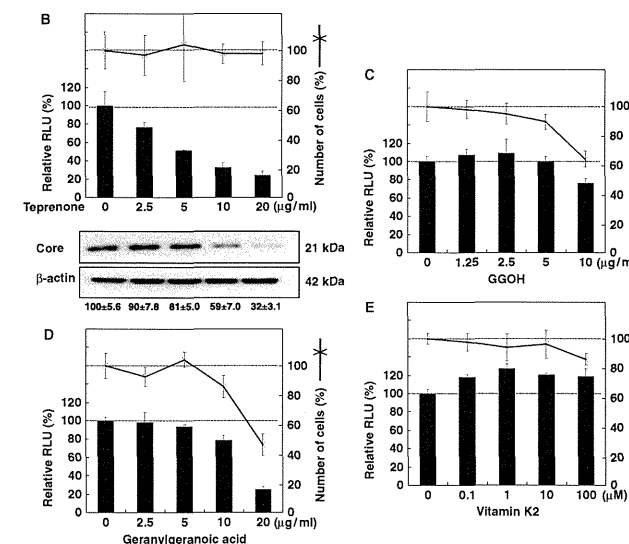
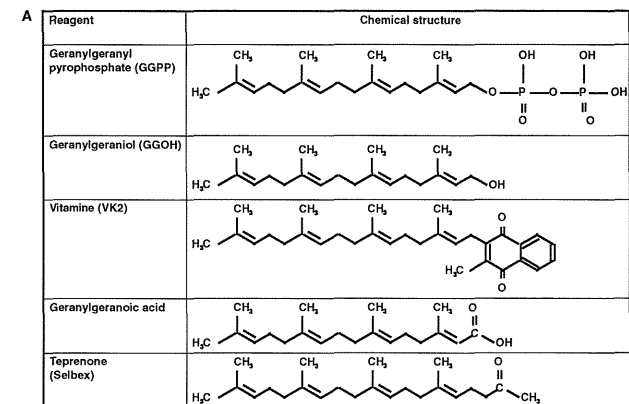


Fig. 2. The effects of geranyl compounds and anti-ulcer agents on hepatitis C virus (HCV) RNA replication. (A) Structures of geranyl compounds. (B) Anti-HCV activity of teprenone on HCV RNA replication in OR6 cells. OR6 cells were treated with teprenone (0, 2.5, 5, 10 and 20 μ g/ml) for 72 h. *Renilla* luciferase (RL) activity for HCV RNA replication is shown as a percentage of control. Each bar represents the average with standard deviations of triplicate data points. Cell viability was also shown as a percentage of control. After 72-h treatment, the production of the Core was analysed by immunoblotting using anti-Core antibody (lower panel). β -actin was used as a control for the amount of protein loaded per lane. The signal intensities of Core from three independent assays were quantified by densitometry and normalized by that of β -actin. Each of the mean \pm standard deviation is under the lower panel. (C to E) OR6 cells were treated with geranylgeraniol (0, 1.25, 2.5, 5 and 10 μ g/ml) (C), geranylgeranoic acid (0, 2.5, 5, 10 and 20 μ g/ml) (D) and VK2 (0, 0.1, 1, 10 and 100 μ M) (E) for 72 h. RL activity and cell viability after treatment were determined as shown in (B).

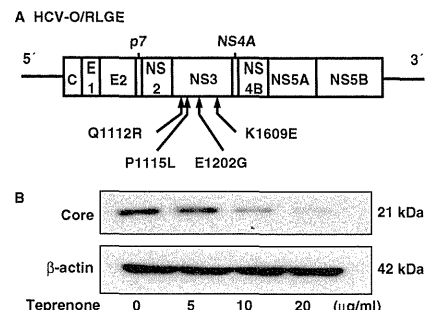


Fig. 3. Teprenone inhibited authentic hepatitis C virus (HCV) RNA replication. (A) Schematic gene organization of genome-length HCV-O/RLGE RNA. The positions of four adaptive mutations – Q1112R, P1115L, E1203G and K1609E – are indicated by arrows. (B) HCV-O/RLGE RNA was introduced into OR6 cells by electroporation as described previously (5). The cells were treated with teprenone (0, 5, 10 and 20 μ g/ml) for 72 h and then the production of the Core was analysed by immunoblotting using anti-Core antibody.

affect cell proliferation within this concentration (Fig. 4). These results suggest that teprenone may be a new candidate as a complement to IFN therapy.

Teprenone exhibited anti-hepatitis C virus activity in the JFH-1 infection system

We examined the anti-HCV activity of teprenone in the JFH-1 infection system (13–15). We treated the cells with teprenone (0, 5, 10 and 20 μ g/ml) at 24-h post-JFH-1 infection and cultured them for 72 h. The culture supernatants and cells were subjected to quantification of the Core by ELISA and western blot analysis respectively. Teprenone decreased the HCV Core in the supernatant (upper panel in Fig. 5A) and in the cells (lower panel in Fig. 5A) in a dose-dependent manner.

We next tested whether or not teprenone (0, 10 and 20 μ g/ml) enhanced IFN- α 's (0, 2.5 and 5 IU/ml) anti-HCV activity in the JFH-1 infection system. As shown in Figure 5B, teprenone enhanced the anti-HCV activity of IFN- α in a dose-dependent manner. These results suggest that teprenone also possessed anti-HCV activity in the JFH-1 infection system.

Teprenone did not inhibit geranylgeranylation

As shown in Figure 2A, the chemical structure of teprenone is similar to that of GGPP. Therefore, we examined the possibility that teprenone inhibits geranylgeranylation. Geranylgeranyl proteins possessed the C-A-A-X motif at the C-terminal of the protein: C is cysteine; A is aliphatic amino acid; and X is typically leucine (or rarely

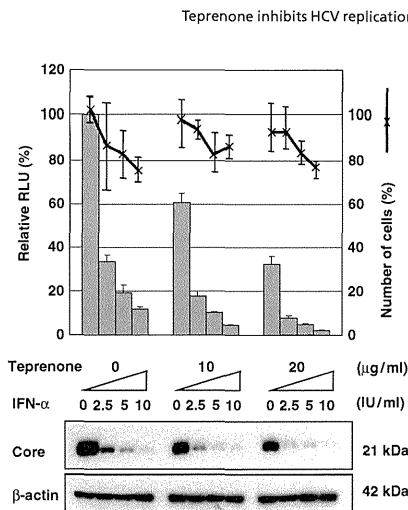


Fig. 4. Teprenone enhanced the anti-hepatitis C virus activity of interferon (IFN)- α . OR6 cells were cotreated with IFN- α (0, 2.5, 5 and 10 IU/ml) and teprenone (0, 10 and 20 μ g/ml) for 72 h. *Renilla* luciferase assay was performed as described in Figure 2B. Production of the Core was analysed by immunoblotting using anti-Core antibody. The cells at 24, 48 and 72 h after treatment were subjected to a WST-1 cell proliferation assay.

isoleucine, valine or phenylalanine). Rap1A is one of the Ras-related proteins and selected to monitor the status of geranylgeranylation. We used anti-Rap1A antibody (sc-1482), which recognized only nongeranylgeranylated Rap1A (21, 22). Therefore, geranylgeranylated Rap1A is not recognized with this antibody. On the other hand, anti-Rap1 antibody (sc-65) recognizes Rap1A and Rap1B independent of the state of geranylgeranylation (22). In the following experiments, we used anti-Rap1A antibody (sc-1482) to monitor the state of geranylgeranylation.

OR6 cells were treated with PTV (1.25 μ M) or teprenone (20 μ g/ml) or neither. The cells were collected after treatment and subjected to luciferase assay and western blot analysis. In the untreated cells, nongeranylgeranylated Rap1A bands were not detected (Fig. 6A). PTV inhibited geranylgeranylation at 3 h and reached a plateau 12 h after treatment along with nongeranylgeranylated Rap1A bands (Fig. 6A). On the other hand, geranylgeranylation was not inhibited in the cells with teprenone treatment (Fig. 6A).

We then tested the effect of mevalonate cotreatment with PTV or teprenone. Mevalonate negated PTV's inhibitory action against geranylgeranylation and led to the loss of PTV's anti-HCV activity (Fig. 6B). However, mevalonate did not affect the anti-HCV activity of teprenone (Fig. 6B). These results indicate that teprenone

Teprenone inhibits HCV replication

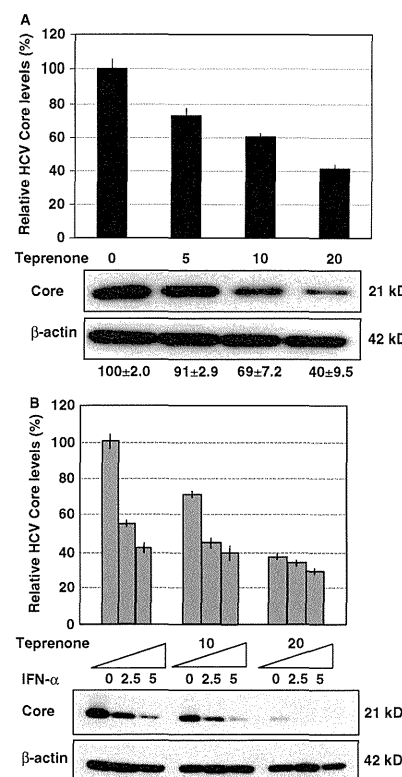


Fig. 5. Teprenone exhibited anti-hepatitis C virus (HCV) activity in the JFH-1 infection system. (A) Teprenone inhibited JFH-1 replication. Huh-7-derived RSC cells were infected with the JFH-1 virus for 24 h and were then treated with teprenone (0, 5, 10 and 20 μ g/ml) for 72 h. The supernatant and the cells were subjected to quantification of the Core by ELISA and western blot analysis respectively. The signal intensities of Core were quantified by densitometry and the mean \pm standard deviation is under the lower panel as shown in Figure 2B. (B) Teprenone enhanced interferon (IFN)- α 's anti-HCV activity in the JFH-1 infection system. JFH-1 virus-infected cells were treated with teprenone (0, 10 and 20 μ g/ml) and IFN- α (0, 2.5 and 5 IU/ml) for 72 h and then subjected to Core quantification by ELISA and western blot analysis as shown in (A).

inhibits HCV RNA replication without the inhibition of geranylgeranylation.

Statins' inhibition of HMG-CoA reductase decreased cholesterol synthesis and led to the increase of HMG-CoA reductase expression by positive feedback (3). The

mRNA of HMG-CoA reductase was increased with PTV treatment but not with teprenone treatment (supporting information, Fig. S3A and B). This result suggests that teprenone, unlike PTV, did not lower the cholesterol synthesis.

The chemical structure of teprenone, which is the major component of Selbex, is similar to that of GGPP, a substrate for geranylgeranyltransferase. Therefore, we ruled out the possibility that teprenone was incorporated into host proteins instead of GGPP and led to the loss of function of the host proteins, when endogenous GGPP was depleted by PTV in OR6 cells. The nongeranylgeranylated Rap1A was detected when OR6 cells were treated with PTV (lane 3; Fig. 6C). However, exogenous GGPP decreased nongeranylgeranylated Rap1A in PTV-treated OR6 cells (lane 4; Fig. 6C). If teprenone was incorporated into Rap1A instead of GGPP and formed a pseudo-geranylgeranylation, Rap1A blotted with anti-Rap1A (sc-1482) would be decreased. Surprisingly, nongeranylgeranylated Rap1A increased in OR6 cells after treatment with PTV and teprenone (compare lanes 3 and 7 in Fig. 6C). Furthermore, it is noteworthy that the total amount of Rap1 was decreased when OR6 cells were treated with PTV and teprenone. These results suggest that teprenone was not incorporated into host protein and unexpectedly enhanced the statin's inhibitory action against geranylgeranylation.

Teprenone enhanced statins' inhibitory action against geranylgeranylation

To further investigate the unexpected results shown in Figure 6C, we tested the geranylgeranyl state and anti-HCV activity using the OR6 assay system. OR6 cells were treated with teprenone (0, 10 and 20 μ g/ml) in combination with PTV (0, 0.25, 0.5 and 1.0 μ M) for 72 h and subjected to western blot analysis for the geranylgeranyl state using anti-Rap1A (sc-1482) and anti-Rap1 (sc-65) antibodies, and for anti-HCV activity using anti-Core, anti-NS5A and anti-NS5B antibodies. Anti-HCV activity was also assessed by a luciferase reporter assay. Teprenone by itself did not inhibit geranylgeranylation (lanes 1–3; Fig. 7A). When teprenone was treated with PTV (0.25 μ M), nongeranylgeranylated Rap1A increased in a dose-dependent manner (lanes 4–6; Fig. 7A). This result indicates that teprenone enhanced PTV's inhibitory action against geranylgeranylation in a dose-dependent manner. This effect of teprenone was also confirmed when PTV was treated at concentrations of 0.5 and 1.0 μ M (lanes 7–12; Fig. 7A). HCV RNA replication and the expression of HCV proteins were decreased when nongeranylgeranylated Rap1As were increased. Next, we examined whether or not this function of teprenone is a common feature against statins. Teprenone enhanced the inhibitory action of ATV, SIV, FLV and LOV but not PRV against geranylgeranylation (lower panel in Fig. 7B). Teprenone also enhanced anti-HCV activity in combination with statins (upper panel in Fig. 7B). These results

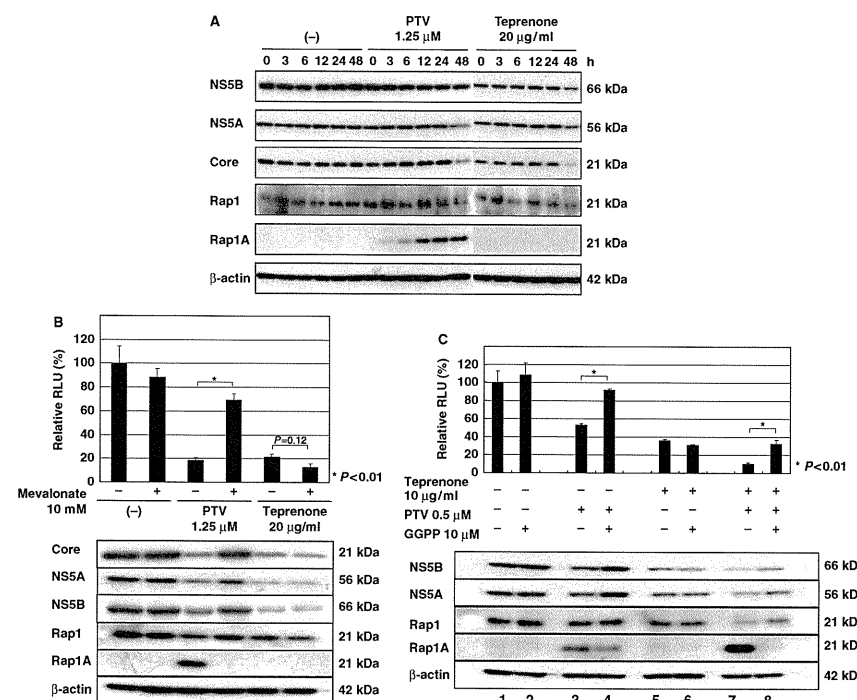


Fig. 6. Teprenone did not inhibit geranylgeranylation. (A) Teprenone did not inhibit geranylgeranylation. OR6 cells were treated with pitavastatin (PTV) (1.25 μ M) or teprenone (20 μ g/ml), or neither for 0, 3, 6, 12, 24 and 48 h. The cells were subjected to western blot analysis for HCV proteins using anti-NS5B, anti-NS5A and anti-Core antibodies, and for geranylgeranylation assay using anti-Rap1A (sc-1482) and anti-Rap1 (sc-65) antibodies. (B) Mevalonate did not affect the anti-HCV activity of teprenone. OR6 cells were treated with PTV (1.25 μ M), teprenone (20 μ g/ml) or neither in the absence or in the presence of mevalonate (10 mM) for 72 h. Then the cells were subjected to luciferase assay (upper panel) and western blot analysis using anti-Core, anti-NS5A, anti-NS5B, anti-Rap1A (sc-1482), anti-Rap1 (sc-65) and anti- β -actin antibodies (lower panel), as shown in (A). (C) Teprenone was not used as a substrate for GGT after the depletion of geranylgeranyl pyrophosphate (GGPP) by statin. OR6 cells were treated with teprenone (0 and 10 μ g/ml), PTV (0 and 0.5 μ M) and GGPP (0 and 10 μ M) in the indicated combination for 72 h. Then the cells were subjected to luciferase assay (upper panel) and geranylgeranyl assay using anti-Rap1A (sc-1482) and anti-Rap1 (sc-65) antibodies (lower panel) as shown in (A).

suggest that teprenone enhances statins' inhibitory action against geranylgeranylation, except for PRV.

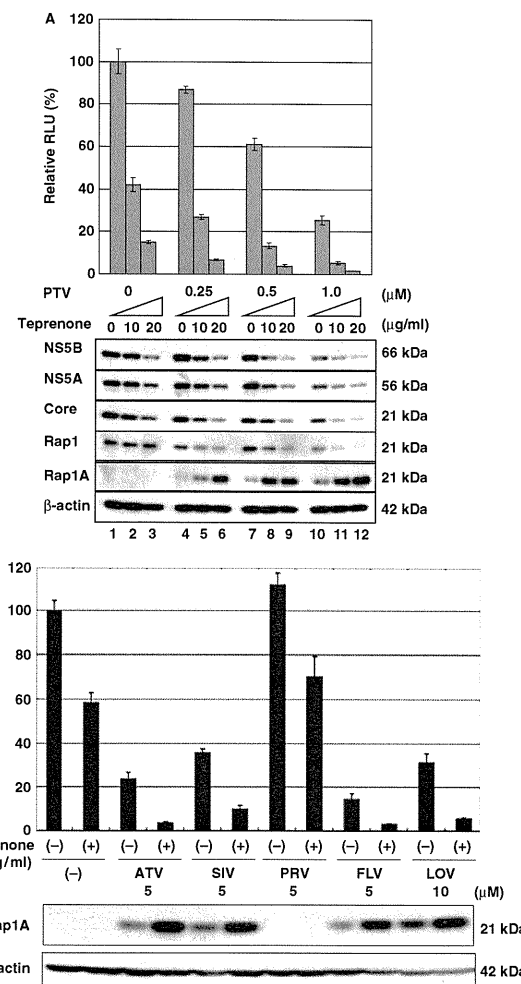
Discussion

In this study, we demonstrated that teprenone inhibited HCV RNA replication. Furthermore, teprenone exhibited anti-HCV activity in the genotype-2a JFH-1 infection system. Teprenone belongs to the geranyl compounds from its chemical structure and anti-ulcer agent from its clinical application. Therefore, we tested other geranyl compounds (GGOH and VK2, as well as geranylgeranoic acid) and

other anti-ulcer agents (ecabet sodium, sofalcone and gefarnate) for their effect on HCV RNA replication. However, only teprenone exhibited anti-HCV activity among the reagents tested. Therefore, the anti-HCV activity of teprenone is a unique feature among these reagents.

The interview form from Selbex providing company Eisai reported the plasma concentration of teprenone. When 150 mg of Selbex was administered orally, its maximum plasma concentration reached 2.2 μ g/ml. This is similar to the EC₅₀ (5.3 μ g/ml) of Selbex *in vitro*.

Ichikawa *et al.* (23) reported that teprenone induced the 2',5'-oligoadenylate synthetases (2',5'-OAS) in



human hepatoma cells. We demonstrated the activation of 2'5'-OAS and IFN-stimulated response element (ISRE) by IFN- α using the reporter assay system in our HuH-7-derived OR6 cells. However, we could not obtain evidence that teprenone activated both 2'5'-OAS and ISRE promoters (supporting information, Fig. S2A and B). Signal transducer and activator of transcription (STAT)1 and STAT2 were not phosphorylated after treatment with teprenone (supporting information, Fig. S2C). This discrepancy may have been caused by the heterogeneity of HuH-7 cells, because OR6 was selected as the clonal cell line and is highly susceptible to HCV RNA replication. Further study is needed to clarify the mechanism underlying teprenone's effect on IFN signalling.

Teprenone reportedly protects the gastric mucosa by inducing HSP (24). From this standpoint, the anti-HCV activity of teprenone was an unexpected result, because recently, it was reported that HSP90 is essential for HCV RNA replication and that an HSP90 inhibitor, geldanamycin, inhibits HCV RNA replication (25, 26). We examined whether or not teprenone induced HSP90 in hepatoma cells and found that it did not (supporting information, Fig. S4).

In this study, we monitored the geranylgeranylated state of Rap1A as a marker using nongeranylgeranylated Rap1A-detectable anti-Rap1A antibody (sc-1482). The least expected result of this sensitive geranylgeranylation assay is that teprenone enhanced statins' inhibitory action against geranylgeranylation. It is not clear in this study as to why teprenone enhanced statins' inhibitory action on geranylgeranylation. One possibility is that teprenone may cause biosynthesis from FPP to cholesterol rather than to GGPP by an unknown mechanism. To clarify this point, further study will be needed. This new function of teprenone may contribute to not only the antiviral field but also other fields, including studies on osteoporosis and on various kinds of antitumours, because geranylgeranylation and farnesylation are targets of the reagent in these fields. For example, statins interfere with the production of GGPP and FPP, which is important in the activation of small G proteins, such as K-ras and the Rho family, and disrupt the growth of malignant cells.

Recently, two important findings have been reported. Firstly, El-Serag *et al.* (8) reported that statins are associated with a reduced risk of HCC. Secondly, Abraldes *et al.* (9) reported that statin lowers portal pressure in patients with cirrhosis. Therefore, as teprenone is a strong adjuvant to statin's inhibitory action against geranylgeranylation, it may further improve portal hypertension in cirrhosis and reduce the risk of HCC in combination with statins. Although teprenone alone possesses modest anti-HCV activity, it will play a significant role in combination with IFN and/or statins in the therapy to HCV-associated liver diseases as an adjuvant like ribavirin. As teprenone is available in clinical use with a low side effect, a clinical study using

Teprenone inhibits HCV replication

teprenone in combination with IFN- α and/or statins is now underway in our institution.

In conclusion, we have shown that the anti-ulcer agent teprenone inhibited HCV RNA replication and enhanced statins' inhibitory action against geranylgeranylation. This newly discovered function of teprenone may contribute to improve the treatment of HCV-associated liver diseases (CH C, cirrhosis and HCC) as an adjuvant to statins.

Acknowledgements

The authors would like to thank Atsumi Morishita, Takashi Nakamura and Midori Takeda for their technical assistance. This work was supported by grants-in-aid for a third-term comprehensive 10-year strategy for cancer control and for research on hepatitis from the Ministry of Health, Labor, and Welfare of Japan. K. A. and K. M. were supported by a Research Fellowship from the Japan Society for the Promotion of Science (JSPS) for Young Scientists.

References

1. Feld JJ, Hoofnagle JH. Mechanism of action of interferon and ribavirin in treatment of hepatitis C. *Nature* 2005; **436**: 967–72.
2. Ikeda M, Abe K, Dansako H, *et al*. Efficient replication of a full-length hepatitis C virus genome, strain O, in cell culture, and development of a luciferase reporter system. *Biochem Biophys Res Commun* 2005; **329**: 1350–9.
3. Ikeda M, Abe K, Yamada M, *et al*. Different anti-HCV profiles of statins and their potential for combination therapy with interferon. *Hepatology* 2006; **44**: 117–25.
4. Ikeda M, Kato N. Modulation of host metabolism as a target of new antivirals. *Adv Drug Deliv Rev* 2007; **59**: 1277–89.
5. Ikeda M, Kato N. Life style-related diseases of the digestive system: cell culture system for the screening of anti-hepatitis C virus HCV reagents: suppression of HCV replication by statins and synergistic action with interferon. *J Pharmacol Sci* 2007; **105**: 145–50.
6. Kim SS, Peng LF, Lin W, *et al*. A cell-based, high-throughput screen for small molecule regulators of hepatitis C virus replication. *Gastroenterology* 2007; **132**: 311–20.
7. Bader T, Fazili J, Madhoun M, *et al*. Fluvastatin inhibits hepatitis C replication in humans. *Am J Gastroenterol* 2008; **103**: 1383–9.
8. El-Serag HB, Johnson ML, Hachem C, Morgana RO. Statins are associated with a reduced risk of hepatocellular carcinoma in a large cohort of patients with diabetes. *Gastroenterology* 2009; **136**: 1601–8.
9. Abraldes JG, Albillas A, Banares R, *et al*. Simvastatin lowers portal pressure in patients with cirrhosis and portal hypertension: a randomized controlled trial. *Gastroenterology* 2009; **136**: 1651–8.
10. Kapadia SB, Chisari FV. Hepatitis C virus RNA replication is regulated by host geranylgeranylation and fatty acids. *Proc Natl Acad Sci USA* 2005; **102**: 2561–6.
11. Ye J, Wang C, Sumpter R Jr, *et al*. Disruption of hepatitis C virus RNA replication through inhibition of host protein geranylgeranylation. *Proc Natl Acad Sci USA* 2003; **100**: 15865–70.
12. Wang C, Gale M Jr, Keller BC, *et al*. Identification of FBL2 as a geranylgeranylated cellular protein required for hepatitis C virus RNA replication. *Mol Cell* 2005; **18**: 425–34.
13. Lindenbach BD, Evans MJ, Syder AJ, *et al*. Complete replication of hepatitis C virus in cell culture. *Science* 2005; **309**: 623–6.
14. Wakita T, Pietschmann T, Kato T, *et al*. Production of infectious hepatitis C virus in tissue culture from a cloned viral genome. *Nat Med* 2005; **11**: 791–6.
15. Zhong J, Gastaminza P, Cheng G, *et al*. Robust hepatitis C virus infection in vitro. *Proc Natl Acad Sci USA* 2005; **102**: 9294–9.
16. Nanke Y, Kotake S, Ninomiya T, *et al*. Geranylgeranylace-tonine inhibits formation and function of human osteoclasts and prevents bone loss in tail-suspended rats and ovariectomized rats. *Calcif Tissue Int* 2005; **77**: 376–85.
17. Kato N, Sugiyama K, Nambu K, *et al*. Establishment of a hepatitis C virus subgenomic replicon derived from human hepatocytes infected in vitro. *Biochem Biophys Res Commun* 2003; **306**: 756–66.
18. Naka K, Ikeda M, Abe K, Dansako H, Kato N. Mizoribine inhibits hepatitis C virus RNA replication: effect of combination with interferon-alpha. *Biochem Biophys Res Commun* 2005; **330**: 871–9.
19. Dansako H, Naganuma A, Nakamura T, *et al*. Differential activation of interferon-inducible genes by hepatitis C virus core protein mediated by the interferon stimulated response element. *Virus Res* 2003; **97**: 17–30.
20. Ariumi Y, Kuroki M, Abe K, *et al*. DDX3 DEAD-box RNA helicase is required for hepatitis C virus RNA replication. *J Virol* 2007; **81**: 13922–6.
21. Hughes A, Rogers MJ, Idris AI, Crockett JC. A comparison between the effects of hydrophobic and hydrophilic statins on osteoclast function in vitro and ovariectomy-induced bone loss in vivo. *Calcif Tissue Int* 2007; **81**: 403–1.
22. Merrell MA, Wakchoure S, Lehenkari PP, Harris KW, Selander KS. Inhibition of the mevalonate pathway and activation of p38 MAP kinase are independently regulated by nitrogen-containing bisphosphonates in breast cancer cells. *Eur J Pharmacol* 2007; **570**: 27–37.
23. Ichikawa T, Nakao K, Nakata K, *et al*. Geranylgeranylace-tonine induces antiviral gene expression in human hepatoma cells. *Biochem Biophys Res Commun* 2001; **280**: 933–9.
24. Hirakawa T, Rokutan K, Niikawa T, Kishi K. Geranylgeranylace-tonine induces heat shock proteins in cultured guinea pig gastric mucosal cells and rat gastric mucosa. *Gastroenterology* 1996; **111**: 345–57.
25. Nakagawa S, Umehara T, Matsuda C, *et al*. Hsp90 inhibitors suppress HCV replication in replicon cells and humanized liver mice. *Biochem Biophys Res Commun* 2007; **353**: 882–8.
26. Okamoto T, Nishimura Y, Ichimura T, *et al*. Hepatitis C virus RNA replication is regulated by FKBP8 and Hsp90. *Embo J* 2006; **25**: 5015–25.

Supporting information

Additional supporting information may be found in the online version of this article:

Fig. S1. The effects of anti-ulcer agents on HCV RNA replication. (A) Cell proliferation assay. OR6 cells were treated with teprenone (0, 2.5, 5, 10, and 20 μ g/ml), and the cells at 24, 48, and 72 hours after treatment were subjected to WST-1 cell proliferation assay. (B) Structures of anti-ulcer agents. (C–E) OR6 cells were treated with acetab sodium (0, 2.5, 5, 10, 20 μ g/ml) (C), sofalcon (0, 2.5, 5, 10, 20 μ g/ml) (D), and gefarnate (0, 2.5, 5, 10, 20 μ g/ml) (E) for 72 hours. Then the cells were subjected to luciferase assay (upper panel) and Western blot analysis using anti-core, and anti- β -actin antibodies (lower panel) as shown in Figure 1B.

Fig. S2. Teprenone didn't activate IFN signaling pathway. (A and B) Luciferase assays for 2'5'OAS and ISRE promoters. p2'5'OAS-luc (A) and pISRE-luc (B) transfected OR6 cells were treated with teprenone (0, 2.5, 5, and 10 μ g/ml) or IFN- α (0, 2.5, 5, and 10 IU/ml) for 6 hours and then subjected to luciferase reporter assay. (C) Teprenone didn't activate STATs in OR6 cells. OR6 cells were treated with IFN- α (500 IU/ml), PTV (1.25 μ M), and teprenone (20 μ g/ml) for 0, 3, 6, and 12 hours. Then the cells were subjected to Western blot analysis using anti-STAT1 (Tyr701), anti-STAT1, anti-pSTAT2 (Tyr689), anti-core, and anti- β -actin antibodies.

Fig. S3. Teprenone treatment didn't cause positive feedback of HMG-CoA reductase (HMGCR). OR6 cells were treated with teprenone (20 μ g/ml), PTV (10 μ mol/L), or neither for 24 hours. The cells were subjected to RT-PCR (A) and real-time RT-quantitative PCR (B) using HMG-CoA reductase-specific primer set. H₂O was used as a negative control. GAPDH was used as an internal control.

Fig. S4. Teprenone didn't induce HSP90 or HSP70 in HuH-7 cells. OR6 cells were treated with teprenone (20 μ g/ml) for 0, 3, 6, 12, 24, and 48 hours. Then the cells were subjected to Western blot analysis using anti-HSP90, anti-HSP70 anti-core, and anti- β -actin antibodies.

Please note: Wiley-Blackwell is not responsible for the content or functionality of any supporting materials supplied by the authors. Any queries (other than missing material) should be directed to the corresponding author for the article.

Hepatitis C Virus Hijacks P-Body and Stress Granule Components around Lipid Droplets[†]

Yasuo Ariumi,^{1,2*} Misao Kuroki,¹ Yukihiro Kusuma,³ Kanae Osugi,⁴ Makoto Hijikata,³ Masatoshi Maki,⁴ Masanori Ikeda,¹ and Nobuyuki Kato¹

Department of Tumor Virology, Okayama University Graduate School of Medicine, Dentistry, and Pharmaceutical Sciences, Okayama 700-8535, Japan;¹ Center for AIDS Research, Kumamoto University, Kumamoto 860-0811, Japan;² Department of Viral Oncology, Institute for Virus Research, Kyoto University, Kyoto 606-8507, Japan;³ and Department of Applied Molecular Biosciences, Graduate School of Biogricultural Sciences, Nagoya University, Nagoya 464-8601, Japan⁴

Received 19 November 2010/Accepted 21 April 2011

The microRNA miR-122 and DDX6/Rck/p54, a microRNA effector, have been implicated in hepatitis C virus (HCV) replication. In this study, we demonstrated for the first time that HCV-JFH1 infection disrupted processing (P)-body formation of the microRNA effectors DDX6, Lsm1, Xrn1, PATL1, and Ago2, but not the decapping enzyme DCP2, and dynamically redistributed these microRNA effectors to the HCV production factory around lipid droplets in HuH-7-derived RSc cells. Notably, HCV-JFH1 infection also redistributed the stress granule components GTPase-activating protein (SH3 domain)-binding protein 1 (G3BP1), ataxin-2 (ATX2), and poly(A)-binding protein 1 (PABP1) to the HCV production factory. In this regard, we found that the P-body formation of DDX6 began to be disrupted at 36 h postinfection. Consistently, G3BP1 transiently formed stress granules at 36 h postinfection. We then observed the ringlike formation of DDX6 or G3BP1 and colocalization with HCV core after 48 h postinfection, suggesting that the disruption of P-body formation and the hijacking of P-body and stress granule components occur at a late step of HCV infection. Furthermore, HCV infection could suppress stress granule formation in response to heat shock or treatment with arsenite. Importantly, we demonstrate that the accumulation of HCV RNA was significantly suppressed in DDX6, Lsm1, ATX2, and PABP1 knockdown cells after the inoculation of HCV-JFH1, suggesting that the P-body and the stress granule components are required for the HCV life cycle. Altogether, HCV seems to hijack the P-body and the stress granule components for HCV replication.

Hepatitis C virus (HCV) is the causative agent of chronic hepatitis, which progresses to liver cirrhosis and hepatocellular carcinoma. HCV is an enveloped virus with a positive single-stranded 9.6-kb RNA genome, which encodes a large polyprotein precursor of approximately 3,000 amino acid (aa) residues. This polyprotein is cleaved by a combination of the host and viral proteases into at least 10 proteins in the following order: core, envelope 1 (E1), E2, p7, nonstructural 2 (NS2), NS3, NS4A, NS4B, NS5A, and NS5B (12, 13, 21). The HCV core protein, a nucleocapsid, is targeted to lipid droplets (LDs), and the dimerization of the core protein by a disulfide bond is essential for the production of infectious virus (24). Recently, LDs have been found to be involved in an important cytoplasmic organelle for HCV production (26). Budding is an essential step in the life cycle of enveloped viruses. The endosomal sorting complex required for transport (ESCRT) system has been involved in such enveloped virus budding machineries, including that of HCV (5).

DEAD-box RNA helicases with ATP-dependent RNA-unwinding activities have been implicated in various RNA metabolic processes, including transcription, translation, RNA splicing, RNA transport, and RNA degradation (32). Previously, DDX3 was identified as an HCV core-interacting pro-

tein by yeast two-hybrid screening (25, 29, 43). Indeed, DDX3 is required for HCV RNA replication (3, 31). DDX6 (Rck/p54) is also required for HCV replication (16, 33). DDX6 interacts with an initiation factor, eukaryotic initiation factor 4E (eIF4E), to repress the translational activity of mRNPs (38). Furthermore, DDX6 regulates the activity of the decapping enzymes DCP1 and DCP2 and interacts directly with Argonaute-1 (Ago1) and Ago2 in the microRNA (miRNA)-induced silencing complex (miRISC) and is involved in RNA silencing. DDX6 localizes predominantly in the discrete cytoplasmic foci termed the processing (P) body. Thus, the P body seems to be an aggregate of translationally repressed mRNPs associated with the translation repression and mRNA decay machinery.

In addition to the P body, eukaryotic cells contain another type of RNA granule termed the stress granule (SG) (1, 6, 22, 30). SGs are aggregates of untranslating mRNAs in conjunction with a subset of translation initiation factors (eIF4E, eIF3, eIF4A, eIFG, and poly(A)-binding protein [PABP]), the 40S ribosomal subunits, and several RNA-binding proteins, including PABP, T cell intracellular antigen 1 (TIA-1), TIA-1-related protein (TIAR), and GTPase-activating protein (SH3 domain)-binding protein 1 (G3BP1). SGs regulate mRNA translation and decay as well as proteins involved in various aspects of mRNA metabolism. SGs are cytoplasmic phase-dense structures that occur in eukaryotic cells exposed to various environmental stress, including heat, arsenite, viral infection, oxidative conditions, UV irradiation, and hypoxia. Impor-

tantly, several viruses target SGs and stress granule components for viral replication (10, 11, 34, 39). Recent studies suggest that SGs and the P body physically interact and that mRNAs may move between the two compartments (1, 6, 22, 28, 30).

miRNAs are a class of small noncoding RNA molecules (~21 to 22 nucleotides [nt] in length). miRNAs usually interact with 3'-untranslated regions (UTRs) of target mRNAs, leading to the downregulation of mRNA expression. Notably, the liver-specific and abundant miR-122 interacts with the 5'-UTR of the HCV RNA genome and facilitates HCV replication (15, 17, 19, 20, 31). Ago2 is at least required for the efficient miR-122 regulation of HCV RNA accumulation and translation (40). However, the molecular mechanism(s) for how DDX6 and miR-122 as well as DDX3 positively regulate HCV replication is not fully understood. Therefore, we investigated the potential role of P-body and stress granule components in HCV replication.

MATERIALS AND METHODS

Cell culture. 293FT cells were cultured in Dulbecco's modified Eagle's medium (DMEM; Invitrogen, Carlsbad, CA) supplemented with 10% fetal bovine serum (FBS). HuH-7-derived RSc cells, in which cell culture-generated HCV-JFH1 (JFH1 strain of genotype 2a) (37) could infect and effectively replicate, were cultured in DMEM with 10% FBS as described previously (3–5, 23).

Plasmid construction. To construct pCDNA3-FLAG-DDX6, a DNA fragment encoding DDX6 was amplified from total RNAs derived from RSc cells by reverse transcription (RT)-PCR using KOD-Plus RNA polymerase (ToyoBo) and the following pairs of primers: 5'-CGGGATCCAAGATGAGCACGCC AGAACAGAGAACCCCTGTT-3' (forward) and 5'-CCGCTCTGAGTAAAGGT TTCTCATCTCTACAGGCTCGCT-3' (reverse). The obtained DNA fragments were subcloned into either BamHI-XbaI site of the pCDNA3-FLAG vector (2), and the nucleotide sequences were determined by BigDye termination cycle sequencing using an ABI Prism 310 genetic analyzer (Applied Biosystems, Foster City, CA).

RNA interference. The following small interfering RNAs (siRNAs) were used: human ATXN2/ATX2/ataxin-2 (siGENOME SMRT pool M-011772-01-005), human PABP1/PABP1c (siGENOME SMRT pool M-019598-01-005), human Lsm1 (siGENOME SMRT pool M-005124-01-005), human Xrn1 (siGENOME SMRT pool M-013754-01-005), human G3BP1 (ON-TARGETplus SMRT pool L-012099-00-005), human PATL1 (siGENOME SMRT pool M-015591-00-005), and siGENOME nontargeting siRNA pool 1 (D-001206-13-05) (Dharmacon, Thermo Fisher Scientific, Waltham, MA), as a control. siRNAs (25 nM final concentration) were transiently transfected into RSc cells (3–5, 23) using Oligofectamine (Invitrogen) according to the manufacturer's instructions. Oligonucleotides with the following sense and antisense sequences were used for the cloning of short hairpin RNA (shRNA)-encoding sequences targeted to DDX6 (DDX6) as well as the control nontargeting shRNA (shCon) in a lentiviral vector: 5'-GATCC CCGGAGAACCTACTGAACTGAGAGACTTCAGAGTTCAGTTCTCC CCTTTTGAAA-3' (sense) and 5'-AGCTTTCACAAAAGGAGGAACCTAA CTCCTGAGTCCTCTGAACTGAGAGTTCCTCCGGG-3' (antisense) for DDX6 and 5'-GATCCGGAACTCTCAGAGGTAATCTACTCTAACAGAGA GTAGATTACCTCTGAACTCTTCTTGTGAAA-3' (sense) and 5'-AGCTTTCAC AAAAGAACCTCAGAGGTAATCTACTCTGAGAGTTCAGTTCTC TGGATTCGGG-3' (antisense) for shCon. The oligonucleotides described above were annealed and subcloned into the BglII-HindIII site, downstream from an RNA polymerase III promoter of pSUPER (8), to generate pSUPER-DDX6 and pSUPER-shCon, respectively. To construct pLV-DDX6 and pLV-shCon, the BamHI-Sall fragments of the corresponding pSUPER plasmids were subcloned into the BamHI-Sall site of pRDI292, an HIV-1-derived self-inactivating lentiviral vector containing a puromycin resistance marker allowing for the selection of transduced cells (7). pLV-DDX6, described previously (3), was used.

Lentiviral vector production. The vesicular stomatitis virus G protein (VSV-G)-pseudotyped HIV-1-based vector system was described previously (27, 44). The lentiviral vector particles were produced by the transient transfection of the second-generation packaging construct pCMV-ΔR8.91 (27, 44), the VSV-G

envelope-expressing plasmid pMDG2, as well as pRDI292 into 293FT cells with FuGene6 reagent (Roche Diagnostics, Mannheim, Germany).

HCV infection experiments. The supernatants were collected from cell culture-generated HCV-JFH1 (37)-infected RSc cells (3–5, 23) at 5 days postinfection and stored at -80°C after filtering through a 0.45-μm filter (Kurabo, Osaka, Japan) until use. For infection experiments with HCV-JFH1, RSc cells (1 × 10⁵ cells/well) were plated onto 6-well plates and cultured for 24 h. We then infected the cells at a multiplicity of infection (MOI) of 1 or 4. The culture supernatants were collected at 48 h postinfection, and the levels of the core protein were determined by an enzyme-linked immunosorbent assay (ELISA) (Mitsubishi Kagaku Bio-Clinical Laboratories, Tokyo, Japan). Total RNA was also isolated from the infected cellular lysates by using an RNeasy mini kit (Qiagen, Hilden, Germany) for analysis of intracellular HCV RNA. The infectivity of HCV-JFH1 in the culture supernatants was determined by a focus-forming assay at 48 h postinfection. HCV-JFH1-infected cells were detected by using anti-HCV core (CP-9 and CP-11 mixture).

Quantitative RT-PCR analysis. The quantitative RT-PCR analysis of HCV RNA was performed by real-time LightCycler PCR (Roche) as described previously (3–5, 14, 23). We used the following forward and reverse primers set for the real-time LightCycler PCR: 5'-ATGAGTCATGTTGGAGTGGAA-3' (forward) and 5'-CTGGCTGACTTCTCCAC-3' (reverse) for DDX3, 5'-ATG AGCACGCCAGAACAGA-3' (forward) and 5'-TTGCTGTCTGTTGCG CCC-3' (reverse) for DDX6, 5'-TACGGGGTCACCCACATG-3' (forward) and 5'-AACGCTGAGCCGCGCTCGGT-3' (reverse) for β-actin, and 5'-AGA GCGCATGTTGCTGGCG-3' (forward) and 5'-CTTGCACACCCACGC TAC-3' (reverse) for HCV-JFH1.

Preparation of anti-PATL1 antibody. The anti-PATL1 antiserum was raised in rabbits using the glutathione S-transferase (GST)-fused PATL1 Ct (C-terminal region of PATL1, aa 450 to 770) as an antigen, and immunoglobulins were affinity purified by using the maltose-binding protein (MBP)-fused PATL1 Ct that was immobilized on an N-hydroxysuccinimide (NHS) column (GE Healthcare Bio-Sciences AB, Uppsala, Sweden).

Preparation of LDs. Lipid droplets (LDs) were prepared as described previously (26). Cells were pelleted by centrifugation at 1,500 rpm. The pellet was resuspended in hypotonic buffer (50 mM HEPES [pH 7.4], 1 mM EDTA, 2 mM MgCl₂) supplemented with a protease inhibitor cocktail (Nacalai Tesque, Kyoto, Japan) and was incubated for 10 min at 4°C. The suspension was homogenized with 30 strokes of a glass Dounce homogenizer using a tight-fitting pestle (Wheaton, Millville, NJ). A 1/10 volume of 10× isotonic buffer (0.2 M HEPES [pH 7.4], 1.2 M potassium acetate (KoAc), 40 mM magnesium acetate [Mg(OAc)₂], and 50 mM diithiothreitol (DTT)) was added to the homogenate. The nuclei were removed by centrifugation at 2,000 rpm for 10 min at 4°C. The supernatant was collected and centrifuged at 16,000 × g for 10 min at 4°C. The supernatant was mixed with an equal volume of 1.04 M sucrose in isotonic buffer (50 mM HEPES, 100 mM KCl, 2 mM MgCl₂, and protease inhibitor cocktail). The solution was set in a 13.2-ml Polycarbonate centrifuge tube (Beckman Coulter, Brea, CA). One milliliter of isotonic buffer was loaded onto the sucrose mixture. The tube was centrifuged at 100,000 × g in an SW41T rotor (Beckman Coulter) for 1 h at 4°C. After the centrifugation, the LD fraction on the top of the gradient solution was recovered in phosphate-buffered saline (PBS). The collected LD fraction was used for Western blot analysis.

Western blot analysis. Cells were lysed in a buffer containing 50 mM Tris-HCl (pH 8.0), 150 mM NaCl, 4 mM EDTA, 1% Nonidet P-40, 0.1% sodium dodecyl sulfate (SDS), 1 mM DTT, and 1 mM phenylmethylsulfonyl fluoride. Supernatants from these lysates were subjected to SDS-polyacrylamide gel electrophoresis, followed by immunoblot analysis using anti-DDX6 (catalog no. M4257 [NT] and M428 [IN]; Anaspec, San Jose, CA), anti-DDX6 (A300-460a; Bethyl Laboratories, Montgomery, TX), anti-adipose differentiation-related protein (ADRP; GTx110204; Genetex, San Antonio, TX), anti-calnexin (NT; Stressgen, Ann Arbor, MI), anti-HCV core (CP-9 and CP-11; Institute of Immunology, Tokyo, Japan), anti-β-actin antibody (A5441; Sigma, St. Louis, MO), anti-ATX2/SCA2 antibody (A302-033A; Bethyl), anti-PABP (sc-32318 [10E10]; Santa Cruz Biotechnology, Santa Cruz, CA), anti-PABP (ab21060; Abcam, Cambridge, United Kingdom), anti-G3BP1 (611126; BD Transduction Laboratories, San Jose, CA), anti-LSM1 (LS-C97364; Life Span Biosciences, Seattle, WA), anti-HSP70 (610607; BD), anti-XRN1 (A300-443A; Bethyl), or anti-PATL1 antibody.

Immunofluorescence and confocal microscopic analysis. Cells were fixed in 3.6% formaldehyde in PBS, permeabilized in 0.1% NP-40 in PBS at room temperature, and incubated with anti-DDX6 antibody (M4257 [NT] and M428 [IN]; Anaspec), anti-DDX3X (LS-C64576; Life Span), anti-DDX6 (A300-460a; Bethyl), anti-HCV core (CP-9 and CP-11), anti-ATX2/SCA2 antibody (A302-033A; Bethyl), anti-ataxin-2 (611378; BD), anti-PABP (ab21060; Abcam), anti-G3BP1 (A302-033A; Bethyl), anti-LSM1 (LS-C97364; Life Span), anti-XRN1

* Corresponding author. Mailing address: Center for AIDS Research, Kumamoto University, 2-2-1 Honjo, Kumamoto 860-0811, Japan. Phone and fax: 81 96 373 6834. E-mail: ariumi@kumamoto-u.ac.jp.
† Published ahead of print on 4 May 2011.

(A300-443A; Bethyl), anti-Dcp2 (A302-597A; Bethyl), anti-human Ago2 (011-22033; Wako, Osaka, Japan), or anti-PATL1 antibody at a 1:300 dilution in PBS containing 3% bovine serum albumin (BSA) for 30 min at 37°C. The cells were then stained with fluorescein isothiocyanate (FITC)-conjugated anti-rabbit antibody (Jackson ImmunoResearch, West Grove, PA) at a 1:300 dilution in PBS containing BSA for 30 min at 37°C. Lipid droplets and nuclei were stained with borodipyromethene (BODIPY) 493/503 (Molecular Probes, Invitrogen) and DAPI (4',6-diamidino-2-phenylindole), respectively, for 15 min at room temperature. Following extensive washing in PBS, the cells were mounted onto slides using a mounting medium of 90% glycerin–10% PBS with 0.01% *p*-phenylene-diamine added to reduce fading. Samples were viewed under a confocal laser scanning microscope (LSM510; Zeiss, Jena, Germany).

Statistical analysis. A statistical comparison of the infectivities of HCV in the culture supernatants between the knockout cells and the control cells was performed by using the Student *t* test. *P* values of less than 0.05 were considered statistically significant. All error bars indicate standard deviations.

RESULTS

HCV infection hijacks the P-body components. To investigate the potential role of P-body components in the HCV life cycle, we first examined the alteration of the subcellular localization of DDX3 or DDX6 by HCV-JFH1 infection using confocal laser scanning microscopy as previously described (2), since both DDX3 and DDX6 were identified previously as P-body components (6). For this, we used Huh-7-derived RSc cells, in which cell culture-generated HCV-JFH1 (JFH1 strain of genotype 2a) (37) can infect and effectively replicate (3, 4, 23). HCV-JFH1-infected RSc cells at 60 h postinfection were stained with anti-HCV core antibody, anti-DDX3, and/or anti-DDX6. Lipid droplets (LDs) and nuclei were stained with BODIPY 493/503 and DAPI (4',6-diamidino-2-phenylindole), respectively. Samples were viewed under a confocal laser scanning microscope. Although we observed that endogenous DDX3 localized in faint cytoplasmic foci in uninfected RSc cells, DDX3 relocalized, formed ringlike structures, and colocalized with the HCV core protein in response to HCV-JFH1 infection (Fig. 1A). On the other hand, endogenous DDX6 was localized in the evident cytoplasmic foci termed P bodies in the uninfected cells (Fig. 1A). DDX6 also relocalized, formed ringlike structures, and colocalized with the core protein in response to HCV-JFH1 infection (Fig. 1A). Although we failed to observe that most of the P bodies of DDX6 perfectly colocalized with DDX3 in uninfected RSc cells (Fig. 1B), we observed a few P bodies of DDX6 colocalized with DDX3 in the uninfected cells (Fig. 1B, arrowheads). Intriguingly, we found that endogenous DDX3 colocalized with endogenous DDX6 in HCV-JFH1-infected cells (Fig. 1B). To further confirm this finding, pHA-DDX3 (41) and pcDNA3-FLAG-DDX6 were cotransfected into 293FT cells. Consequently, we observed that hemagglutinin (HA)-DDX3 colocalized with FLAG-DDX6 in 293FT cells coexpressing HA-DDX3 and FLAG-DDX6 (Fig. 1B), suggesting cross talk of DDX3 with DDX6. Recently, LDs have been found to be involved in an important cytoplasmic organelle for HCV production (26). Indeed, both DDX3 and DDX6 were recruited around LDs in response to HCV infection, while these proteins did not colocalize with LDs in uninfected naïve RSc cells (Fig. 1C). Furthermore, both DDX3 and DDX6 accumulated in the LD fraction of the HCV-JFH1-infected RSc cells; however, we could not detect both proteins in the LD fraction from uninfected control cells (Fig. 1D), suggesting that DDX3 and

DDX6 are recruited around LDs in response to HCV infection.

These results suggest that HCV-JFH1 infection disrupts P-body formation. Therefore, we further examined whether or not HCV-JFH1 disrupts the P-body formations of other microRNA effectors, including Ago2; the Sm-like protein Lsm1, which is a subunit of heptameric-ring Lsm1-7, involved in decapping; the 5'-to-3' exonuclease Xrn1; the decapping activator PATL1; and the decapping enzyme DCP2 (6, 21, 30). As expected, HCV-JFH1 disrupted the P-body formations of Ago2, Lsm1, and Xrn1 as well as PATL1 (Fig. 2). Lsm1, Xrn1, or PATL1 relocalized, formed ringlike structures, and colocalized with the HCV core protein in response to HCV-JFH1 infection, whereas they were localized predominantly in P bodies in uninfected RSc cells (Fig. 2). In fact, we observed that DDX6 colocalized with Ago2, a P-body marker (Fig. 2). In contrast, HCV-JFH1 failed to disrupt the P-body formation of DCP2 (Fig. 2). Thus, these results suggest that HCV disrupts P-body formation through the hijacking of P-body components.

HCV hijacks stress granule components. Since Nonhoff et al. recently reported that DDX6 interacted with ataxin-2 (ATX2) (28), we examined the potential cross talk among DDX6, ATX2, and HCV. Although ATX2 and G3BP1, a well-known stress granule component (36), were dispersed in the cytoplasm at 37°C, both proteins formed discrete aggregates termed stress granules and colocalized with each other in response to heat shock at 43°C for 45 min, indicating that ATX2 is also stress granule component (Fig. 3A). We did not observe prominent colocalization between DDX6 and ATX2 at 37°C (Fig. 3B). In contrast, we found that DDX6 was recruited, juxtaposed, and partially colocalized with stress granules of ATX2 in response to heat shock at 43°C for 45 min in the uninfected RSc cells (Fig. 3B). Notably, ATX2 was recruited, formed the ring-like structures, and partially colocalized with DDX6 in response to HCV-JFH1 infection even at 37°C (Fig. 3B). Furthermore, we noticed that ATX2 was recruited around LDs in HCV-JFH1-infected cells at 72 h postinfection, while ATX2 did not colocalize with LDs in uninfected cells (Fig. 3C), suggesting the colocalization of ATX2 with the HCV core protein in infected cells. Indeed, ATX2 colocalized with the HCV core protein in HCV-JFH1-infected RSc cells at 37°C (Fig. 3D). Moreover, HCV-JFH1 infection induced the colocalization of the core protein with other stress granule components, G3BP1 or PABP1 as well as ATX2 (Fig. 4 and 5). To further confirm our findings, we examined the time course of the redistribution of DDX6 and G3BP1 after inoculation with HCV-JFH1. Consequently, we still detected the P-body formation of DDX6 and dispersed G3BP1 in the cytoplasm, and we did not observe a colocalization between the HCV core protein and DDX6 at 12 and 24 h postinfection (Fig. 4). In contrast, we found that the P-body formation of DDX6 began to be disrupted at 36 h postinfection (Fig. 4). Consistently, G3BP1 formed stress granules at 36 h postinfection (Fig. 4). We then noticed a ringlike formation of DDX6 or G3BP1 and colocalization with the HCV core protein after 48 h postinfection (Fig. 4), suggesting that the disruption of P-body formation and the hijacking of P-body and stress granule components occur in a late step of HCV infection.

We then examined whether or not HCV-JFH1 infection

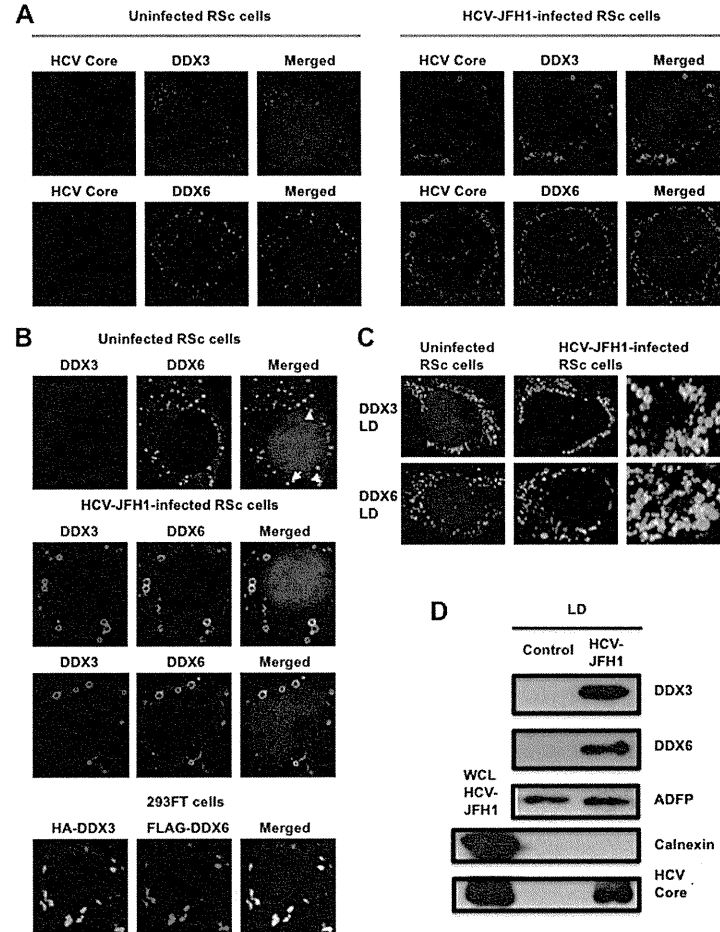


FIG. 1. Dynamic recruitment of DDX3 and DDX6 around lipid droplets (LDs) in response to HCV-JFH1 infection. (A) HCV-JFH1 disrupts the P-body formation of DDX6. Cells were fixed at 60 h postinfection and were then examined by confocal laser scanning microscopy. Cells were stained with anti-HCV core (CP-9 and CP-11 mixture) and either anti-DDX3 (54257 and 54258 mixture) or anti-DDX6 (A300-460A) antibody and then visualized with FITC (DDX3 or DDX6) or Cy3 (core). Images were visualized by using confocal laser scanning microscopy. The two-color overlay images are also exhibited (merged). Colocalization is shown in yellow. (B) HCV-JFH1 recruits DDX3 or DDX6 around LDs. Cells were stained with either anti-DDX3 or anti-DDX6 antibody and were then visualized with Cy3 (red). Lipid droplets and nuclei were stained with BODIPY 493/503 (green) and DAPI (blue), respectively. A high-magnification image is also shown. (C) Colocalization of DDX3 with DDX6. HCV-JFH1-infected RSc cells at 60 h postinfection were stained with anti-DDX3 (L-S-C64576) and anti-DDX6 (A300-460A) antibodies. 293FT cells cotransfected with 100 ng of pcDNA3-FLAG-DDX6 and 100 ng of pHA-DDX3 (41) were stained with anti-FLAG-Cy3 and anti-HA-FITC antibodies (Sigma). (D) Association of DDX3 and DDX6 with LDs in response to HCV-JFH1 infection. The LD fraction and whole-cell lysates (WCL) were collected from uninfected RSc cells (control) or HCV-JFH1-infected RSc cells at 5 days postinfection. The results of Western blot analyses of DDX3, DDX6, and the LD marker ADPF and the endoplasmic reticulum (ER) marker calnexin in the LD fraction are shown.

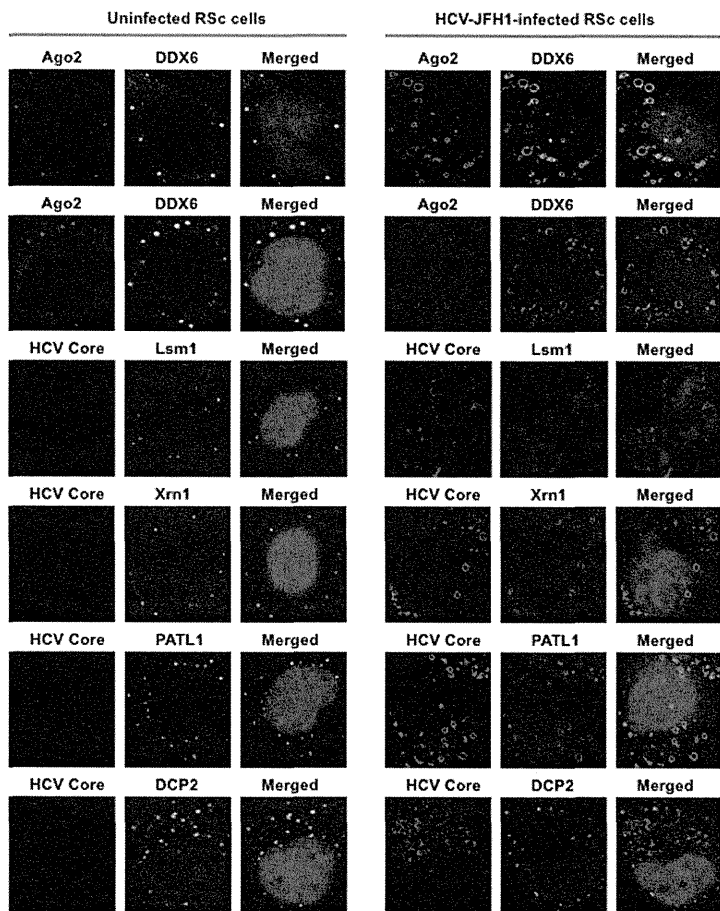


FIG. 2. HCV disrupts the P-body formation of microRNA effectors. Uninfected RSC cells and HCV-JFH1-infected RSC cells at 72 h postinfection were stained with anti-humanAGO2 (011-22033) and anti-DDX6 (A300-460A) antibodies. The cells were also stained with anti-HCV core and anti-Lsm1 (LS-C97364), anti-Xrn1 (A300-443A), anti-PATL1, or anti-DCP2 (A302-597A) antibodies and were examined by confocal laser scanning microscopy.

could affect the stress granule formation of G3BP1, ATX2, or PABP1 in response to heat shock or treatment with arsenite. These stress granule components dispersed in the cytoplasm at 37°C, whereas these proteins formed stress granules in response to heat shock at 43°C for 45 min or treatment with 0.5 mM arsenite for 30 min (Fig. 5). Furthermore, Western blot analysis of cell lysates of uninfected or HCV-JFH1-infected cells at 72 h postinfection showed similar protein expression levels of ATX2, PABP1, HSP70, DDX3, DDX6, and Lsm1 but not G3BP1 (Fig. 6), suggesting that HCV-JFH1 infection does not affect host mRNA translation.

P-body and stress granule components are required for HCV replication. Finally, we investigated the potential role of

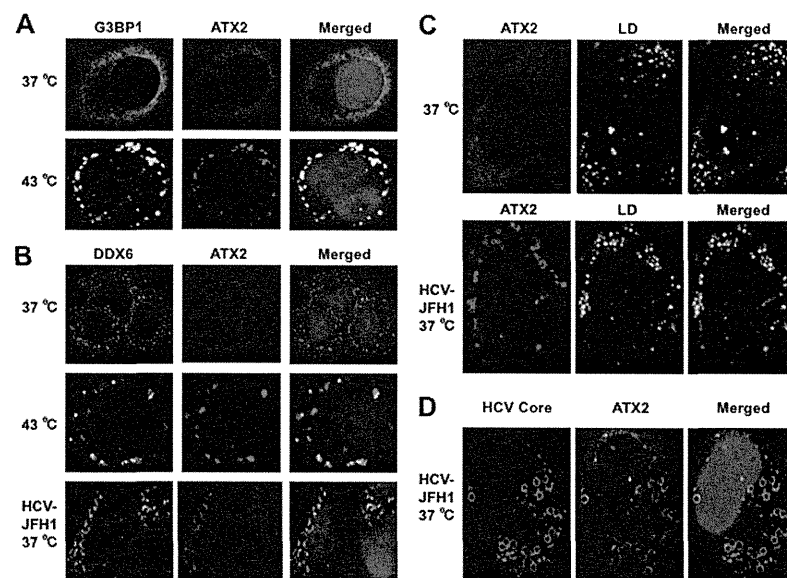


FIG. 3. Dynamic redistribution of ataxin-2 (ATX2) around LDs in response to HCV-JFH1 infection. (A) ATX2 is a stress granule component. RSC cells were incubated at 37°C or 43°C for 45 min. Cells were stained with anti-G3BP1 (A302-033A) and anti-ATX2 (A93520) antibodies and were examined by confocal laser scanning microscopy. (B) Dynamic redistribution of DDX6 and ATX2 in response to heat shock or HCV infection. RSC cells after heat shock at 43°C for 45 min or 72 h after inoculation with HCV-JFH1 were stained with anti-DDX6 and anti-ATX2 (A93520) antibodies. (C) HCV relocates ataxin-2 to LDs. HCV-JFH1-infected RSC cells at 72 h postinfection were stained with anti-ATX2 (A93520) antibody and BODIPY 493/503. (D) ATX2 colocalizes with the HCV core protein. HCV-JFH1-infected RSC cells at 72 h postinfection were stained with anti-ATX2/SCA2 (A301-118A) and anti-HCV core antibodies.

P-body and stress granule components in the HCV life cycle. We first used lentiviral vector-mediated RNA interference to stably knock down DDX6 as well as DDX3 in RSC cells. We used puromycin-resistant pooled cells 10 days after lentiviral transduction in all experiments. Real-time LightCycler RT-PCR analysis of DDX3 or DDX6 demonstrated a very effective knockdown of DDX3 or DDX6 in RSC cells transduced with lentiviral vectors expressing the corresponding shRNAs (Fig. 7A). Importantly, shRNAs did not affect cell viabilities (data not shown). We next examined the levels of HCV core and the infectivity of HCV in the culture supernatants as well as the level of intracellular HCV RNA in these knockdown cells 24 h after HCV-JFH1 infection at an MOI of 4. The results showed that the accumulation of HCV RNA was significantly suppressed in DDX3 or DDX6 knockdown cells (Fig. 7B). In this context, the release of the HCV core protein and the infectivity of HCV in the culture supernatants were also significantly suppressed in these knockdown cells (Fig. 7C and D). This finding suggested that DDX6 is required for HCV replication, like DDX3. To further examine the potential role of other P-body and stress granule components in HCV replication, we used RSC cells transiently transfected with a pool of siRNAs specific for ATX2, PABP1, Lsm1, Xrn1, G3BP1, and PATL1 as well as a pool of control siRNAs (siCon) following HCV-

JFH1 infection. In spite of the very effective knockdown of each component (Fig. 7E), the siRNAs used in these experiments did not affect cell viabilities (data not shown). Consequently, the accumulation of HCV RNA was significantly suppressed in ATX2, PABP1, or Lsm1 knockdown cells (Fig. 7F), indicating that ATX2, PABP1, and Lsm1 are required for HCV replication. In contrast, the level of HCV RNA was not affected in Xrn1 knockdown cells (Fig. 7F), suggesting that Xrn1 is unrelated to HCV replication. Furthermore, we observed a moderate effect of siG3BP1 and siPATL1 on HCV RNA replication (Fig. 7F). Altogether, HCV seems to hijack the P-body and stress granule components around LDs for HCV replication.

DISCUSSION

So far, the P body and stress granules have been implicated in mRNA translation, RNA silencing, and RNA degradation as well as viral infection (1, 6, 22, 30). Host factors within the P body and stress granules can enhance or limit viral infection, and some viral RNAs and proteins accumulate in the P body and/or stress granules. Indeed, the microRNA effectors DDX6, GW182, Lsm1, and Xrn1 negatively regulate HIV-1 gene expression by preventing the association of viral mRNA

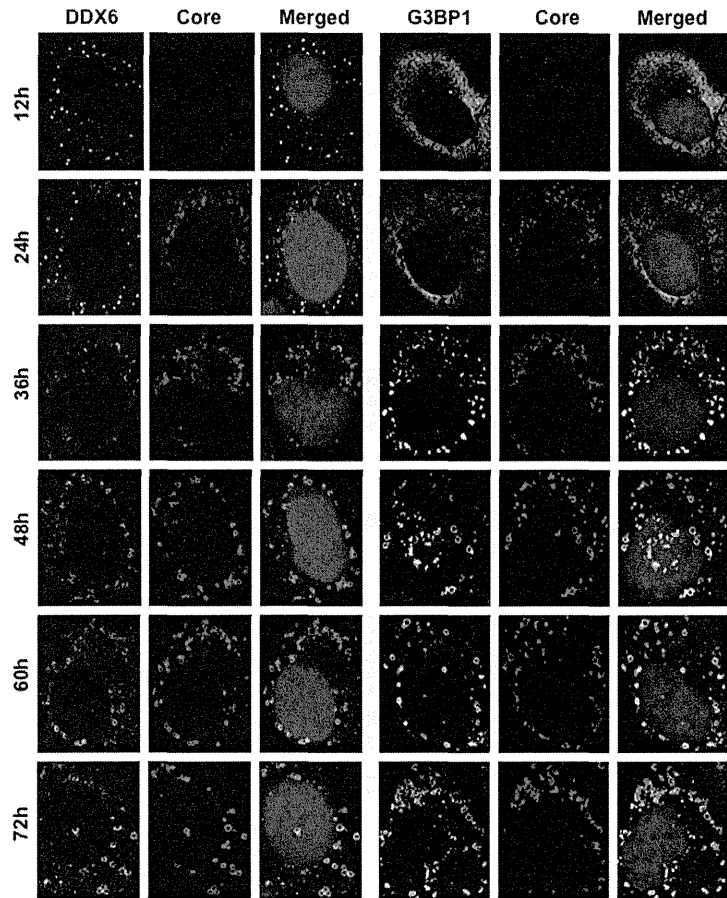


FIG. 4. Dynamic redistribution of DDX6 and G3BP1 in response to HCV-JFH1 infection. RSc cells at the indicated times (hours) after inoculation with HCV-JFH1 were stained with anti-HCV core and either anti-DDX6 (A300-460A) or anti-G3BP1 (A302-033A) antibodies.

with polysomes (9). In contrast, miRNA effectors such as DDX6, Lsm1, PatL1, and Ago2 positively regulate HCV replication (Fig. 7B and F) (16, 31, 33). We have also found that DDX3 and DDX6 are required for HCV RNA replication (3) (Fig. 7B) and that DDX3 colocalized with DDX6 in HCV-JFH1-infected RSc cells (Fig. 1B), suggesting that DDX3 co-modulates the DDX6 function in HCV RNA replication. In this regard, the liver-specific miR-122 interacts with the 5'-UTR of the HCV RNA genome and positively regulates HCV replication (15, 17, 19, 20, 31). Since miRNAs usually interact with DDX6 and Ago2 in miRISC and are involved in RNA silencing, DDX6 and Ago2 may be required for miR-122-

dependent HCV replication. Indeed, quite recently, a study showed that Ago2 is required for miR-122-dependent HCV RNA replication and translation (40). However, little is known regarding how miR-122 and DDX6 positively regulate HCV replication. Accordingly, we have shown that these miRNA effectors, including DDX6, Lsm1, Xrn1, and Ago2, accumulated around LDs and the HCV production factory and colocalized with the HCV core protein in response to HCV infection (Fig. 1 and 2). However, the decapping enzyme DCP2 did not accumulate and colocalize with the core protein (Fig. 2). Consistent with this finding, Scheller et al. reported previously that the depletion of DCP2 by siRNA did not affect HCV

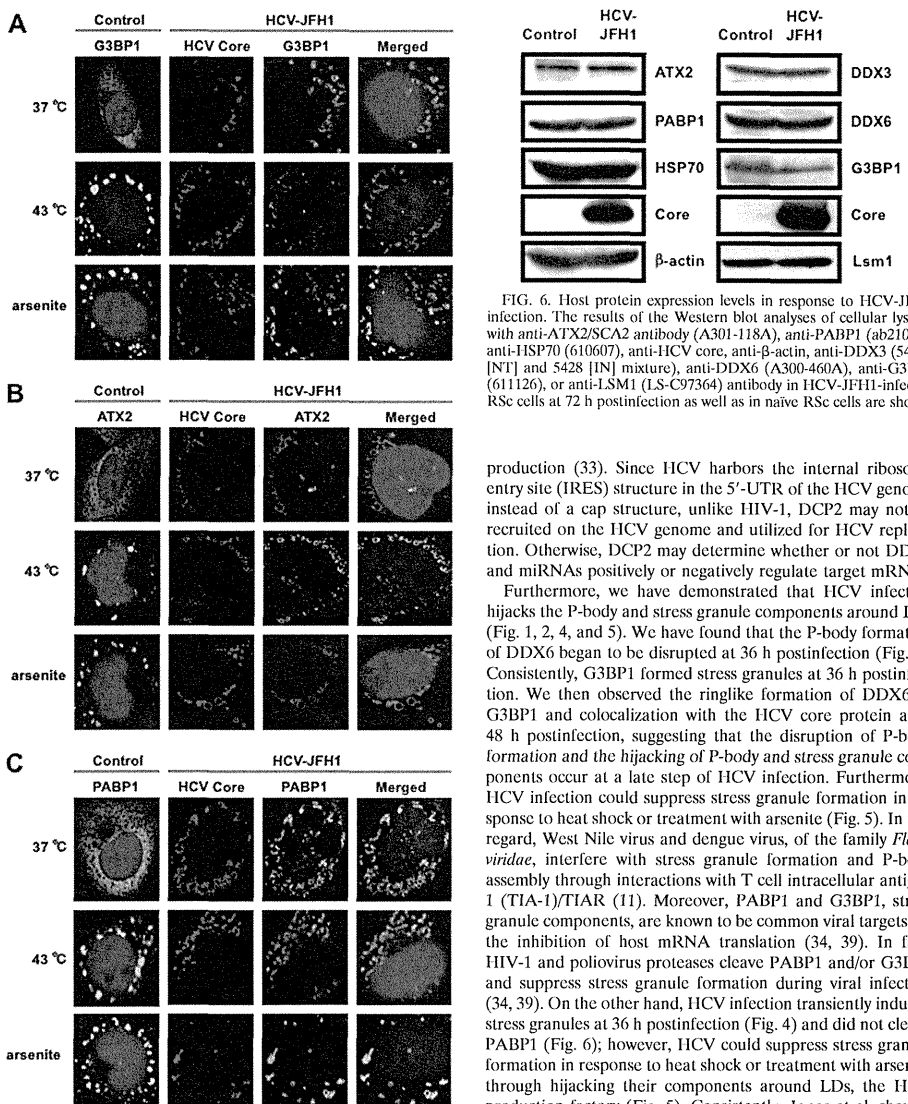


FIG. 5. HCV suppresses stress granule formation in response to heat shock or treatment with arsenite. Naive RSc cells or HCV-JFH1-infected RSc cells at 72 h postinfection were incubated at 37°C or 43°C for 45 min. Cells were also treated with 0.5 mM arsenite for 30 min. Cells were stained with anti-HCV core and anti-G3BP1 (A), anti-ATX2 (B), or anti-PABP1 (ab21060) (C) antibodies and were examined by confocal laser scanning microscopy.

FIG. 6. Host protein expression levels in response to HCV-JFH1 infection. The results of the Western blot analyses of cellular lysates with anti-ATX2/SCA2 antibody (A301-118A), anti-PABP1 (ab21060), anti-HSP70 (610607), anti-HCV core, anti-β-actin, anti-DDX3 (54257 [INT] and 5428 [IN] mixture), anti-DDX6 (A300-460A), anti-G3BP1 (611126), or anti-Lsm1 (LS-C97364) antibody in HCV-JFH1-infected RSc cells at 72 h postinfection as well as in naive RSc cells are shown.

production (33). Since HCV harbors the internal ribosome entry site (IRES) structure in the 5'-UTR of the HCV genome instead of a cap structure, unlike HIV-1, DCP2 may not be recruited on the HCV genome and utilized for HCV replication. Otherwise, DCP2 may determine whether or not DDX6 and miRNAs positively or negatively regulate target mRNA.

Furthermore, we have demonstrated that HCV infection hijacks the P-body and stress granule components around LDs (Fig. 1, 2, 4, and 5). We have found that the P-body formation of DDX6 began to be disrupted at 36 h postinfection (Fig. 4). Consistently, G3BP1 formed stress granules at 36 h postinfection. We then observed the ringlike formation of DDX6 or G3BP1 and colocalization with the HCV core protein after 48 h postinfection, suggesting that the disruption of P-body formation and the hijacking of P-body and stress granule components occur at a late step of HCV infection. Furthermore, HCV infection could suppress stress granule formation in response to heat shock or treatment with arsenite (Fig. 5). In this regard, West Nile virus and dengue virus, of the family *Flaviviridae*, interfere with stress granule formation and P-body assembly through interactions with T cell intracellular antigen 1 (TIA-1)/TIA1 (11). Moreover, PABP1 and G3BP1, stress granule components, are known to be common viral targets for the inhibition of host mRNA translation (34, 39). In fact, HIV-1 and poliovirus proteases cleave PABP1 and/or G3BP1 and suppress stress granule formation during viral infection (34, 39). On the other hand, HCV infection transiently induced stress granules at 36 h postinfection (Fig. 4) and did not cleave PABP1 (Fig. 6); however, HCV could suppress stress granule formation in response to heat shock or treatment with arsenite through hijacking their components around LDs, the HCV production factory (Fig. 5). Consistently, Jones et al. showed that HCV transiently induces stress granules of enhanced green fluorescent protein (EGFP)-G3BP at 36 h after infection with the cell culture-generated HCV (HCVcc) reporter virus Jc1FLAG2 (p7-nsGluc2A); however, those authors did not show the recruitment of EGFP-G3BP to LDs (18). Although we do not know the exact reason for this apparent discrepancy,

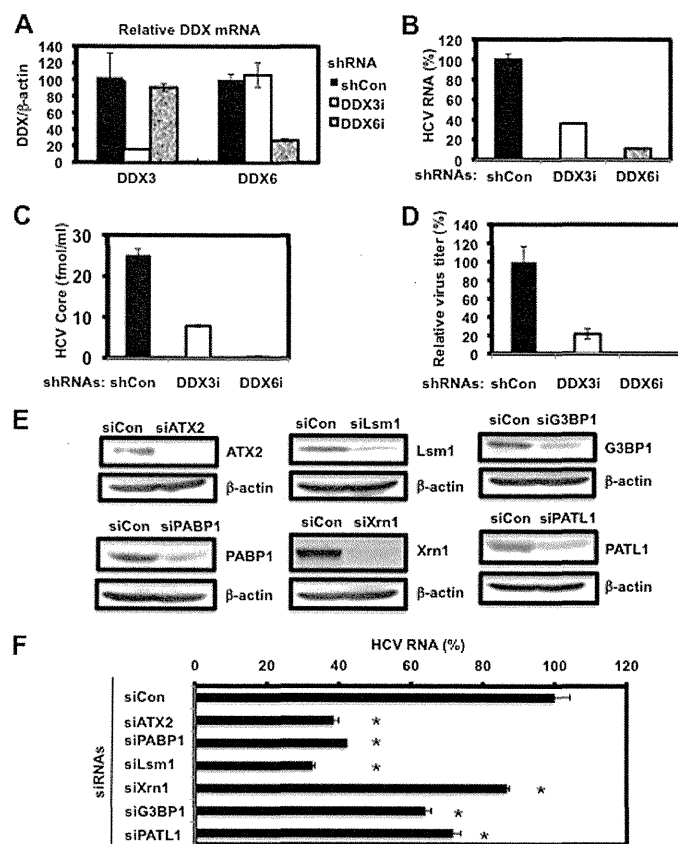


FIG. 7. Requirement of P-body and stress granule components for HCV replication. (A) Inhibition of DDX3 or DDX6 mRNA expression by the shRNA-producing lentiviral vector. Real-time LightCycler RT-PCR for DDX3 or DDX6 was also performed for β -actin mRNA in RSC cells expressing shRNA targeted to DDX3 (DDX3i) or DDX6 (DDX6i) or the control nontargeting shRNA (shCon) in triplicate. Each mRNA level was calculated relative to the level in RSC cells transduced with the control nontargeting lentiviral vector (shCon), which was assigned as 100%. Error bars in this panel and other panels indicate standard deviations. (B) Levels of intracellular genome-length HCV-JFH1 RNA in the cells at 24 h postinfection at an MOI of 4 were monitored by real-time LightCycler RT-PCR. Results from three independent experiments are shown. Each HCV RNA level was calculated relative to the level in RSC cells transduced with a control lentiviral vector (shCon), which was assigned as 100%. (C) The levels of HCV core in the culture supernatants from the stable knockdown RSC cells 24 h after inoculation of HCV-JFH1 at an MOI of 4 were determined by ELISA. Experiments were done in triplicate, and columns represent the mean core protein levels. (D) The infectivity of HCV in the culture supernatants from stable-knockdown RSC cells 24 h after inoculation of HCV-JFH1 at an MOI of 4 was determined by a focus-forming assay at 24 h postinfection. Experiments were done in triplicate, and each virus titer was calculated relative to the level in RSC cells transduced with a control lentiviral vector (shCon), which was assigned as 100%. (E) Inhibition of ATX2, PABP1, Lsm1, Xrn1, G3BP1, or PATL1 protein expression by 72 h after transient transfection of RSC cells with a pool of control nontargeting siRNA (siCon) or a pool of siRNAs specific for ATX2, PABP1, Lsm1, Xrn1, G3BP1, or PATL1 (25 nM), respectively. The results of Western blot analyses of cellular lysates with anti-ATX2, anti-PABP1, anti-Lsm1, anti-Xrn1, anti-G3BP1, anti-PATL1, or anti- β -actin antibody are shown. (F) Levels of intracellular genome-length HCV-JFH1 RNA in the cells at 48 h postinfection at an MOI of 1 were monitored by real-time LightCycler RT-PCR. RSC cells were transiently transfected with a pool of control siRNA (siCon) or a pool of siRNAs specific for ATX2, PABP1, Lsm1, Xrn1, G3BP1, and PATL1 (25 nM). At 48 h after transfection, the cells were inoculated with HCV-JFH1 at an MOI of 1 and incubated for 2 h. The culture medium was then changed and incubated for 22 h. Experiments were done in triplicate, and each HCV RNA level was calculated relative to the level in RSC cells transfected with a control siRNA (siCon), which was assigned as 100%. Asterisks indicate significant differences compared to the control treatment (*, $P < 0.01$).

Labor, and Welfare of Japan; and by the Viral Hepatitis Research Foundation of Japan. M.K. was supported by a research fellowship from the JSPS for young scientists.

REFERENCES

- Anderson, P., and N. Kedersha. 2007. Stress granules: the Tao of RNA triage. *Trends Biochem. Sci.* 33:141–150.
- Ariumi, Y., et al. 2003. Distinct nuclear body components, PML and SMRT, regulate the *trans*-acting function of HTLV-1 Tax oncoprotein. *Oncogene* 22:1611–1619.
- Ariumi, Y., et al. 2007. DDX3 DEAD-box RNA helicase is required for hepatitis C virus RNA replication. *J. Virol.* 81:13922–13926.
- Ariumi, Y., et al. 2008. The DNA damage sensors ataxia-telangiectasia mutated kinase and checkpoint kinase 2 are required for hepatitis C virus RNA replication. *J. Virol.* 82:9639–9646.
- Ariumi, Y., et al. 2011. The ESCRT system is required for hepatitis C virus production. *PLoS One* 6:e14517.
- Beckham, C. J., and R. Parker. 2008. P bodies, stress granules, and viral life cycles. *Cell Host Microbe* 3:206–212.
- Bridge, A. J., S. Pebernard, A. Duxer, A. L. Nicoula, and R. Iggo. 2003. Induction of an interferon response by RNAi vectors in mammalian cells. *Nat. Genet.* 34:263–264.
- Brummelkamp, T. R., R. Bernard, and R. Agami. 2002. A system for stable expression of short interfering RNAs in mammalian cells. *Science* 296:550–553.
- Chable-Bessia, C., et al. 2009. Suppression of HIV-1 replication by microRNA effectors. *Retrovirology* 6:26.
- Cristea, I. M., et al. 2010. Host factors associated with the Sindbis virus RNA-dependent RNA polymerase: role for G3BP1 and G3BP2 in virus replication. *J. Virol.* 84:6720–6732.
- Emara, M. M., and M. A. Branton. 2007. Interaction of TIA-1/TIA1 with West Nile and dengue virus products in infected cells interferes with stress granule formation and processing body assembly. *Proc. Natl. Acad. Sci. U. S. A.* 104:9041–9046.
- Hijikata, M., N. Kato, Y. Ootsuyama, M. Nakagawa, and K. Shimotohno. 1991. Gene mapping of the putative structural region of the hepatitis C virus genome by *in vitro* processing analysis. *Proc. Natl. Acad. Sci. U. S. A.* 88:5547–5551.
- Hijikata, M., et al. 1993. Proteolytic processing and membrane association of putative nonstructural proteins of hepatitis C virus. *Proc. Natl. Acad. Sci. U. S. A.* 90:10773–10777.
- Ikeda, M., et al. 2005. Efficient replication of a full-length hepatitis C virus genome, strain O, in cell culture, and development of a luciferase reporter system. *Biochem. Biophys. Res. Commun.* 329:1350–1359.
- Jangra, R. K., M. Yi, and S. M. Lemon. 2010. Regulation of hepatitis C virus translation and infectious virus production by the microRNA miR-122. *J. Virol.* 84:6615–6625.
- Jangra, R. K., M. Yi, and S. M. Lemon. 2010. DDX6 (Rek/p54) is required for efficient hepatitis C virus replication but not IRES-directed translation. *J. Virol.* 84:6810–6824.
- Ji, H., et al. 2008. MicroRNA-122 stimulates translation of hepatitis C virus RNA. *EMBO J.* 27:3300–3310.
- Jones, C. T., et al. 2010. Real-time imaging of hepatitis C virus infection using a fluorescent cell-based reporter system. *Nat. Biotechnol.* 28:167–171.
- Jopling, C. L., M. Yi, A. M. Lancaster, S. M. Lemon, and P. Sarnow. 2005. Modulation of hepatitis C virus RNA abundance by a liver-specific microRNA. *Science* 309:1577–1581.
- Jopling, C. L., S. Schütz, and P. Sarnow. 2008. Position-dependent function for a tandem microRNA miR-122-binding site located in the hepatitis C virus RNA genome. *Cell Host Microbe* 4:77–85.
- Kato, N., et al. 1990. Molecular cloning of the human hepatitis C virus genome from Japanese patients with non-A, non-B hepatitis. *Proc. Natl. Acad. Sci. U. S. A.* 87:9524–9528.
- Kedersha, N., and P. Anderson. 2007. Mammalian stress granules and processing bodies. *Methods Enzymol.* 431:61–81.
- Kuroki, M., et al. 2009. Arsenic trioxide inhibits hepatitis C virus RNA replication through modulation of the glutathione redox system and oxidative stress. *J. Virol.* 83:2338–2348.
- Kushima, Y., T. Wakita, and M. Hijikata. 2010. A disulfide-bonded dimer of the core protein of hepatitis C virus is important for virus-like particle production. *J. Virol.* 84:9118–9127.
- Maniwa, N., and H. J. Worman. 1999. Hepatitis C virus core protein binds to a DEAD box RNA helicase. *J. Biol. Chem.* 274:15751–15756.
- Miyanari, Y., et al. 2007. The lipid droplet is an important organelle for hepatitis C virus production. *Nat. Cell Biol.* 9:1089–1097.
- Naldini, L., et al. 1996. In vivo gene delivery and stable transduction of nondividing cells by a lentiviral vector. *Science* 272:263–267.
- Nonhoff, U., et al. 2007. Ataxin-2 interacts with the DEAD/H-box RNA helicase DDX6 and interferes with P-bodies and stress granules. *Mol. Biol. Cell* 18:1385–1396.
- Owsiaka, A. M., and A. H. Patel. 1999. Hepatitis C virus core protein interacts with a human DEAD box protein DDX3. *Virology* 257:330–340.

30. Parker, R., and U. Sheth. 2007. P bodies and the control of mRNA translation and degradation. *Mol. Cell* 25:635–646.
31. Randall, G., et al. 2007. Cellular cofactors affecting hepatitis C virus infection and replication. *Proc. Natl. Acad. Sci. U. S. A.* 104:12884–12889.
32. Rocak, S., and P. Linder. 2004. DEDD-box proteins: the driving forces behind RNA metabolism. *Nat. Rev. Mol. Cell Biol.* 5:232–241.
33. Schelter, N., et al. 2009. Translation and replication of hepatitis C virus genomic RNA depends on ancient cellular proteins that control mRNA fates. *Proc. Natl. Acad. Sci. U. S. A.* 106:13517–13522.
34. Smith, R. W., and N. K. Gray. 2010. Poly(A)-binding protein (PABP): a common viral target. *Biochem. J.* 426:1–11.
35. Tingting, P., F. Caiyun, Y. Zhiqiang, Y. Pengyan, and Y. Zhenghong. 2006. Subproteomic analysis of the cellular proteins associated with the 3' untranslated region of the hepatitis C virus genome in human liver cells. *Biochem. Biophys. Res. Commun.* 347:683–691.
36. Tourrière, H., et al. 2003. The RasGAP-associated endoribonuclease G3BP assembles stress granules. *J. Cell Biol.* 160:823–831.
37. Wakita, T., et al. 2005. Production of infectious hepatitis C virus in tissue culture from a cloned viral genome. *Nat. Med.* 11:791–796.
38. Weston, A., and J. Sommerville. 2006. Xp54 and related (DDX6-like) RNA helicase: roles in messenger RNP assembly, translation regulation and RNA degradation. *Nucleic Acids Res.* 34:3082–3094.
39. White, J. P., A. M. Cardenas, W. E. Marissen, and R. E. Lloyd. 2007. Inhibition of cytoplasmic mRNA stress granule formation by a viral proteinase. *Cell Host Microbe* 2:295–305.
40. Wilson, J. A., C. Zhang, A. Huys, and C. D. Richardson. 2011. Human Ago2 is required for efficient miR-122 regulation of HCV RNA accumulation and translation. *J. Virol.* 85:2342–2350.
41. Yedavalli, V. S., C. Neveut, Y. H. Chi, L. Kleiman, and K. T. Jeang. 2004. Requirement of DDX3 DAEQ box RNA helicase for HIV-1 Rev-RRE export function. *Cell* 119:381–392.
42. Yi, Z., et al. 2006. Subproteomic study of hepatitis C virus replicon reveals Ras-GTPase-activating protein binding protein 1 as potential HCV RC component. *Biophys. Biochem. Res. Commun.* 350:174–178.
43. You, L. R., et al. 1999. Hepatitis C virus core protein interacts with cellular putative RNA helicase. *J. Virol.* 73:2841–2853.
44. Zufferey, R., D. Nagy, R. J. Mandel, L. Naldini, and D. Trono. 1997. Multiply attenuated lentiviral vector achieves efficient gene delivery in vivo. *Nat. Biotechnol.* 15:871–875.



Contents lists available at ScienceDirect

Biochemical and Biophysical Research Communications

journal homepage: www.elsevier.com/locate/ybbrc

Plural assay systems derived from different cell lines and hepatitis C virus strains are required for the objective evaluation of anti-hepatitis C virus reagents

Youki Ueda, Kyoko Mori, Yasuo Ariumi, Masanori Ikeda, Nobuyuki Kato*

Department of Tumor Virology, Okayama University Graduate School of Medicine, Dentistry, and Pharmaceutical Sciences, 2-5-1 Shikata-cho, Okayama 700-8558, Japan

ARTICLE INFO

Article history:

Received 8 April 2011

Available online 17 May 2011

Keywords:

HCV

HCV RNA replication system

Li23 cells

Reporter assay for anti-HCV reagents

ABSTRACT

Persistent hepatitis C virus (HCV) infection causes chronic liver diseases and is a global health problem. HuH-7 hepatoma-derived cells are widely used as the only cell-based HCV replication system for HCV research, including drug assays. Recently, using different hepatoma Li23-derived cells, we developed an HCV drug assay system (ORL8), in which the genome-length HCV RNA (O strain of genotype 1b) encoding renilla luciferase replicates efficiently. In this study, using the HuH-7-derived OR6 assay system that we developed previously and the ORL8 assay system, we evaluated 26 anti-HCV reagents, which other groups had reported as anti-HCV candidates using HuH-7-derived assay systems other than OR6. The results revealed that more than half of the reagents showed different anti-HCV activities from those in the previous studies, and that anti-HCV activities evaluated by the OR6 and ORL8 assays were also frequently different. In further evaluation using the HuH-7-derived AH1 assay system, which was developed using the AH1 strain of genotype 1b, several reagents showed different anti-HCV activities in comparison with those evaluated by the OR6 and ORL8 assays. These results suggest that the different activities of anti-HCV reagents are caused by the differences in cell lines or HCV strains used for the development of assay systems. Therefore, we conclude that plural HCV assay systems developed using different cell lines or HCV strains are required for the objective evaluation of anti-HCV reagents.

© 2011 Elsevier Inc. All rights reserved.

1. Introduction

Hepatitis C virus (HCV) infection frequently causes chronic hepatitis, which often leads to liver cirrhosis and hepatocellular carcinoma. Since approximately 170 million people are infected with HCV worldwide, HCV infection is a serious global health problem [1]. Although the combination of pegylated-interferon (PEG-IFN) and ribavirin is the standard therapy worldwide, only half of the patients receiving this treatment exhibit a sustained virologic response [2]. HCV is an enveloped virus with a positive single-stranded RNA virus of the *Flaviviridae* family. The HCV genome encodes a large polyprotein precursor of approximately 3000 amino acids, which is cleaved into 10 proteins in the following order: Core, envelope 1 (E1), E2, p7, non-structural 2 (NS2), NS3, NS4A, NS4B, NS5A, and NS5B [3,4].

To date, HuH-7 hepatoma-derived cells are used as the only cell culture system for robust HCV replication in HCV research, including drug assays. We have also developed a HuH-7-derived drug assay system (OR6), in which genome-length HCV RNA (O strain of genotype 1b derived from an HCV-positive blood donor) encoding renilla luciferase (RL) efficiently replicates [5]. Recently, we found a new human hepatoma cell line, Li23, that enables robust

HCV RNA replication [6], and we showed that the gene expression profile of Li23 cells was distinct from that of HuH-7 cells, although both cell lines had similar liver-specific expression profiles [7]. In that study, we identified three genes (New York esophageal squamous cell carcinoma 1, β -defensin-1, and galectin-3) showing Li23-specific expression profiles by a comparative analysis using several other hepatic cell lines [7]. We further developed Li23-derived drug assay systems (ORL8 and ORL11), which are relevant to the HuH-7-derived OR6 assay system [6]. During the process of evaluating the ORL8 and ORL11 assay systems using anti-HCV reagents such as IFNs, we noticed that these assay systems were frequently more sensitive to anti-HCV reagents than the OR6 assay system [6]. Furthermore, we recently found that ribavirin at clinically achievable concentrations (approximately 10 μ M) effectively inhibited HCV RNA replication in both the ORL8 and ORL11 assay systems, but not in the OR6 assay system [8]. This finding led to the clarification of the anti-HCV mechanism of ribavirin, and we demonstrated that ribavirin's anti-HCV activity was mediated by the inhibition of inosine monophosphate dehydrogenase, a key enzyme in the guanosine biosynthetic pathway [8]. From these findings, we supposed that the anti-HCV reagents reported to date might show different activities among the different drug assay systems. To test this assumption, we evaluated 22 anti-HCV reagents that were reported using HuH-7-derived assay systems other than OR6, using the OR6 and ORL8 assay systems. Four additional

* Corresponding author. Fax: +81 86 235 7392.

E-mail address: nkato@md.okayama-u.ac.jp (N. Kato).

reagents predicted by antiviral activity other than HCV were also evaluated. Furthermore, a recently developed HuH-7-derived AH1R assay system (AH1 strain of genotype 1b derived from a patient with acute hepatitis) (Mori et al., in preparation) was also used for the evaluation. Here, we report that plural assay systems derived from different cell lines and different HCV strains are required for the objective evaluation of anti-HCV reagents.

2. Materials and methods

2.1. Cell cultures

HuH-7-derived ORG and AH1R cells were maintained in medium containing G418 (0.3 mg/ml) as described previously [5]. Li23-derived ORL8 cells were also maintained in medium containing G418 (0.3 mg/ml) as described previously [6].

2.2. Reagents

Acetylsalicylic acid, cephalotaxine, clemizole, curcumin, isoliquiritigenin, nitazoxanide, and tizoxanide were purchased from Sigma-Aldrich (St. Louis, MO). Cantharidin, 2'-deoxy-5-fluorouridine, griseofulvin, guanazole, homoharringtonine, resveratrol, and Y7632 were purchased from WAKO Pure Chemical Industries, Ltd. (Osaka, Japan). Artemisinin and bisindolyl maleimide 1 were purchased from Alexis Biochemicals (San Diego, CA). Artesunate and silibinin A were purchased from Ikt Laboratories (St. Paul, MN). Esomeprazole and neflifavir were purchased from Toronto Research Chemicals (North York, ON, Canada). Cinanserin hydrochloride and HA1077 were purchased from Tocris Bioscience (Bristol, UK). 6-Azauridine was purchased from MP Biomedicals (Solon, OH). Carvedilol was purchased from Calbiochem (San Diego, CA). Hemin was purchased from Alfa Aesar (Ward Hill, MA). Methotrexate was purchased from Tokyo Chemical Industry (Tokyo, Japan). Cinanserin hydrochloride, guanazole, HA1077, and Y7632 were dissolved in the culture medium for Li23-derived cells. Artesunate was dissolved in 0.5% NaHCO₃ solution. Other reagents were dissolved in dimethyl sulfoxide.

2.3. RL assay

RL assay was performed as described previously [6]. Briefly, the cells were plated onto 24-well plates (2 × 10⁴ cells per well) in triplicate and then treated with each reagent at several concentrations for 72 h. After treatment, the cells were subjected to luciferase assay using the RL assay system (Promega, Madison, WI). From the assay results, the 50% effective concentration (EC₅₀) of each reagent was determined.

2.4. WST-1 cell proliferation assay

The cells were plated onto 96-well plates (1 × 10³ cells per well) in triplicate and then treated with each reagent at several concentrations for 72 h. After treatment, the cells were subjected to the WST-1 cell proliferation assay (Takara Bio, Otsu, Japan) according to the manufacturer's protocol. From the assay results, the 50% cytotoxic concentration (CC₅₀) of each reagent was determined.

2.5. Western blot analysis

The preparation of cell lysates, sodium dodecyl sulfate-polyacrylamide gel electrophoresis, and immunoblotting analysis were performed as previously described [9]. The antibodies used in this study were those against HCV Core (CP11; Institute of Immunology, Tokyo, Japan) and β-actin (AC-15, Sigma-Aldrich)

as the control for the amount of protein loaded per lane. Immuno-complexes were detected with the Renaissance enhanced chemiluminescence assay (Perkin-Elmer Life Sciences, Boston, MA).

2.6. Selective index (SI)

The SI value of each reagent was determined by dividing the CC₅₀ value by the EC₅₀ value.

3. Results

3.1. Evaluation of 26 reagents for anti-HCV activity using ORG and ORL8 assay systems

To obtain candidates for the evaluation of anti-HCV activity using ORG and ORL8 assay systems, we first searched the literature in the PubMed database using the key words (HCV or hepatitis C) and (inhibit or antiviral or suppress or block); this yielded approximately 4500 reports published between January 2003 and April 2010. From these results, we further selected the reports in which the EC₅₀ values of reagents were determined or estimated by the HuH-7-derived HCV assay systems using the Con-1 strain (genotype 1b) [10], N strain (genotype 1b) [11], or HCV JFH-1 strain (genotype 2a) [12]. We finally chose 22 commercially available reagents for the evaluation of anti-HCV activity using ORG and ORL8 assay systems. Four reagents predicted from the antiviral activity (hepatitis B virus, cytomegalovirus, etc.) other than HCV were also included in the evaluation study. The 26 selected reagents and their references are listed in Supplementary Table S1.

For each of the 26 reagents, we determined the EC₅₀ value by RL assay and the CC₅₀ value by WST-1 assay using the ORG or ORL8 assay system, and calculated the SI value by dividing the CC₅₀ value by the EC₅₀ value. For each reagent, we first compared the EC₅₀ value obtained from the ORG or ORL8 assay with that of the previous study. Consequently, we classified the 26 reagents into five classes, A to E (Table 1). Eight reagents (methotrexate, artemisinin, artesunate, clemizole, hemin, 6-azauridine, acetylsalicylic acid, and isoliquiritigenin with the order of the SI value in the ORL8 assay) belonged to class A, in which the EC₅₀ value obtained by either the ORG or ORL8 assay was less than one-third of that in the previous study (Supplementary Table S1 and Table 1). Artesunate, an artemisinin-derivative possessing antiviral activity against cytomegalovirus, herpesvirus, Epstein-Barr virus etc., was included in class A by the comparison with the data on anti-cytomegalovirus activity. In this class, we especially noticed that methotrexate (an anti-cancer drug) showed very strong anti-HCV activity (EC₅₀ 0.1 μM; CC₅₀ > 200 μM; SI > 2000) in the ORL8 assay (upper panel in Fig. 1A and Table 1), whereas methotrexate showed very weak anti-HCV activity (EC₅₀ > 200 μM; CC₅₀ > 200 μM) in the ORG assay as well as in a previous report [13] (upper panel in Fig. 1A and Table 1). This drastic difference was confirmed by Western blot analysis (lower panels in Fig. 1A). These results indicate that only the ORL8 assay is drastically sensitive to methotrexate, and suggest that the anti-HCV activity of methotrexate depends on the types of hepatic cells. The comparison of the EC₅₀ values of other reagents belonging to class A revealed that the ORL8 assay was more sensitive than the ORG assay (1.9–15-fold) to artemisinin, artesunate, clemizole, acetylsalicylic acid, and 6-azauridine, and conversely the ORG assay was more sensitive than the ORL8 assay (2–2.5-fold) to hemin and isoliquiritigenin (Table 1). Furthermore, the CC₅₀ values of clemizole and 6-azauridine also differed more than twofold between the ORG and ORL8 assays (Table 1). These results suggest that the anti-HCV activities of these reagents are affected by the kind of assay systems used. Especially, we noticed that artemisinin and artesunate (antimalarial drugs) showed higher SI values in the

Table 1
Anti HCV activities of 26 reagents evaluated in this study.

Class	Assay	Cell origin	HCV strain	HuH-7		ORG		ORL8		AH1R	
				Con-1, N, JFH-1, etc.	EC ₅₀	SI	EC ₅₀	SI	EC ₅₀	SI	EC ₅₀
A	Methotrexate			> 100	–	> 200	–	> 200	> 2000	170	<0.9
A	Artemisinin			> 100	> 100	> 200	0.1	370	16	310	58
A	Artesunate ^b			> 177	> 2.3	380	4.7	370	15	5.3	4
A	Artesunate ^b			> 78	> 3.8	81	2.7	34	15	4.1	4.9
A	Clemizole			> 15	> 2.5	3.9	2.3	0.22	22	11	<0.3
A	Hemin			> 20	> 2.5	8	11	0.5	22	11	7.3
A	6-Azauridine			> 52	> 2.4	22	10	1.8	2.0	7.2	6.5
A	6-Azauridine			> 100	> 1.0	100	1.2	10	1.5	14	4.2
A	Acetylsalicylic acid			> 100	2.0	8 ^d	2.6 ^d	1.6	2.4 ^d	ND	–
A	Isoliquiritigenin			< 24	< 1.0	4 ^d	1.6 ^d	12	3.1	15	ND
B	Nelfinavir			> 10	> 1.0	24	3.9	26	2.4	68	5.7
B	2'-Deoxy-5-fluorouridine			< 15	< 1.0	9.9	32	31	1.0	36	13
B	Resveratrol			> 10	> 1.0	15	35	4.3	8.1	42	7.7
B	Cantharidine ^c			> 10	> 1.0	3.5	12	1.5	5.4	16	ND
B	Homoharringtonine ^c			> 10	> 1.0	0.3	0.28	38*	2.1	0.11	2.6
B	Homoharringtonine ^c			> 10	> 1.0	0.5	0.17	18*	45*	45*	1.2
B	Crucumin			> 15	> 1.0	15	18	1.3	19	1.7	ND
B	Griseofulvin			> 10	> 1.0	207	34	16	14	1.6	ND
B	Cinanserin hydrochloride			> 10	> 1.0	6.1	4.4	33	1.3	39	ND
B	Cephalotaxine ^c			> 10	> 1.0	10	25	35	35	1.1	–
C	Tizoxanide			> 100	> 1.0	60	35	29	38	0.8	4.8
C	Nitazoxanide			> 100	> 1.0	15	11	11	24	2.5	ND
C	Nitazoxanide			> 100	> 1.0	38	181	11	3.9	17	7.2
D	Guanazole			< 100	< 1.0	0.21	2.8	200	170	<0.9	2.2
D	HA1077			> 100	> 1.0	50	3.3	> 200	> 200	<0.9	<0.9
E	Bisindolyl maleimide 1			> 100	> 1.0	15	50	> 50	> 50	> 50	> 50
E	Esomeprazole			> 100	> 1.0	5	8.1	1.3	15	1.0	1.5
E	Y27632			> 100	> 1.0	ND	6.2	1.0	27	20	0.8
E	Carvedilol			> 100	> 1.0	50	80	> 80	> 80	39	<0.5
E	Silibinin A			> 100	> 1.0	17	4.4	1.2	6.6	8.8	6.3
E	Silibinin A			> 100	> 1.0	4.5	3.7	0.1	26	0.3	0.3
E	Silibinin A			> 100	> 1.0	23	85	89	89	96	0.3

ND, not determined.

^a Assay used in previous reports.

^b Reported as anti-cytomegalovirus reagent.

^c Reported as anti-hepatitis B virus reagent. EC₅₀ and CC₅₀ values are indicated by the order of μM except 'd' (μM) and 'e' (nM).

ORL8 assay than previously reported [14,15]. The anti-HCV profiles of artemisinin and artesunate in the ORG and ORL8 assays are shown in Fig. 1B and Supplementary Fig. 1A, respectively. In addition, the comparison of SI values revealed that the ORG assay was more sensitive to hemin and isoliquiritigenin than the HuH-7-derived assays (Con-1 and N strains) used in the previous reports (Supplementary Table S1), suggesting that the HCV strains used in the assay systems affect the evaluation of anti-HCV reagents.

Nine reagents (nelfinavir, 2'-deoxy-5-fluorouridine, resveratrol, cantharidin, homoharringtonine, crucumin, griseofulvin, cinanserin hydrochloride, and cephalotaxine with the order of SI value in the ORL8 assay) were placed in class B, in which the EC₅₀ values obtained by the ORG and ORL8 assays were similar (more than one-third to less than threefold) to those in the previous study (Table 1 and Supplementary Table S1). Cantharidin, homoharringtonine, and cephalotaxine, all of which possess anti-hepatitis B virus activity, were placed in class C, in which the data on anti-hepatitis B virus activity (Supplementary Fig. 1).

Tizoxanide and nitazoxanide belonged to class C, in which the EC₅₀ values obtained by both the ORG and ORL8 assays were more than threefold higher than in the previous study (Table 1 and Supplementary Table S1). Guanazole and HA1077 were placed in class D, in which there was no anti-HCV activity in both the ORG and ORL8 assays (Table 1). No anti-HCV activity of guanazole and HA1077 was also confirmed by Western blot analysis (data not shown). Lastly, five reagents (Bisindolyl maleimide 1, esomeprazole, Y27632, carvedilol, and silibinin A) were placed in class E, in which pro-HCV activity was exhibited in both ORG and ORL8 assays. We unexpectedly observed that these reagents enhanced the HCV RNA replication level. As a

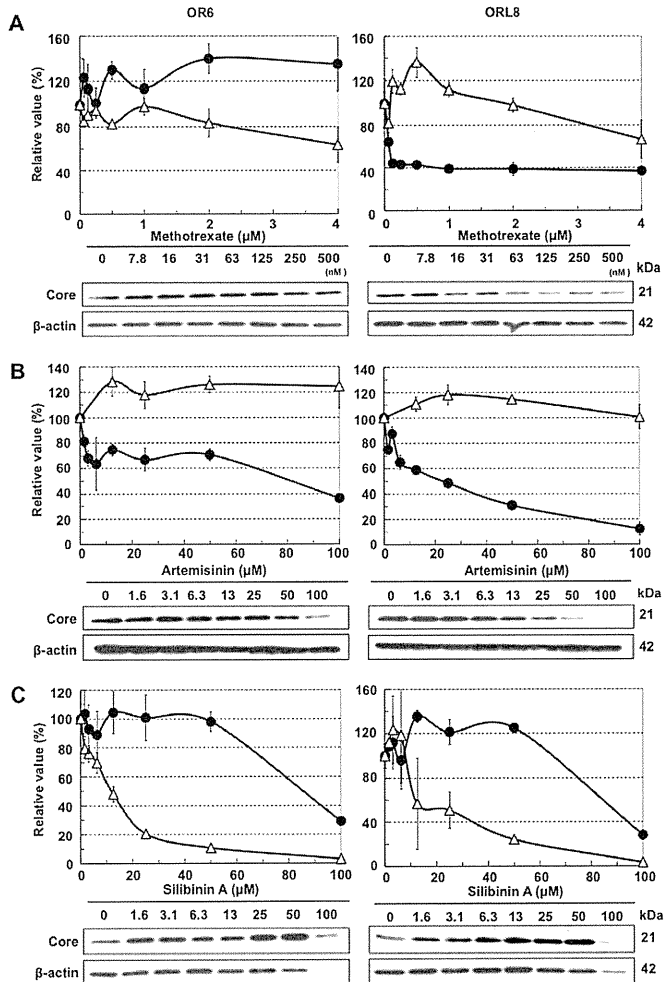


Fig. 1. Anti-HCV profiles of representative reagents in the OR6 and ORL8 assay systems. (A) Methotrexate sensitivities on genome-length HCV RNA replication in the OR6 and ORL8 assay systems. OR6 and ORL8 cells were treated with methotrexate for 72 h, followed by RL assay (black circle in the upper panel) and WST-1 assay (open triangle in the upper panel). The relative value (%) calculated at each point, when the level in nontreated cells was assigned to 100%, is presented here. Western blot analysis of the treated cells for the HCV Core was also performed (lower panel). (B) Artemisinin sensitivities on genome-length HCV RNA replication in the OR6 and ORL8 assay systems. RL assay, WST-1 assay, and Western blot analysis were performed as described in (A). (C) Silibinin A sensitivities on genome-length HCV RNA replication in the OR6 and ORL8 assay systems. RL assay, WST-1 assay, and Western blot analysis were performed as described in (A).

representative reagent, pro-HCV profiles of silibinin A are shown in the upper panel of Fig. 1C. These pro-HCV profiles were confirmed by Western blot analysis (lower panels in Fig. 1C for silibinin A and data not shown for the other reagents). Since the anti-HCV activity of silibinin A was detected by the HCV replicon assay system using the Con-1 strain [14], the converse effects obtained by our assay systems using the O strain may

be due to the difference in HCV strains. In summary, the differences in anti-HCV activities observed among HuH-7- and Li23-derived assay systems used in this study and the other HuH-7-derived assay systems used in the previous studies suggest that the activities of anti-HCV reagents differ depending on which HCV strains and cell lines are used in the evaluation assays.

3.2. Evaluation of 18 reagents for anti-HCV activity using AH1R assay system

We previously established a HuH-7-derived cell line (AH1), which harbors genome-length HCV RNA (AH1 strain of genotype 1b) derived from a patient with acute hepatitis [16]. To further examine the effect of the HCV strain on anti-HCV reagent activity, we developed an AH1R assay system that is based on the AH1 cell line and that corresponds to the OR6 assay system (Mori et al., in preparation).

Using the AH1R assay system, we further evaluated the anti-HCV activities of 18 reagents, which showed differential anti-HCV activity between the OR6 and ORL8 assays, or showed either no anti-HCV activity or pro-HCV activity in both the OR6 and ORL8 assays. The results of the evaluation are shown in Table 1. The comparisons of the data obtained by the OR6 and AH1R assays revealed that the difference in the EC_{50} value from reagent to reagent was held within the range of one-third to threefold. However, we noticed that the EC_{50} value (5.3 μ M) of artemisinin in the AH1R assay was remarkably lower than that (81 μ M) in the OR6 assay (Supplementary Fig. 2 and Table 1), suggesting that artemisinin's anti-HCV activity differs depending on the HCV strain. Furthermore, the results of the AH1R assay revealed that cephalotaxine, belonging to class B, would be recategorized into class D. In summary, some reagents showed differential anti-HCV activities between the HuH-7-derived OR6 (O strain) and AH1R (AH1 strain) assay systems, although most of the reagents showed similar levels of anti-HCV activity in both assays. Taking together the results of the previous and present studies, we conclude that plural assay systems derived from different cell lines and HCV strains are needed for the objective evaluation of anti-HCV reagents.

4. Discussion

In the present study, we demonstrated for the first time that a Li23-cell-derived drug assay system, not a HuH-7-derived system, was important to use for the objective evaluation of anti-HCV reagents. In addition, we demonstrated that assay systems derived from different HCV strains were also necessary for the objective evaluation of anti-HCV reagents.

Among the 26 reagents evaluated by our assay systems, methotrexate showed the most drastic differences between the HuH-7- and Li23-derived assay systems in terms of anti-HCV activity. Although methotrexate showed very weak anti-HCV activity in the HuH-7-derived assay (Con-1 strain) used in a previous study [13] as well as in our OR6 and AH1R assays (O and AH1 strains), the ORL8 assay revealed very strong anti-HCV activity (SI > 2000). Such drastic differences in both assays suggest that some host factor or factors required for HCV RNA replication are different between these two cell lines, although the anti-HCV target of methotrexate is unclear. Since methotrexate is currently used as an anti-cancer drug or anti-rheumatic drug and its EC_{50} value for HCV RNA replication is 0.1 μ M, it may be a potential candidate for enhancing the effects of the current combination therapy of PEG-IFN and ribavirin.

The anti-HCV activities of two antimalarial drugs, artemisinin and its derivative artesunate, are interesting. Although Paeshuyse et al. [14] showed that artemisinin possessed weak or moderate anti-HCV activity using a HuH-7- or HuH-6-derived subgenomic HCV replicon system, artemisinin's anti-HCV mechanism was unclear. On the other hand, Efferth et al. [15] reported that artesunate, the most studied artemisinin-derivative for the treatment of severe malaria, possessed antiviral activity against Epstein-Barr virus, human cytomegalovirus, human herpesvirus 6A, herpes simplex virus 1, and so on, except for HCV with the low micromolar

range, although artesunate's precise antiviral mechanism was ambiguous. Therefore, we supposed, and our assay systems clearly detected, that both artemisinin and artesunate possess anti-HCV activity. Especially, the AH1R assay was the most sensitive to artesunate (EC_{50} 0.22 μ M). Preliminary experiments for the anti-HCV mechanisms of these reagents showed that they did not induce the oxidative stress (data not shown), and that they did not induce the IFN-signaling pathway (data not shown), and that they did not induce the oxidative stress (data not shown) as observed in the treatment with a broad range of anti-HCV reagents, including cyclosporine A [8,17]. Further studies are needed to clarify the anti-HCV mechanisms of these reagents. Since the largest SI value of artemisinin was 58 in the AH1R assay and that of artesunate was 16 in the ORL8 assay, these reagents may be also useful for the treatment of patients with chronic hepatitis.

In this study, we demonstrated that many anti-HCV reagents showed differential anti-HCV activities among different assay systems (OR6, ORL8, and AH1R) on HCV RNA replication. These results suggest that reliance on only a single assay system may lead to an incorrect evaluation of anti-HCV candidates. Therefore, we propose that plural assay systems derived from different cell lines and HCV strains should be used in order to evaluate anti-HCV candidates. Furthermore, plural assay systems derived from at least two different cell origins would be also useful for the screening of anti-HCV candidates.

Acknowledgments

We thank Yusuke Wataya and Hye-Sook Kim for their helpful discussions. This work was supported by grants-in-aid for research on hepatitis from the Ministry of Health, Labor, and Welfare of Japan. K. M. was supported by a Research Fellowship for Young Scientists from the Japan Society for the Promotion of Science.

Appendix A. Supplementary data

Supplementary data associated with this article can be found, in the online version, at doi:10.1016/j.bbrc.2011.05.061.

References

- [1] D.L. Thomas, Hepatitis C epidemiology, *Curr. Top. Microbiol. Immunol.* 242 (2000) 25–41.
- [2] S. Chevalliez, J.M. Pawlinsky, Interferon-based therapy of hepatitis C, *Adv. Drug. Deliv. Rev.* 59 (2007) 1222–1241.
- [3] N. Kato, M. Hijikata, Y. Ootsuyama, et al., Molecular cloning of the human hepatitis C virus genome from Japanese patients with non-A, non-B hepatitis, *Proc. Natl. Acad. Sci. USA* 87 (1990) 9524–9528.
- [4] N. Kato, Molecular virology of hepatitis C virus, *Acta Med. Okayama* 55 (2001) 133–159.
- [5] M. Ikeda, K. Abe, H. Dansako, et al., Efficient replication of a full-length hepatitis C virus genome, strain O, in cell culture, and development of a luciferase reporter system, *Biochem. Biophys. Res. Co.* 329 (2005) 1350–1359.
- [6] N. Kato, K. Mori, K. Abe, et al., Efficient replication systems for hepatitis C virus using a new human hepatoma cell line, *Virus Res.* 146 (2009) 41–50.
- [7] K. Mori, M. Ikeda, Y. Ariumi, N. Kato, Gene expression profile of Li23 a new human hepatoma cell line that enables robust hepatitis C virus replication: comparison with HuH-7 and other hepatic cell lines, *Hepatol. Res.* 40 (2010) 1248–1253.
- [8] K. Mori, M. Ikeda, Y. Ariumi, et al., Mechanism of action of ribavirin in a novel hepatitis C virus replication cell system, *Virus Res.* 157 (2011) 61–70.
- [9] N. Kato, K. Sugiyama, K. Namba, et al., Establishment of a hepatitis C virus subgenomic replicon derived from human hepatocytes infected in vitro, *Biochem. Biophys. Res. Co.* 306 (2003) 756–766.
- [10] V. Lohmann, F. Korner, J. Koch, et al., Replication of subgenomic hepatitis C virus RNAs in a hepatoma cell line, *Science* 285 (1999) 110–113.
- [11] M. Ikeda, M. Yi, K. Li, S.M. Lemon, Selectable subgenomic and genome-length dicistrionic RNAs derived from an infectious molecular clone of the HCV-N strain of hepatitis C virus replicate efficiently in cultured HuH7 cells, *J. Virol.* 76 (2002) 2997–3006.
- [12] T. Wakita, T. Pietschmann, T. Kato, et al., Production of infectious hepatitis C virus in tissue culture from a cloned viral genome, *Nat. Med.* 11 (2005) 791–796.

[13] L.J. Stuyver, T.R. McBrayer, P.M. Tharnish, et al., Dynamics of subgenomic hepatitis C virus replicon RNA levels in HuH-7 cells after exposure to nucleoside antimetabolites, *J. Virol.* 77 (2003) 10689–10694.

[14] J. Paeshuyse, L. Coelmont, I. Villegent, et al., Hemin potentiates the anti-hepatitis C virus activity of the antimalarial drug artemisinin, *Biochem. Biophys. Res. Co.* 348 (2006) 139–144.

[15] T. Efferth, M.R. Romero, D.G. Wolf, et al., The antiviral activities of artemisinin and artesunate, *Clin. Infect. Dis.* 47 (2008) 804–811.

[16] K. Mori, K. Abe, H. Dansako, et al., New efficient replication system with hepatitis C virus genome derived from a patient with acute hepatitis C, *Biochem. Biophys. Res. Co.* 371 (2008) 104–109.

[17] M. Yano, M. Ikeda, K. Abe, et al., Comprehensive analysis of the effects of ordinary nutrients on hepatitis C virus RNA replication in cell culture, *Antimicrob. Agents Ch.* 51 (2007) 2016–2027.

ORIGINAL ARTICLE—LIVER, PANCREAS, AND BILIARY TRACT

Geranylgeranylacetone has anti-hepatitis C virus activity via activation of mTOR in human hepatoma cells

Shigeyuki Takeshita · Tatsuki Ichikawa · Naota Taura · Hisamitsu Miyaaki · Toshihisa Matsuzaki · Masashi Otani · Toru Muraoka · Motohisa Akiyama · Satoshi Miuma · Eisuke Ozawa · Masanori Ikeda · Nobuyuki Kato · Hajime Isomoto · Fuminao Takeshima · Kazuhiko Nakao

Received: 27 July 2010 / Accepted: 29 August 2011
© Springer 2011

Abstract

Background Geranylgeranylacetone (GGA), an isoprenoid compound which includes retinoids, has been used orally as an anti-ulcer drug in Japan. GGA acts as a potent inducer of anti-viral gene expression by stimulating ISGF3 formation in human hepatoma cells. This drug has few side effects and reinforces the effect of IFN when administered in combination with peg-IFN and ribavirin. This study verified the anti-HCV activity of GGA in a replicon system. In addition, mechanisms of anti-HCV activity were examined in the replicon cells.

Methods OR6 cells stably harboring the full-length genotype 1 replicon containing the *Renilla* luciferase gene, ORN/C-5B/KE, were used to examine the influence of the anti-HCV effect of GGA. After treatment, the cells were harvested with Renilla lysis reagent and then subjected to a luciferase assay according to the manufacturer's protocol. **Result** The results showed that GGA had anti-HCV activity. GGA induced anti-HCV replicon activity in a time- and dose-dependent manner. GGA did not activate the tyrosine 701 and serine 727 on STAT-1, and did not induce HSP-70 in OR6 cells. The anti-HCV effect depended on the GGA induced mTOR activity, not STAT-1

activity and PKR. An additive effect was observed with a combination of IFN and GGA.

Conclusions GGA has mTOR dependent anti-HCV activity. There is a possibility that the GGA anti-HCV activity can be complimented by IFN. It will be necessary to examine the clinical effectiveness of the combination of GGA and IFN for HCV patients in the future.

Keywords mTOR · STAT-1 · Interferon · HCV · GGA

Abbreviations

IFN	Interferon
HCV	Hepatitis C virus
STAT	Signal transducers and activators of transcription
ISGF-3	IFN-stimulated gene factor 3
ISRE	IFN-stimulated regulatory element
PKR	Double-stranded RNA-dependent protein kinase
Rapa	Rapamycin
PI3-K	Phosphatidylinositol 3-kinase
mTOR	Mammalian target of rapamycin
GGA	Geranylgeranylacetone
siRNA	Small interfering RNA

Introduction

Currently, chronic hepatitis C virus (HCV) infection is the major cause of hepatocellular carcinoma worldwide [1]. Therefore, an anti-HCV strategy is important for prevention of carcinogenesis. The treatment of HCV with a combination of pegylated interferon (IFN) and ribavirin is effective in 80% of HCV genotype 2 or 3 cases, but less than 50% of genotype 1 cases. New anti-HCV agents have been developed to inhibit the life cycle of HCV and are

S. Takeshita · T. Ichikawa (✉) · N. Taura · H. Miyaaki · T. Matsuzaki · M. Otani · T. Muraoka · M. Akiyama · S. Miuma · E. Ozawa · H. Isomoto · F. Takeshima · K. Nakao
Department of Gastroenterology and Hepatology,
Graduate School of Biomedical Sciences,
Nagasaki University, 1-7-1 Sakamoto,
Nagasaki 852-8501, Japan
e-mail: ichikawa@net.nagasaki-u.ac.jp

M. Ikeda · N. Kato
Department of Molecular Biology,
Graduate school of Medicine and Dentistry,
Okayama University, Okayama, Japan